Disko-Nuussuaq: Structural mapping and GIS compilation to better define petroleum exploration targets on Disko and Nuussuaq

John R. Hopper, Gunver K. Pedersen, Erik V. Sørensen, Pierpaolo Guarnieri, Niels H. Schovsbo, Henrik Nøhr-Hansen, Thomas F. Kokfelt, Morten L. Hjuler, Christian Knudsen, Peter Johannessen & Willy L. Weng

GEUS

Disko-Nuussuaq: Structural mapping and GIS compilation to better define petroleum exploration targets on Disko and Nuussuaq

John R. Hopper, Gunver K. Pedersen, Erik V. Sørensen, Pierpaolo Guarnieri, Niels H. Schovsbo, Henrik Nøhr-Hansen, Thomas F. Kokfelt, Morten L. Hjuler, Christian Knudsen, Peter Johannessen & Willy L. Weng

Contents

1. Executive Summary

This report summarizes the key outcomes of the MMR/GEUS project "Disko–Nuussuaq: Structural mapping and GIS compilation to better define petroleum exploration targets on Disko and Nuussuaq". It is intended to provide a succinct overview of the structure and stratigraphy of the region to accompany the GIS project that was compiled. The project was carried out at GEUS during 2015 and 2016.

Beginning in the late 1980s and early 1990s, GGU undertook a series of campaigns to assess the resource potential of western Greenland, including the areas onshore Disko–Nuussuaq where outcrops of the Nuussuaq Basin are well exposed. As a result of this early work, the potential for oil and gas is now proven (Bojesen-Koefoed et al. 1999). Oil and gas shows occur in many shallow core holes and wells and several mineral exploration wells in the region were abandoned because of gas overpressure. Oil seeps have been documented over a large area, with five distinct oil types sourced from Mesozoic and Paleocene shales known to occur (Figure 1.1).

While there is little doubt of an active petroleum system, there remain key problems with understanding the structural development of the basin and with understanding the distribution and quality of the source rocks. This hampers the prediction of locations where large accumulations might be found. The purpose of this project was compile as much of the relevant information available into a new GIS project with the aim of reassessing the structural development of the region. The report includes a brief summary of the regional setting followed by four main chapters: a chapter on the structural framework that includes a new structure map based on photogrammetry, interpretation of offshore seismic data, and a review of existing geologic and structural maps of the region; a chapter summarizing the sedimentological and volcanic successions of the region; a chapter on the petrophysical characteristics of likely reservoir rocks in region; and a chapter on the sediment composition and provenance. This is followed by a brief review of the potential prospectivity of various areas and recommendations for future work needed to further de-risk exploration in the region. In this report, it should be noted that frequent references are made to figures from key publications. The word 'figure' is capitalized when referring to figures in this report, but is non-capitalized when referring to the figure number within a cited publication.

1.1 What's new in this compilation

The compilation here is built on previous GIS compilations for the Baffin Bay and West Greenland regions and includes several important updates as well as new mapping. The following list summarizes the key new information provided in the compilation:

- new map of the Tunoqqu surface based on recently acquired aerial photos over Nuussuaq showing a large anticline structure;

- Late Cretaceous–Eocene structural elements map highlighting the main depocentres and structural highs that likely controlled the distribution of key source rock formations;

• documentation of important inversion structures through central Nuussuaq and northern Disko;

• stratigraphic correlation panels calibrated to the 2012 timescale that supplement the vertical geological sections of Pedersen et al. (1993, 2002, 2003, 2005, & 2006); two sets are provided, a general overview covering the Cretaceous–Cenozoic and a detailed view of the Paleocene for the volcanic stratigraphy;

• inferred stratigraphic distribution maps of key source and reservoir rock formations based on the known outcrops and structural mapping;

• complete database of all wells and shallow cores with links to public and freely available reports;

• georeferenced lithostratigraphic columns of key localities (from Dam et al. 2009);

• database of georeferenced field photos, oblique photos, and selected aerial photos showing local geology, terrain, and structures;

• database of key petrophysical data relevant to potential reservoirs;

• updated biostratigraphic range charts and information;

• vectorized versions of previously published structural maps of the region;

• vectorized cross-sections and profiles across key structures (both new and previously published);

• high resolution digital elevation model that can be used as an overlay on various maps.

1.2 Acknowledgements
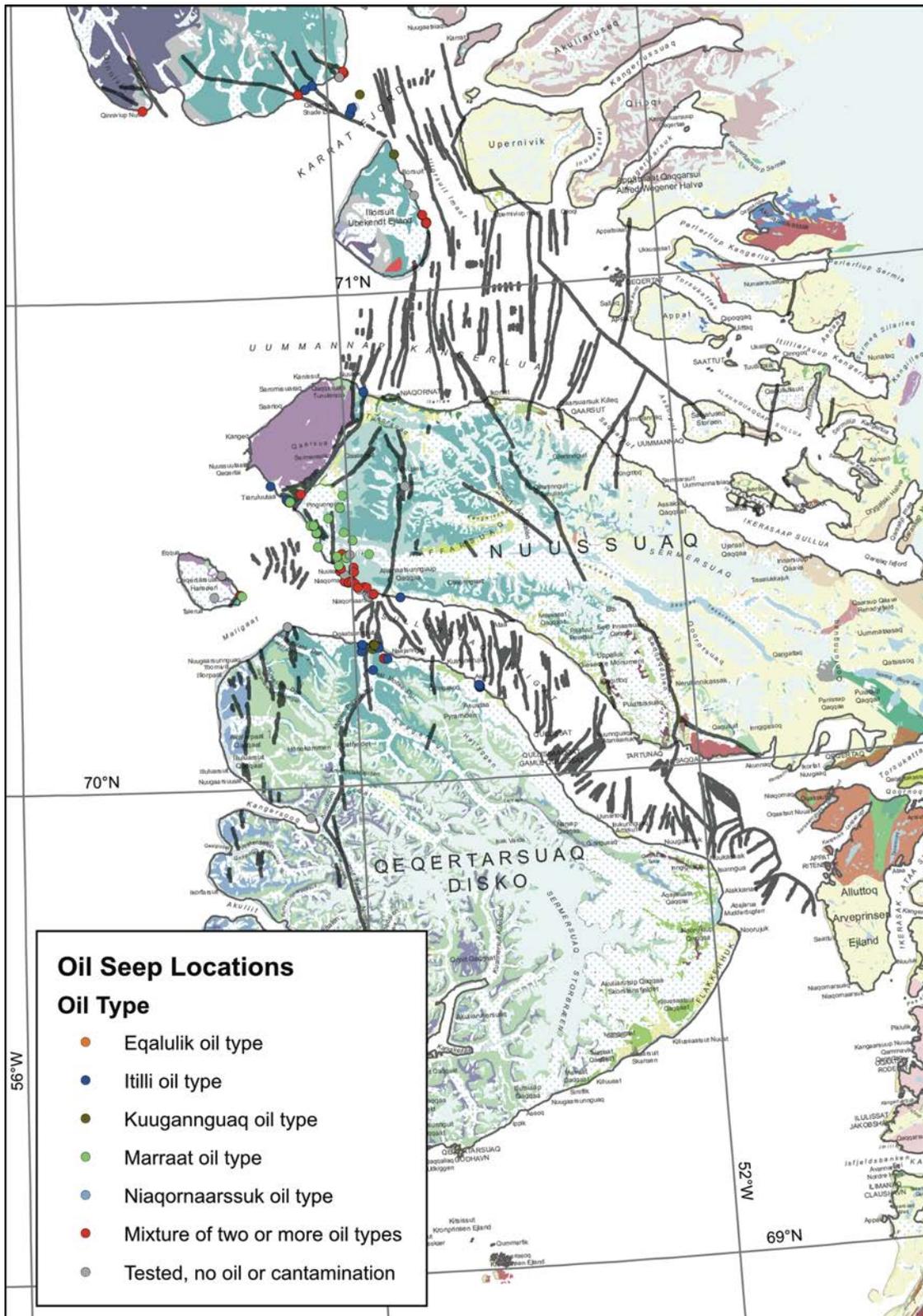
Figure 1.1. *1:500 000 geological map of Disko and Nuussuaq where the Nuussuaq Basin is well exposed. Grey lines are faults interpreted by Marcussen et al. (2002). Oil seep locations are concentrated in the south-western part of Nuussuaq, but additional seeps are found along the north coast of both Disko and Nuussuaq, on Ubekendt Ejland, and on Svartenhuk Halvø.*

2. Regional setting

The overall tectonic setting of the Labrador Sea and Baffin Bay is reasonably well established and a regional review by Balkwill et al. (1990) still provides the basic framework. The onshore areas of West Greenland, Baffin Island, and Labrador are dominated by Precambrian basement rocks of the North American Archaean Craton and surrounding Proterozoic mobile belts (Tappe et al. 2007). Mesozoic continental rifting separated Greenland from North America, culminating in seafloor spreading in the Labrador Sea and Baffin Bay during the Palaeogene and linking Atlantic spreading to the Arctic Ocean (e.g., Oakey & Chalmers 2012). The history of extension is recorded primarily in the offshore basins that make up the continental margins of Greenland and Canada. Most of what is known about the Mesozoic and younger history comes from exploration wells and regional seismic data collected over the last several decades. An important exception is the Nuussuaq Basin, onshore central West Greenland, where Cretaceous–Paleocene sedimentary rocks crop out.

A comprehensive review of the Labrador Sea margins and seafloor spreading is provided in Chalmers and Pulvertaft (2001) and more recent summaries of these margins are available in Keen et al. (2012) and Dickie et al. (2011). The Labrador Sea and Baffin Bay are separated by the Davis Strait high, a complex transform margin that is dominantly continental crust and strongly affected by volcanism (Funck et al. 2007; Gerlings et al. 2009). The Baffin Bay is the northernmost extent of seafloor spreading between Greenland and North America and is bounded to the north by the Palaeozoic–Mesozoic Franklinian and Sverdrup basins, which form the northern margins of Canada and Greenland along the Arctic Ocean. The Baffin Bay margins are summarised in Harrison et al. (2011), Gregersen et al. (2013), and Alsulmai et al (2015).

Figure 2.1 shows the regional tectonic elements map from Oakey & Chalmers (2012) and Figure 2.2 shows the summary stratigraphy of the main basin areas of the regions from Fensome et al. (2016), which is the most recent revision of the regional stratrigraphy.

The Nuussuaq Basin is well exposed onshore Disko Island and Nuussuaq Peninsula, with additional important outcrops on Ubekendt Island and Svartenhuk Pensinsula. The basin is located at north-easternmost corner of the Davis Straight high and was part of a complex zone of transfer systems that linked extension in the Labrador Sea to the Baffin Bay and the Melville Bay Graben (Gregersen et al. 2013).

Major Mesozoic basin formation occurred in two phases, with a first phase in the Early Cretaceous and a second phase in the Late Cretaceous to Paleocene, culminating with breakup and seafloor spreading. Dykes along SW Greenland indicate that regional extension began already in the Jurassic (Larsen et al. 2009). However, no Jurassic sediments are known from either the Canadian or Greenland margins. Along the Labrador shelf, the onset of major extension is marked by a volcanic episode represented by the Valanginian–Hauterivian Alexis Formation volcanic rocks and intra-volcanic sediments (Balkwill et al. 1990). Along the Greenland margin, the Early Cretaceous rift phase is inferred primarily from seismic interpretation of the offshore areas (Chalmers & Pulvertaft 2001). The oldest sediments penetrated by wells are Upper Cretaceous and the significant thickness of

deeper sedimentary sequences is evidence that the first rift phase was important offshore West Greenland as well. The oldest sedimentary rocks in the Nuussuaq Basin are ?Aptian–Albian terrestrial deposits of the Kome and Atane formations (Dam et al. 2009).

This first phase of rifting was followed by a period of thermal subsidence and quiescence during the mid-Cretaceous with a second major phase of rifting beginning in the Campanian which continued into the Paleocene (Chalmers et al. 1999). The thermal subsidence phase was marked by a major marine transgression, probably beginning in the Cenomanian–Turonian, and resulted in deposition of the Itilli Fm, which includes important deep marine mudstones.

Major uplift occurred during the latest Cretaceous and early Paleocene that is considered to be related to the arrival of the Iceland mantle plume beneath Greenland (e.g., Storey et al. 1998; Nielsen et al. 2002; Larsen et al. 2015). Large volume volcanism occurred, forming the West Greenland volcanic province during the Paleocene and Eocene (see Larsen et al. 2015 for a recent summary). This volcanism was coincident with the earliest known true seafloor spreading in the Labrador Sea and Baffin Bay (Oakey & Chalmers 2012; Keen et al. 2012). Onshore West Greenland, the oldest known volcanic rocks are ~62 Ma and are hyaloclastite deposits of the lower Vaigat Fm, which were deposited into a marine basin. The basin eventually filled with volcanic material and was then covered by subaerially erupted lava flows that make up the overlying volcanic succession (see Larsen et al. 2015 for the volcanic stratigraphy).

At the end Paleocene to early Eocene, a major regional plate adjustment occurred as the North Atlantic Ocean opened. This resulted in a significant change in spreading direction between Greenland and North America. This change in plate configuration seems to have affected the Nuussuaq Basin in complex ways, with the development of wrenching (Green et al. 2013) during the adjustment between Chrons C25N and C24N. By C24N, the plate configuration stabilized and the area around the Nuussuaq Basin was dominated by strike-slip faulting with some rifting at the northeast extension of the Ungava fault system in Davis Strait. Sea floor spreading ceased in the Baffin Bay and Labrador Sea by Chron C13N in the late Eocene.

The end Eocene was marked by a period of uplift and non-deposition during the Oligocene. The lack of Oligocene deposition along the surrounding margins remains one of the more enigmatic problems of the Cenozoic history of the region (Fensome et al. 2016). Large contourite drift deposits developed during the middle Miocene (Knutz et al. 2015) and by the late Miocene, renewed uplift of the margin occurred, followed by a second phase of uplift and doming in the Pleistocene that generated the present day high topography of the region (Green et al. 2013). The uplift and subsidence history of the West Greenland margin has been recently reviewed by Green et al. (2013) and is summarized in Figures 2.3 and 2.4.
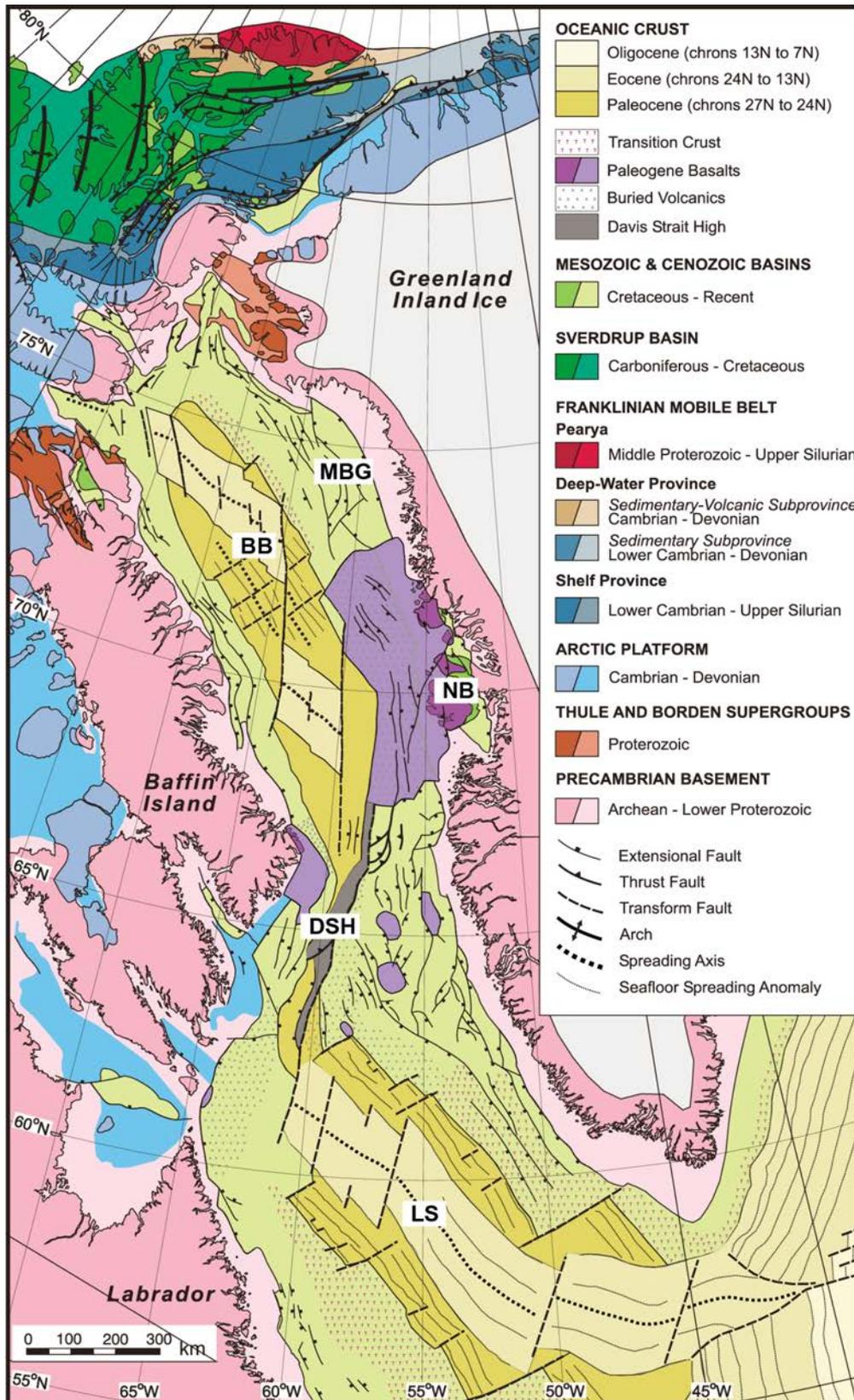
Figure 2.1. *Regional geology of the Baffin Bay and Labrador Sea (figure 2 of Chalmers and Oakey 2012). See Chalmers and Oakey for references. NB - Nuussuaq Basin; LS - Labrador Sea; BB - Baffin Bay; - MBG - Melville Bay Graben.*
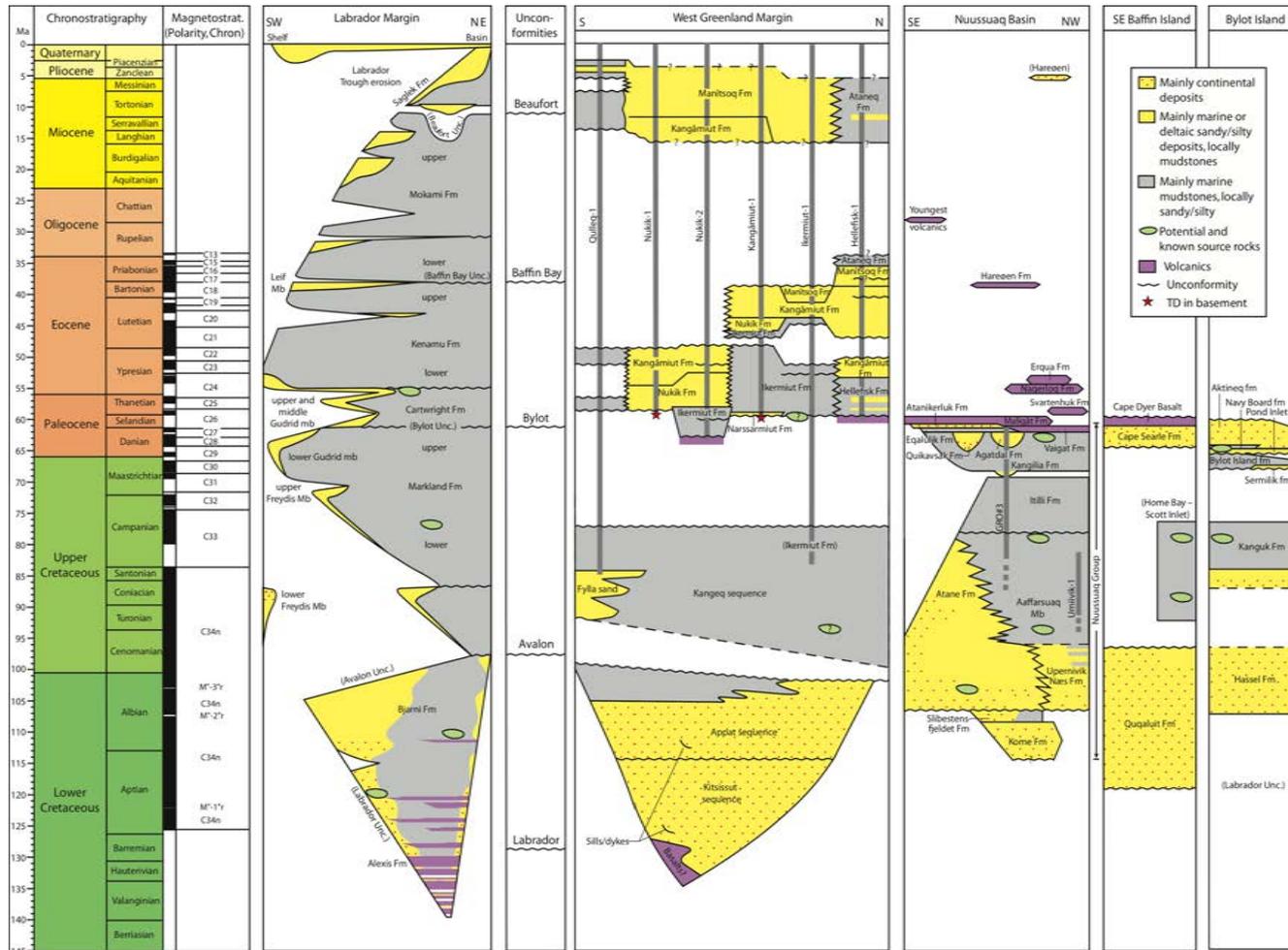
Figure 2.2. The formations recognized in six offshore wells and two onshore wells are illustrated. Please note that the vertical axis shows the age and not thickness of each formation. Several formations include significant hiatuses, which were not recognized during the initial descriptions of the sections drilled. The ages of the formations are mainly derived from Nøhr-Hansen (2003), Fensome et al. (2016), Rasmussen et al. (2003), and Rasmussen & Sheldon (2003). Lithostratigraphy from Rolle (1985) and Dam et al. (2009). Figure from Fensome et al. (2016).

Fig. 38. Summary of the subsidence and uplift history of the Nuussuaq Basin. **A**: Schematic diagram showing estimates of uplift and subsidence derived from the geological record that affected the Nuussuaq Basin between Early Cretaceous rifting and shortly after mid-Paleocene break-up (Fig. 37). **B**: Enlargement of part of **A**. The record is from Dam *et al.* (2009) except where otherwise cited and refers to an area on the south coast of Nuussuaq marked on Fig. 36 (photos in Fig. 39). An episode of rifting took place probably in the Aptian (depositing TSS1) followed by thermal subsidence that started in the Albian (Chalmers *et al.* 1999). The Atane Formation (TSS2) was deposited during the latter event. It is at least 3 km thick but a reflection seismic line on the south coast of Nuussuaq (Chalmers *et al.* 1999, fig. 9) shows that the sediments at this location are at least 6 km thick and may be 8 km thick. An episode of uplift followed by renewed subsidence and deposition of the Itilli Formation (TSS3) took place in the Campanian. Faulting, uplift and erosion of major submarine channels in the Maastrichtian led to the complete erosion of TSS3 at some localities such as the one represented here. The Kangilia Formation (TSS4) was deposited in the renewed subsidence after this event (Fig. 39A). Two episodes in the late Danian uplifted the surface to above sea level and the fluvial Quikavsak Formation (TSS5) was deposited in the river channels (Fig. 39B). Submarine volcanism commenced in the western Nuussuaq Basin at this time. The volcanism built up a volcanic island and became subaerial at the same time as the eastern Nuussuaq Basin subsided by 600–700 m. Subaerial lava flows from the west flowed into this basin (TSS7), filling it as a hyaloclastite delta (Fig. 39C). Subsidence continued, however, as shown by the deposition of a succession of lava flows with hyaloclastite bases and subaerial tops (Fig. 39D) and eventually entirely sub-aerial lavas. Deposition of a later (Eocene) subaerial volcanic succession (TSS8) followed a hiatus in the volcanism. Arrows indicate episodes of uplift (red) and subsidence (blue). **Subs. during SFS**: Subsidence during sea-floor spreading. **TSS**: tectonic stratigraphic sequences in Fig. 37 (Dam *et al.* 2009).
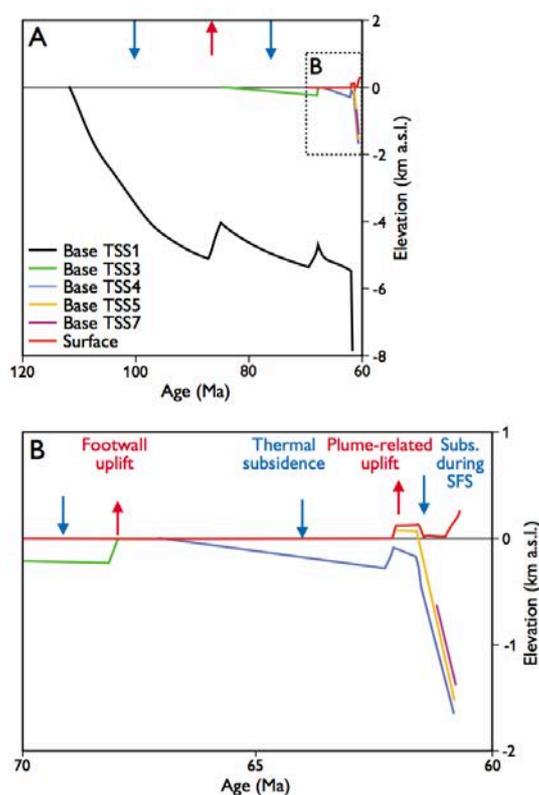
Figure 2.3. *Green et al. (2013) figure 38 along with original caption summarizing the uplift and subsidence history of the Nuussuaq Basin. The references cited in the original caption are not necessarily included in the reference list of this report.*
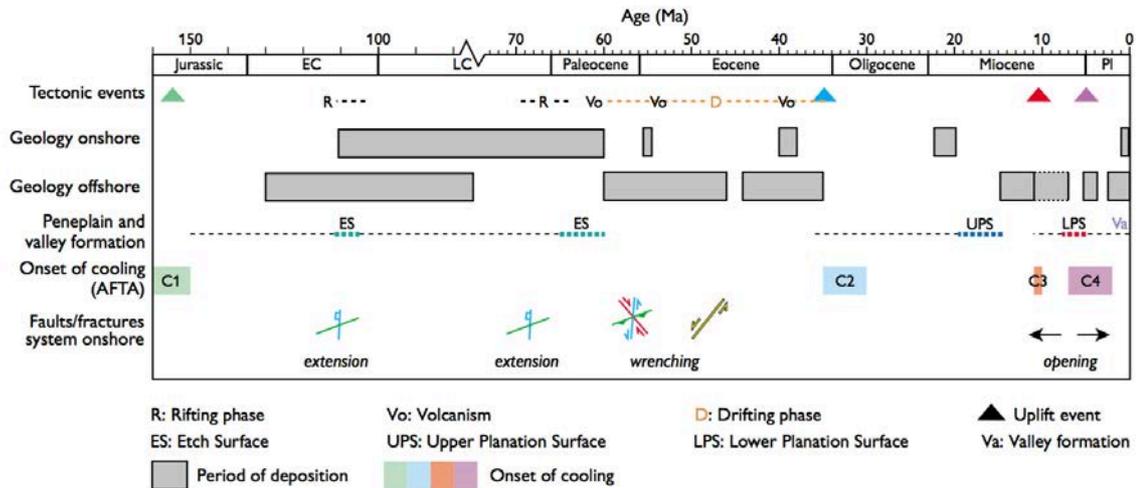
Fig. 48. Summary of stratigraphy offshore and onshore West Greenland, cooling events identified onshore from AFTA, peneplain formation and valley incision, and key regional tectonic events as seen in the structural systems onshore. Onshore and offshore unconformities correspond to regional tectonic events that are identified by stratigraphic landscape analysis and constrained in time by the cooling events defined by AFTA. Weathering and erosion of the etch surface (**ES**) in basement rocks took place following Late Jurassic exhumation (cooling event **C1**, Table 2) and prior to Early Cretaceous burial, and renewed development took place prior to Paleocene volcanism. Following post-breakup subsidence and burial, a first phase of uplift and exhumation that began at the Eocene–Oligocene transition (**C2**), led to the formation of the Upper Planation Surface (**UPS**) during the Oligo–Miocene (see Fig. 54). This surface was offset by reactivated faults, resulting in megablocks that were tilted and uplifted to present-day altitudes of up to 2 km in two phases that began in the Late Miocene and in the latest Miocene–Pliocene, **C3** and **C4**, respectively. The C3 uplift led to incision below the uplifted UPS and thus to formation of the Lower Planation Surface (**LPS**). The peneplains and incised valleys thus reveal information on erosion from periods in the past from where there exist no other geological data. Dotted line: maximum age range of sediments. Onshore stratigraphy from Fig. 37 and Schmidt *et al.* (2005), Pedersen *et al.* (2006). Offshore stratigraphy from Fig. 43. **EC**: Early Cretaceous. **LC**: Late Cretaceous. **Pl**: Plio–Pleistocene. Modified from Bonow *et al.* 2007b and Japsen *et al.* (2009).

Figure 2.4. *Figure 48 from Green et al. (2013) along with original figure caption summarizing the main tectonic events and uplift events in West Greenland. The references cited in the original caption are not necessarily included in the reference list of this report.*

3. Structural framework

John R. Hopper, Pierpaolo Guarnieri, & Erik Vest Sørensen

3.1 Introduction

The structural framework of the Nuussuaq Basin is highly complex. Chalmers et al. (1999) provided an interpretation of seismic, magnetic, and gravity data to establish the overall structural setting of the basin and its relation to the West Greenland margin. They concluded that *"At present the sequence of events that created the Nuussuaq Basin is not clear"*. While much work has been done on the stratigraphic and volcanic successions since that time (Chapter 4), comparatively little has been done on the structural development. Several phases of deformation are known to have affected the basin, generating structures in multiple directions that cross-cut each other. The sparse data offshore in combination with the poor exposure of key structures onshore remains a key barrier to fully understanding the structural evolution of the basin. Nevertheless, while the original conclusion of Chalmers et al. (1999) still holds today, a general outline of the key tectonic events and structural trends that developed is still possible.

The summary here provides a brief overview of the main structures following the general format laid out in Chalmers et al. (1999). A summary structural elements map is provided based on the previous work, but with several key differences, the most important of which is the recognition from recent mapping that the lower volcanic succession shows evidence for compression and inversion (Sørensen 2011). As part of this project, this inversion has been further documented and possible examples of inversion structures on seismic data offshore are highlighted. In addition, some examples from field photos further documenting inversion are shown.

The main previously published structural maps of the region are shown in Figures 3.1–3.4 (Chalmers et al. 1998; Chalmers et al. 1999; Marcussen et al. 2002). The Nuussuaq Basin is situated at the north-eastern edge of a complex system of rift basins and transfer systems that linked extension and seafloor spreading in the Labrador Sea to the Baffin Bay. It lies along strike of the Ungava fault zone, which is a major strike-slip boundary along the Davis Strait high that developed during Labrador Sea/Baffin Bay opening. The basin was formed by two major phases of extension, first in the Early Cretaceous and then in the Late Cretaceous, with an intervening quiescent period of thermal subsidence. The arrival of the Iceland plume beneath Greenland in the Paleocene resulted in significant volcanism that covered much of the basin and an evident uplift documented by the unconformable basal contact of the volcanic sequence. The oldest known volcanic rocks of the Vaigat Fm erupted during Chron C27N (Larsen et al. 2015), which is also the oldest undisputed magnetic anomaly in the Labrador Sea. In addition, Oakey & Chalmers (2012) interpret the oldest magnetic anomaly in the Baffin Bay as C27N. Thus there is a close association with the onset of volcanism in the basin and the initiation of seafloor spreading between Greenland and Canada.

The earliest seafloor spreading was directed in a NE–SW direction and was accommodated along mostly NW–SE striking extensional fault systems (Oakey & Chalmers 2012). The Cretaceous kinematic history is much less well constrained, but it is likely that initial extension was in a similar direction. This is indicated by dominantly NW–SE striking early main boundary faults throughout the region (e.g., Whittaker 1997 and Gregersen et al. 2013 in the Baffin Bay; Chalmers et al 1993 in the Labrador Sea). Between Disko Bugt and Nuuk along West Greenland, however, the main boundary faults are all N–S striking (Chalmers et al. 1993). In the Nuussuaq Basin, the early main boundary faults also appear to be dominantly NW–SE striking in the northernmost parts on Ubekendt Island and Svartenhuk Halvø. The situation is less clear on Nuussuaq and Disko, where both N–S trends and NW–SE trends are mapped, further emphasizing that the Nuussuaq Basin is located at a key juncture linking the Baffin Bay basins to the Labrador Sea.

The second phase of extension, which began in the Campanian, appears to have been accommodated by N–S striking faults within the Nuussuaq Basin, with complicated splay and transfer systems linking them to older fault systems. In addition, the older fault system was very likely reactivated in many places. These later faults dissect the basin and resulted in complicated structural patterns within the basin, as is demonstrated by complex structures mapped on seismic reflection data in the offshore areas (Marcussen et al. 2002).

As documented in Oakey & Chalmers (2012), significant changes in the kinematic evolution of the Baffin Bay and Labrador Sea occurred during the latest Paleocene–Eocene that are thought to be related to the opening of the North Atlantic Ocean. In their model, three distinct poles of rotation are required to satisfy the available magnetic constraints: one from C27N to C25N, one from C25N to C24N, and one from C24N to C13N, after which spreading ceased. The apparent onset of inversion in the offshore basins began in the Late Paleocene based on seismic-stratigraphic interpretation constrained by wells (Gregersen & Bidstrup 2008). The inversion documented in this report in Section 3.3 is thought to be at this time as well (Guarnieri 2015) and may be related to regional changes in plate motion that began in the latest Paleocene during Chrons 25N–24N.

The Eocene was marked by nearly north–south extension in the Baffin Bay, which was linked to the Labrador Sea along major NE–SW oriented strike slip fault systems through the Davis Strait high. A single fault, the Itilli Fault, in the Nuussuaq basin has this orientation as described further below. The Eocene was marked by large scale flood volcanism in the region. Notably, the only Eocene volcanic rocks preserved are northwest of the Itilli Fault. It is presumed that the Eocene volcanic rocks covered most of the Nuussuaq Basin, but have since been eroded away during subsequent post-breakup uplift events that form the present day high topography of the region (Green et al. 2013).

3.2   Structural elements of the Nuussuaq Basin

This section summarizes the main structural elements as faults and basement highs that were active during the Cretaceous–Paleocene development of the basin, observed onshore as well as several key structures inferred from geophysical data. Figure 3.5 shows a structural summary map highlighting the main Cretaceous structures and structural elements and Figure 3.6 shows geological cross sections through several key areas. The maps build

on the work of Chalmers et al. (1999). Key gravity modelling profiles that this latter work is based on are shown in Figure 3.7 and include the structures discussed below. Figure 3.8 shows the regional magnetic anomaly field (Gaina et al. 2011) and Figure 3.9 shows the tilt derivative of a high resolution magnetic survey over the region (Thorning & Stemp 1998).

There remain key questions regarding the timing of movement on the faults exposed onshore in relation to the sedimentary successions within the basin (see Pulvertaft 1979, 1989a,b and Chalmers et al. 1999). The Early Cretaceous boundary fault system may have been farther east than the current distribution of sedimentary outcrop would imply. In the depth to basement maps in Chalmers et al. (1999), the easternmost parts of the Nuussuaq Basin show 3–5 km thick sediments overlying basement. Thick sediments well in excess of 5 km are restricted to areas west of the Kuugannguaq–Qunnilik Fault and fault P, with an important exception to the north just west of the Ikorfat Fault (Figure 3.3).

The present day boundary of the Nuussuaq Basin is marked by NNW–SSE striking faults linked by presumed ENE–WSW striking transfer systems. In the area covered by this project, the main boundary between the basin and the Precambrian basement are found on Nuussuaq at Kuuk along the north coast, and along the eastern edge of Sarqaqdalen along the south coast. To the south, the boundary fault system is entirely offshore in Disko Bugt and its position can only be inferred from magnetic anomaly and gravity data. To the north, the boundary fault is exposed on Upernikvik Ø and on Svartenhuk Halvø. Where exposed the faults are steeply dipping towards the basin (SW) from 47°–73° (Chalmers et al. 1999).

Pre-existing structural trends within underlying basement place important controls on subsequent evolution of rifted basins (e.g., Ring 1994). Pre-existing fabrics are often oblique to later regional extension directions and influence key aspects of the later fault systems including the preferred main fault direction and fault splays and displacements, as well as the development of transfer and linkage systems between faults (Morley et al. 2004).

3.2.1   Structural trends in the Precambrian basement

The Precambrian geology of the Disko Bugt region is summarized in a collection of papers edited by Kalsbeek (1999) and in mapping by Garde (1994). The basement east of Disko Bugt and in eastern Nuussuaq is dominated by NW–SE trending ductile shear zones and brittle faults related to the Paleoproterozoic Nagssugtoqidian and Rinkian orogenic belts (Connelly et al. 2006). This is parallel to the overall trend of the main boundary faults described in Chalmers et al. (1999) as well as to the main boundary fault of the Melville Bay graben farther north.

The areas east of Uummannaq and south of Disko Bugt show several sets of brittle faults described by Chalmers et al. (1999) as primarily left-lateral strike slip with displacements up to 1.2 km. They are oriented NNE–SSW. The age of these faults is not noted in any information available to this project, so it is not clear if these are older trends or if they are related to younger tectonics.

The magnetic anomaly map shows several distinct lineations that are related to older dykes. An ENE–WSW anomaly extends into the Vaigat south of Saqqaq (Figure 3.9). This

trend is suggested below to be similar to possible transfer faults linking the main normal faults of the basin.

3.2.2   The Nuussuaq Ridge

The Nuussuaq ridge is a NW–SE trending basement high bounded to the SW by the Kuuk and Ikorfat–Saqqaqdalen faults and described as the NE-dipping Qaarsut ramp by Chalmers et al. (1999). Note that the Nuussuaq Ridge is a structural feature that is not highlighted or named in previous works. It is shown in Figures 3.5–3.7. The basement exposed along the ridge is interpreted as the result of footwall-crest erosion during block-tilting initiated in the Early Cretaceous. This is indicated by the onlap of more than 800 m thick succession of sandstones, heteroliths and mudstones of fluvial, estuarine, deltaic and lacustrine origin of Early Cretaceous age. The crest is unconformably covered by subaerial volcanic rocks of the Vaigat Fm suggesting that it was a structural high before the Late Paleocene.

3.2.3   The Disko Gneiss Ridge

The Disko Gneiss Ridge is a north–south trending ~20 km wide zone on Disko where Precambrian rocks crop out. The ridge extends at least as far north as the Kuugannauq Valley where borehole FP93-3-1 penetrated ~55 m of shales and sandstones before reaching gneissic basement at 100 m depth (~150 m above sea level; Olshefsky & Jerome 1994). The ridge appears to completely disappear farther north. Along strike toward Nuussuaq, seismic line GGU/NU94-01 shows at least 8 km of sedimentary sequences along the south coast of Nuussuaq between the K–Q Fault and fault P. Thick sediments are also indicated in the gravity models along the Vaigat. A NW–SE trending fault is inferred, fault M, to accommdate this.

Similar to the Nuussuaq ridge, the Disko Gneiss ridge is interpreted as the footwall crest of a rotated block formed during the initial rifting in the Early Cretaceous. The N–S trend of the ridge as mapped by Chalmers et al. (1999) and highlighted by the magnetic map (Figure 3.8) is interpreted as the result of combined fault activity starting during the Early Cretaceous when the ridge probably formed a NW–SE trending footwall crest and segmented later, by the Late Cretaceous and younger faults.

The western edge of the ridge aligns with the K–Q fault (section 3.2.6), but there is no significant displacement of the basalts across the boundary here. In the north, the subaerial lava flows of the upper Vaigat Fm onlap the basement, and in the south, the Maligât Fm onlaps the basement. The western edge is considered in most maps to be a continuous normal fault, but it is unclear that this is the case. The gravity modelling suggests a N–S striking fault south of Disko that changes strike to NW–SE underneath Kangerluk (Chalmers 1998). The central part of the Disko Gneiss Ridge shows no strong evidence for a fault. The gravity modelling suggests instead a gradual deepening of the basin to the SW away from Disko, which would be inconsistent with a significant west dipping normal fault along the ridge.

The eastern edge of the ridge is likely bounded by an east dipping fault based on the gravity modelling. The depth to basement below central Disko east of the ridge appears to be quite deep, up 8 km along fault C. The models in Chalmers (1998) suggest that central Disko may be deep graben, requiring the eastern edge of the Disko Gneiss Ridge to be fault controlled.

The ages of faults associated with the Disko Gneiss Ridge are similarly uncertain. In the paleogeographic reconstructions in Dam et al. (2009), the ridge does not appear as a topographic high until the Late Cretaceous, implying that it emerged as a major structural feature in association with Campanian faulting. The overall N–S strike would be consistent with the general development of Chalmers et al. (1999) suggesting that Campanian rifting was accommodated along dominantly N–S structures. However, the deep basins seem to require Early Cretaceous extension as well. Here it is suggested that the Disko Gneiss Ridge could be a series of en échelon horst structures that began to develop already during the Early Cretaceous phase of rifting along NW–SE striking structures with NE–SW transfer systems. These were modified in some places by later faulting in the Campanian. Given the lack of displacement of the upper Vaigat, motion must have ceased by the late Paleocene.

3.2.4   Kuuk Fault

The Kuuk Fault is exposed on the north side of Nuussuaq and represents the easternmost limit of sedimentary rock outcrop on Nuussuaq. East of the Kuuk Fault, Maligât Fm basalts overly Precambrian basement. The fault is described by Chalmers et al. (1999) as linked to the Ikorfat Fault by the Qaarsut ramp. Late Albian sediments are cut abruptly by the fault with no change in facies towards the fault (Pulvertaft 1989). In addition, interpretation of the Upper Albian sediments does not suggest the presence of a fault scarp at the position of the Kuuk Fault during the mid-Cretaceous (Midtgaard 1996a). Tilting of the sediments towards the fault must have been pre-Maastrichtian, however, since Maastrichtian mudstones unconformably overlie the Upper Albian rocks east of Ikorfat (Chalmers et al. 1999). Thus the Kuuk fault is interpreted as a Campanian fault that formed during the second major phase of basin formation. The Early and mid-Cretaceous deposits found in this region are interpreted by Chalmers et al. (1999) to result from thermal subsidence of the basin following the first main phase of Early Cretaceous extension. Some early maps showed a connection and fault splay system from the Kuuk Fault to the Saqqaqdalen Fault to south. However mapping by Pulvertaft (1979, 1989b) could find no evidence for this.

3.2.5   Ikorfat and Saqqaqdalen faults

The Ikorfat and Saqqaqdalen faults together form a major NW–SE striking fault system. The Ikorfat Fault is exposed on the north side of Nuussuaq and the Saqqadalen Fault is exposed on the south side of Nuussuaq. Although they are typically drawn on regional maps as a single fault, It is more likely that they are connected by splay faults and transfer systems. Together with Kuuk Fault, they are interpreted as part the boundary fault system defining the eastern edge of the Nuussuaq Basin that formed during the second phase of extension (Chalmers et al. 1999). Thus, they are also thought to be Campanian in age. However, they remained active into the Paleocene as there is evidence that they displace

the Vaigat formation (Pedersen et al. 1996) and Maastrichtian mudstones are displaced as much as 725 m. The Campanian section is suggested by Chalmers et al. (1999) to have been downthrown out of sight. Any motion on the fault ceased by the end of the Paleocene, however. Dolerite sheets dated to 55 Ma (Storey et al. 1998) intrude the Saqqaqdalen fault and are undeformed.

3.2.6   Kuugannguaq–Qunnilik (K–Q) Fault, Gassø Fault & Fault P

Th Kuugannguaq fault on Disko and the Qunnilik Fault on Nuussuaq is a major structure within the Nuussuaq Basin and is the most prominent N–S striking fault that can be mapped. Downthrow of Tunoqqu surface is as much as 700 m to the west across this fault on Nuussuaq, but less further south on Disko (Chalmers et al. 1999). In the gravity modeling of Chalmers et al. (1998), a significant fault just to the east of the K–Q fault is also indicated and is referred to as fault P. There may be an expression of this fault on the south coast of Nuussuaq where a 400 m difference in elevation of the hyaloclastite units is observed (Pedersen et al. 1993; Chalmers 1998). Otherwise this fault is primarily based on interpretation of gravity and seismic data (Chalmers 1998; Marcussen et al. 2002). The Gassø fault, to the west of the K–Q Fault, is another significant structure mapped onshore. It strikes N–S and shows post-Vaigat downthrow to the west of nearly 1 km (Chalmers 1998).

The K–Q and P faults mark the location where the depth to basement becomes significantly greater to the west. Basement to the west of these faults reaches as deep as 8–11 km, whereas to the east, depth to basement is typically 5 km. In the general development outlined in Chalmers et al. (1999), these may have been the main boundary faults during the first phase of extension in the Early Cretaceous. This would explain the significantly deeper basement to the west and lack of evidence for pre-Campanian motion on the faults exposed on Nuussuaq to the east (the Kuuk, Ikorfat, and Saqqaqdalen faults). The faults, however, also displace the basalt, showing that they were active throughout the basin development into the Paleocene.

Collectively, these faults also define the area where the most significant oil seepage occurs. The vast majority of oil seeps are mapped between the K–Q Fault and Itilli Fault. Important exceptions to this include the Asuk seep location on the north coast of Disko, which is approximately 50 km east of the Kuugannguaq Fault.

3.2.7   Itilli Fault

The Itilli Fault is a well-defined structure that strikes NE–SW along the north-western part of the Nuussuaq Basin. Although there are small scale NE–SW striking structures that act is transfer or linkage systems within the basin, the Itilli fault is the only regional scale structure with this orientation. It is exposed on the south-eastern corner of Harøen and continues across the entire Nuussuaq Peninsula where it can also be mapped in seismic data. No Eocene basalts crop out to the southeast of the fault zone. Chalmers et al. (1999) suggest about a kilometre of down to northwest throw along the fault, although it is thought to be primarily a sinistral strike slip feature that forms the north-eastern continuation of the Unga-

va fault zone into the Nuussuaq Basin. In the Itilli valley along the southeast edge of the fault, an east plunging anticline has been mapped, and along the northwest edge near the south coast of Nuussuaq, a series of small NW–SE striking normal faults. These structures, compressional to the southeast and extensional to the northwest, are consistent with the local stress field that would be predicted by dominantly left-lateral strike slip. The Itilli Fault is considered a young feature that formed after seafloor spreading and volcanism began. Chalmers et al. (1999) suggest that it formed in the Eocene. Interpretation of apatite fission track data show elevated temperatures near the Itilli fault during the late Eocene (35 Ma). This is interpreted as evidence that the fault was still active at that time (Green et al. 2013). No such elevated temperatures are found of this age to the southeast within the main parts of the Nuussuaq Basin, however, suggesting that tectonic activity at this point was limited to the Itilli Fault.

3.2.8   Additional faults within the basin on Nuussuaq

Chalmers et al. (1999) describe several additional faults within the basin that are thought to only affect the Cretaceous–Paleocene sediments. These are difficult to document, however, because they located in steep ravines that are difficult to access and are covered by scree. A few have been documented primarily along the south coast of Nuussuaq. They are briefly noted here because one has significance for the inversion discussed in the next section. To the west of Kingittok on the south coast of Nuussuaq, Santonian–Campanian sedimentary rocks are found and to the east, sedimentary rocks are Cenomanian in age. This requires a fault, the Kingittok Fault, that is considered by Chalmers et al. (1999) to strike NW-SE with down-throw to the west. The overlying subaerial lavas, however, show down sagging to the east (Pedersen & Dueholm 1992), indicating late Paleocene reversal of motion on the Kingittok fault (Chalmers et al. 1999).

3.3   Possible inversion structures

3.3.1   Evidence for inversion

Detailed photogrammetric mapping of the volcanic marker horizons that make up the Tunoqqu surface (Sørensen 2011) show that the surface, which was sub-horizontal at time of formation, is now segmented into areas of different elevation and structural trends as a result of later tectonic deformation. This is most notable on Nuussuaq where the western part is elevated and in parts highly faulted (Figure 3.11). Around Qunnilik the surface has been uplifted and faulted into many small blocks by numerous faults, so that it now forms an asymmetric anticline with a steeper dipping western limb and a gently dipping eastern limb (Figure 3.12). Measured vertical displacement on faults varies by two orders of magnitude from a few metres to around 100 m, whereas the elevation difference between the axial parts of the syncline and anticline amounts to around 700 m. The limbs of the anticline are coincident with two pre-Tunoqqu extensional faults (K–Q and Fault P) that are oriented obliquely to the Itilli fault.

Additional evidence for inversion is shown in Figures 3.13–3.19. These include a pop-up structure and reverse fault within the Atane formation along the north coast of Disko near Asuk (Figure 3.13); a small anticline observed within the Slibestensfjeldet Fm along the north coast of Nuussuaq and small fault that may have reversal (Figures 3.14, 3.15); a large syncline near faults that show evidence for reversal in a seismic profile offshore north of Nuussuuaq near the Ikorfat Fault (Figure 3.16); and several examples of folding and possible reverse faults on seismic data in the Vaigat (Figures 3.17–3.18). These last examples are along strike of the fold axes mapped in Tunoqqu surface.

3.3.2   Timing of inversion

The exact timing of the inversion is difficult to resolve. However, seismic-stratigraphic interpretation of data offshore West Greenland (Gregersen & Bidstrup 2008) indicates that the offshore areas off central West Greenland experienced a period of inversion in late Paleocene times. It is reasonable to assume that this also marks the onset of inversion in the Disko–Nuussuaq region. The inversion must post-date the deposition of the Naujánguit Member (Vaigat Fm) and probably also post-dates the deposition of the Maligát Fm. The Disko–Nuussuaq region was probably dominated by a NE–SW directed extensional palaeostress regime during the eruption of the Vaigat Fm lavas prior to the inversion. There is a strong clustering of NW–SE directed Vaigat Fm dykes on Disko indicating NE–SW directed extension similar to the direction of the earliest seafloor spreading (Oakey & Chalmers 2012). The latest Paleocene to Eocene of the Disko–Nuussuaq region therefore documents a period of time with marked changes in tectonic regime. These changes can eventually be linked to the rotation of Greenland in the late Paleocene and the opening of the North Atlantic Ocean. Calculation of rotation of Greenland based on palaeostress along the East Greenland margin prior the opening of the North Atlantic Ocean (Guarnieri 2015) predicts an E–W directed compressional palaeostress regime in the Disko–Nuussuaq region during the latest Paleocene. This could potentially be the driving force for the inversion.

Whether the inversion was a short-lived event or took place during a longer period of time is less clear from the present data. In any case the NE–SW trending Itilli fault that is an important strike-slip fault during the Eocene and shows a left-lateral movement that seems to be incompatible with compression along N–S trending faults such as the K–Q fault and other faults that are oblique to the Itilli fault. For this reason the activity of the fault post-dates the tectonic inversion, suggesting a short-lived period for the compressive event.
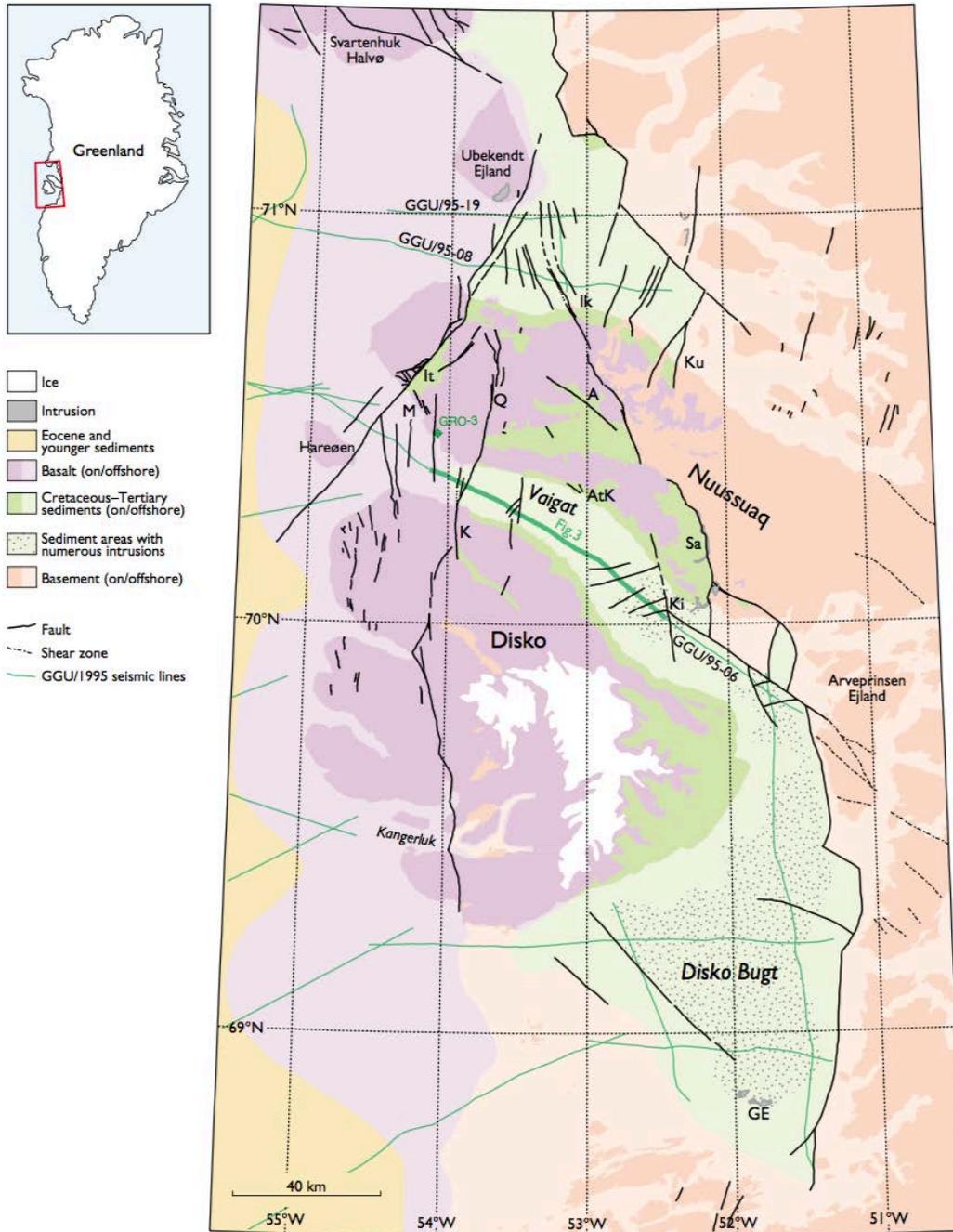
Figure 3.1. *Structural map of the Nuussuaq Basin from Chalmers et al. (1998). Green lines are the 1995 seismic lines. A vectorized version is available in the GIS project. Ik - Ikorfat; Ku - Kuuk; I - Itilli; M - Marraat Killiit; Q - Qunnilik; AtK - Ataata Kuua; A - Agatdalen; Sa - Saqqaqdalen; K - Kuuganguaq; Ki - Kingittoq; GE - Grønne Ejland.*
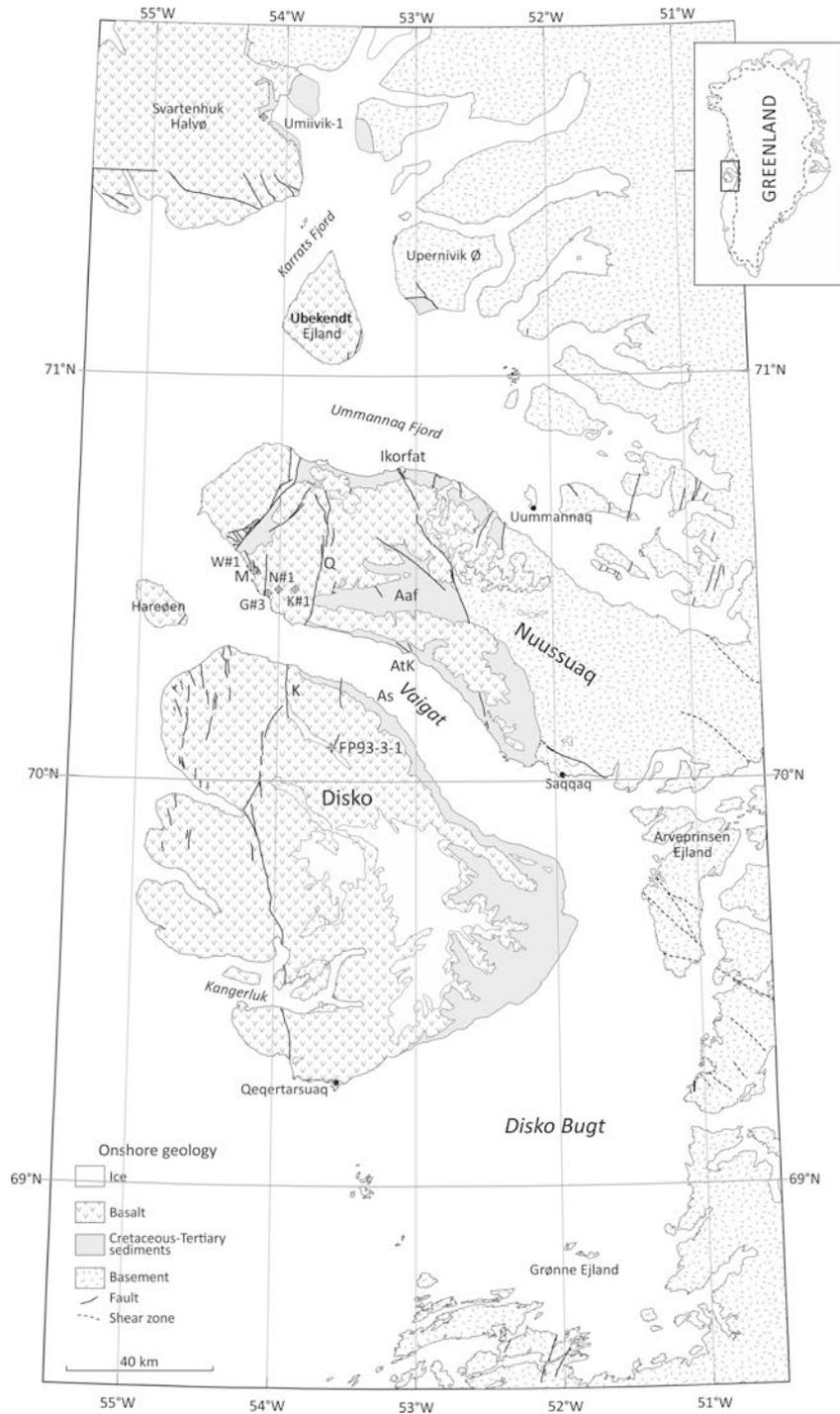
Figure 3.2. *Structural map published in Chalmers et al. (1999). A - Agatdalen; Aaf - Aaffarsuaq; Ap - Appat; As - Asuk; AtK - Ataata Kuua; G#3 - GRO-3 well; Ik - Ikorfat; It - Itilli; K - Kuuganguaq; Ki - Kingittoq; Ku - Kuuk; K#1 - GANK-1 borehole; M - Marraat and the Marraaat-1 borehole; Ni - Niaqornaarsuk; NK - Nuuk Killeq; N#1 - GANE-1 borehole; Q - Qunnilik; Qa - Qaarsut; S - Salleq; Sa - Saqqaqdalen; Tu - Tupersuartaa; W#1 - GANW-1 borehole.*
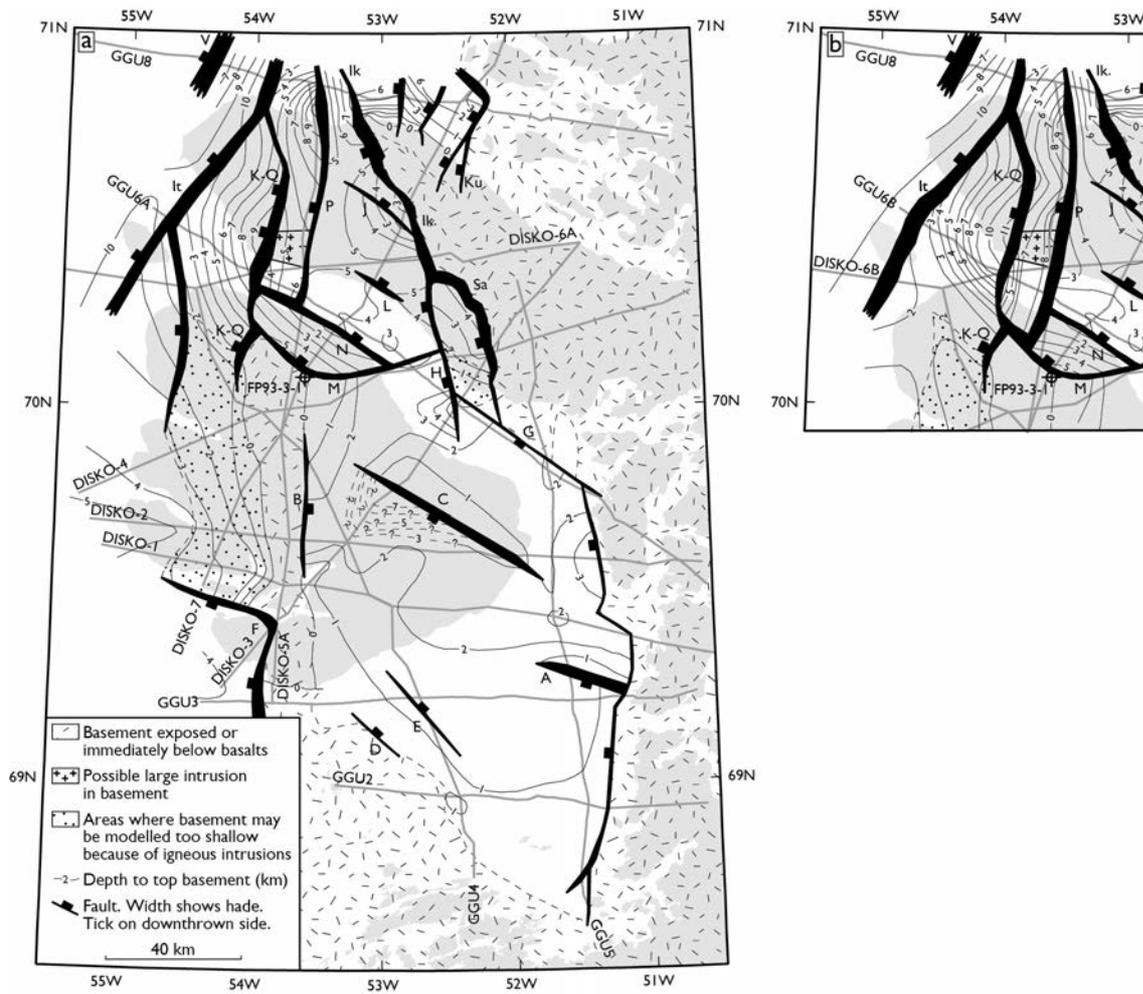
Figure 3.3. *Structural maps from Chalmers et al. (1999) based interpretation of seismic data and gravity modelling. Vectorized versions are available in the GIS project.*
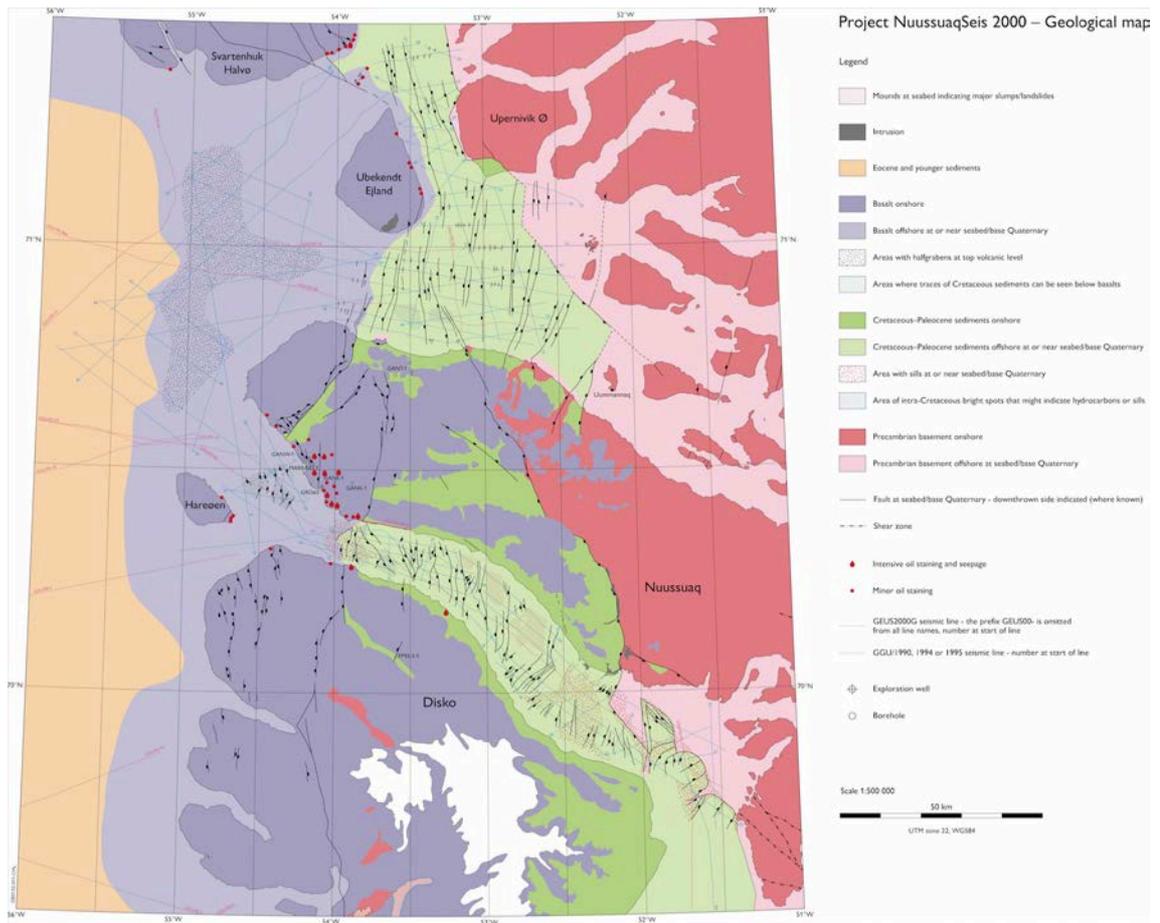
Figure 3.4. *Structural map published in Marcussen et al. (2002) based on interpretation of seismic reflection data collected in 2000. A vectorized version is available in the GIS project and a large scale print is available with the original report.*
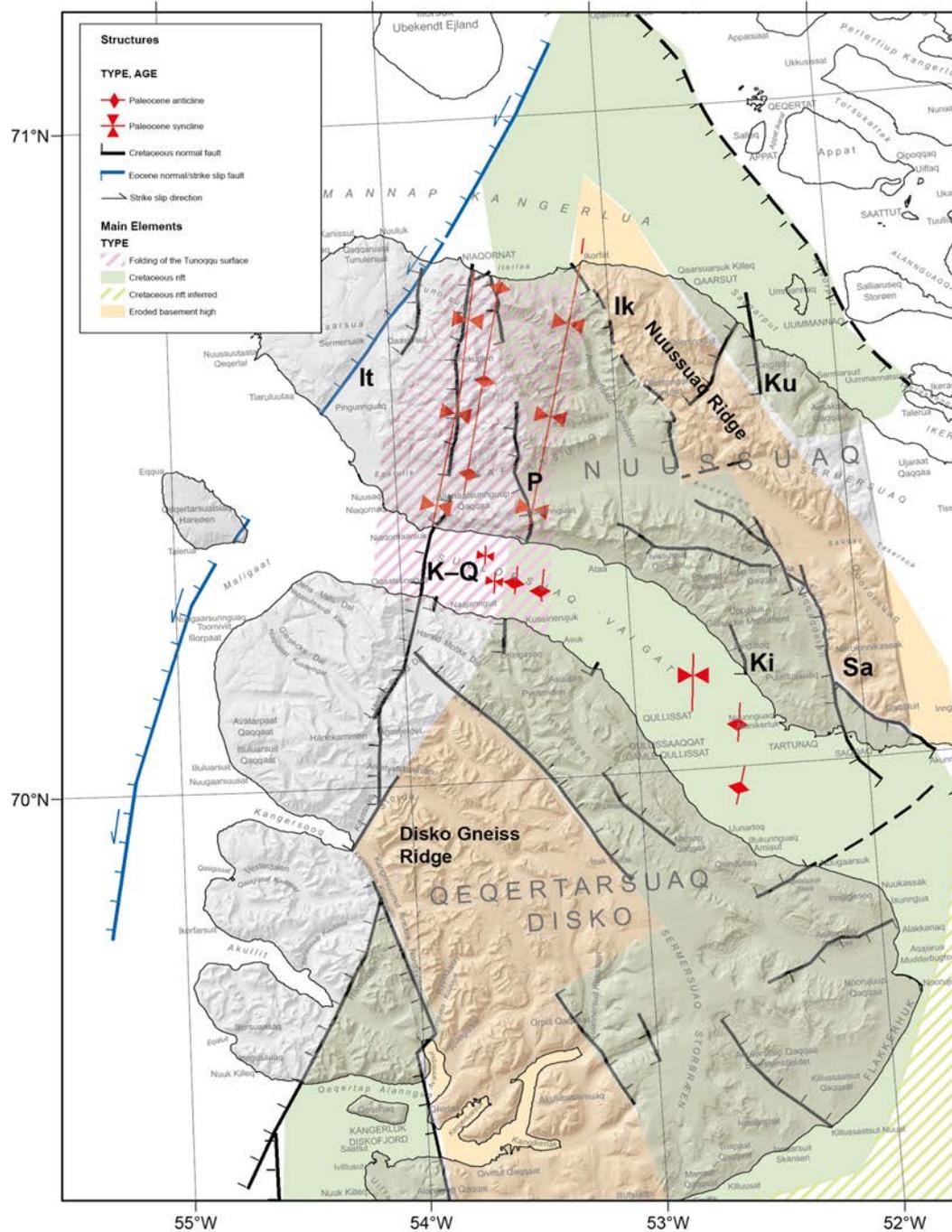
Figure 3.5. *Structural setting of the Cretaceous basins and highs based on this work. The red structures highlight the inversion discussed in the text. Sections 3.2 and 3.3 for complete discussion. Key faults are: Ik - Ikorfat; It - Itilli; K–Q -Kuuganguaq–Qunnilik; Ki - Kingittoq; Ku - Kuuk; P; Sa - Saqqaqdalen.*
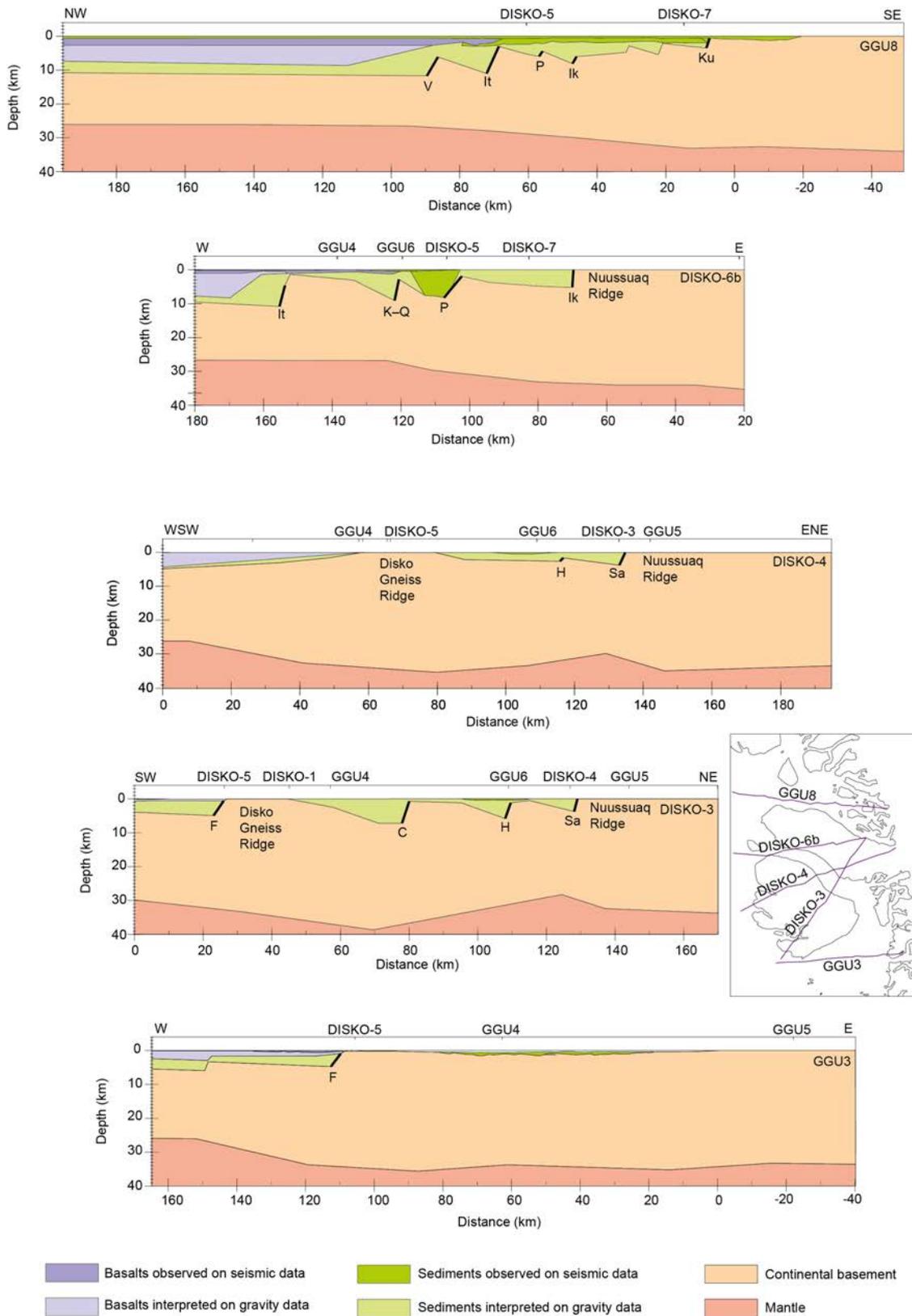
Figure 3.6. *Selected crustal models from Chalmers (1998) highlighting some of the key structures discussed in the text. Note that in general, basins deepen to the NE along SW dipping normal faults. Abbreviations as in previous figures.*
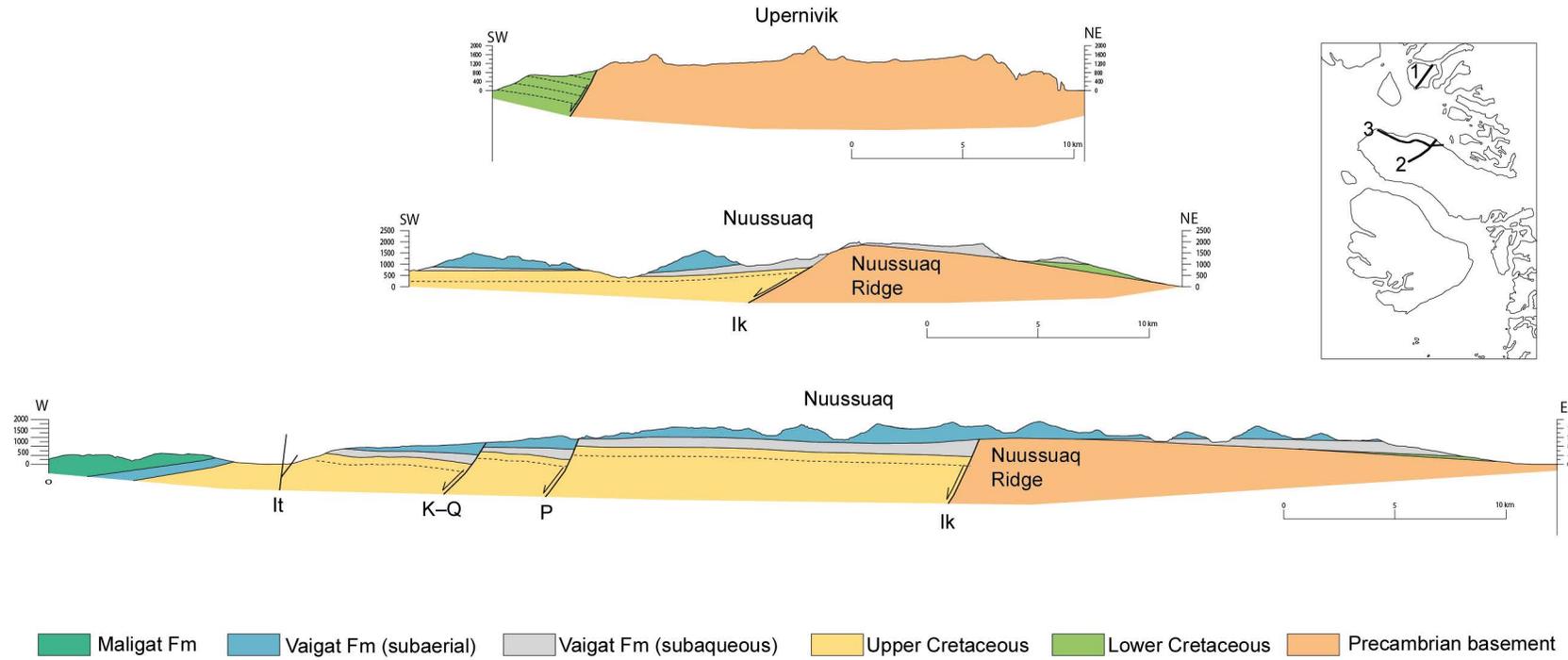
Figure 3.7. *Geological cross sections with no vertical exaggeration to highlight some of the key structural relationships. Note in profile 2 that the lower Cretaceous onlaps the basement, suggesting that the Nuussuaq ridge was a structural high at this time. See also Figure 3.10.*
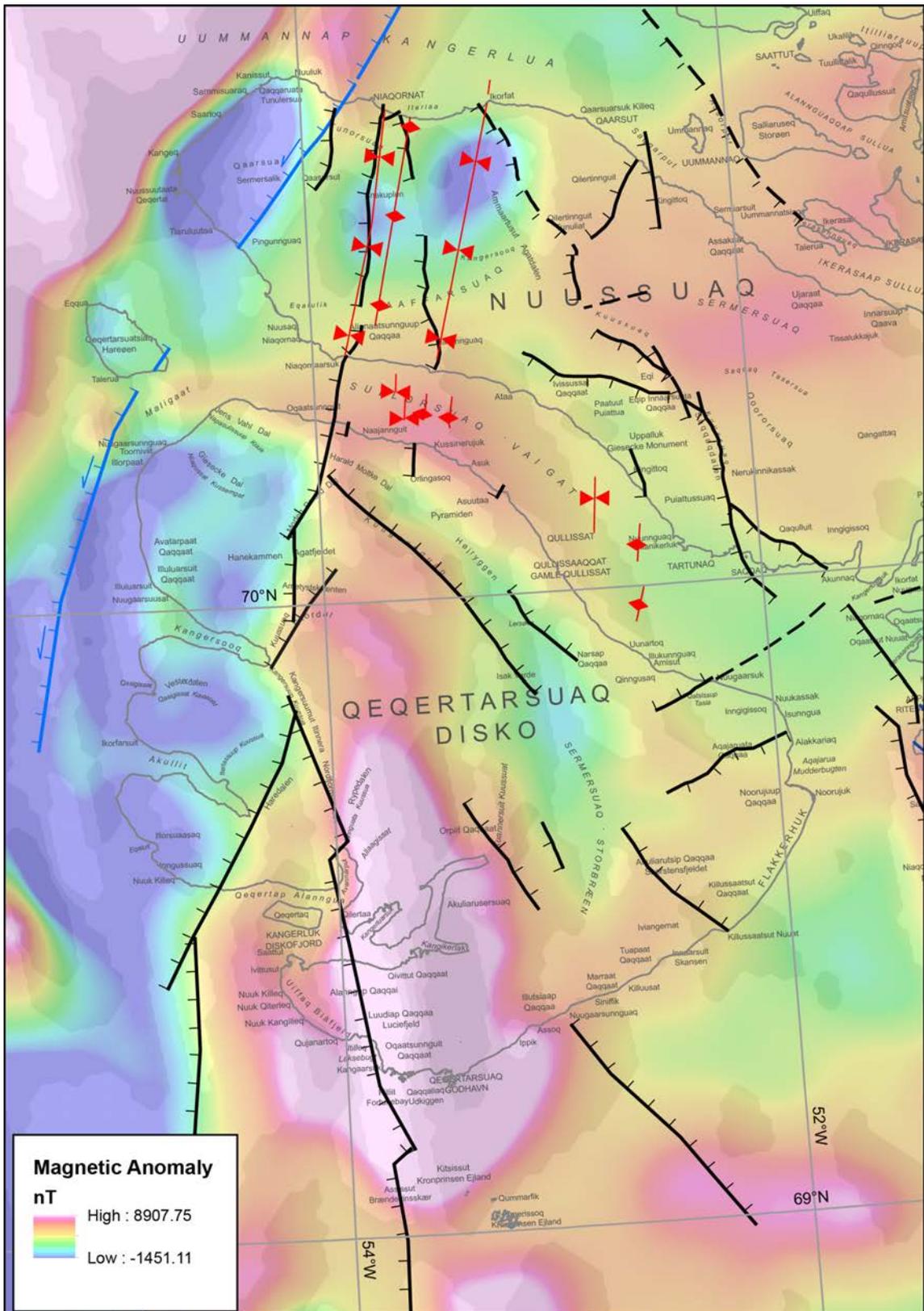
Figure 3.8. *CAMPGM magentic anomaly map (from Gaina et al. 2011). Structures from Figure 3.5 are overlain. See Figure 3.5 legend for structural symbols.*
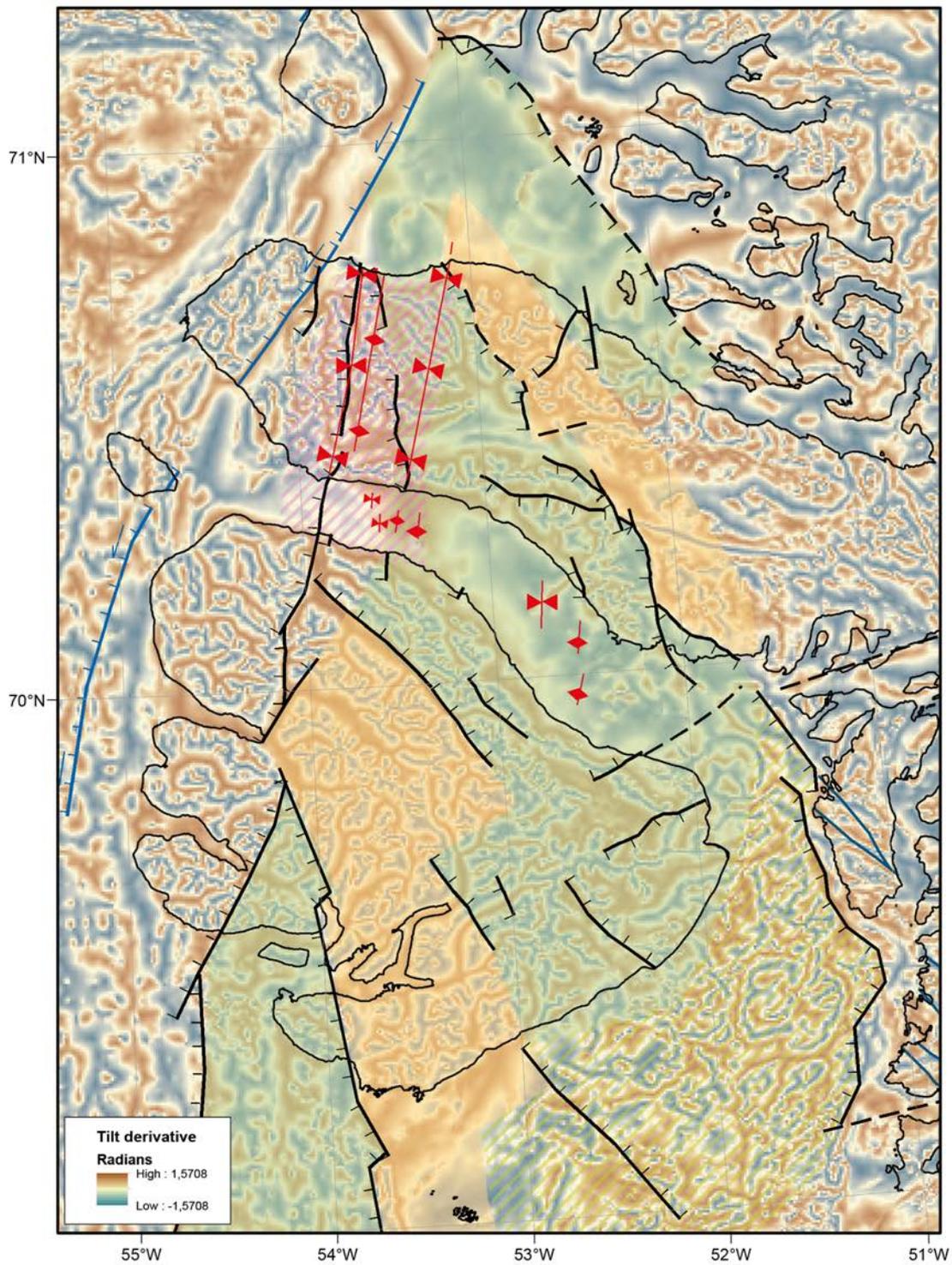
Figure 3.9. *Tilt derivative of the magnetic anomaly. From a high resolution aeromagnetic survey by GEUS in 1997 (Thorning & Stemp 1998) and merged with TGS offshore aeromagnetic data from 2006. See Figure 3.5 legend for structural symbols.*
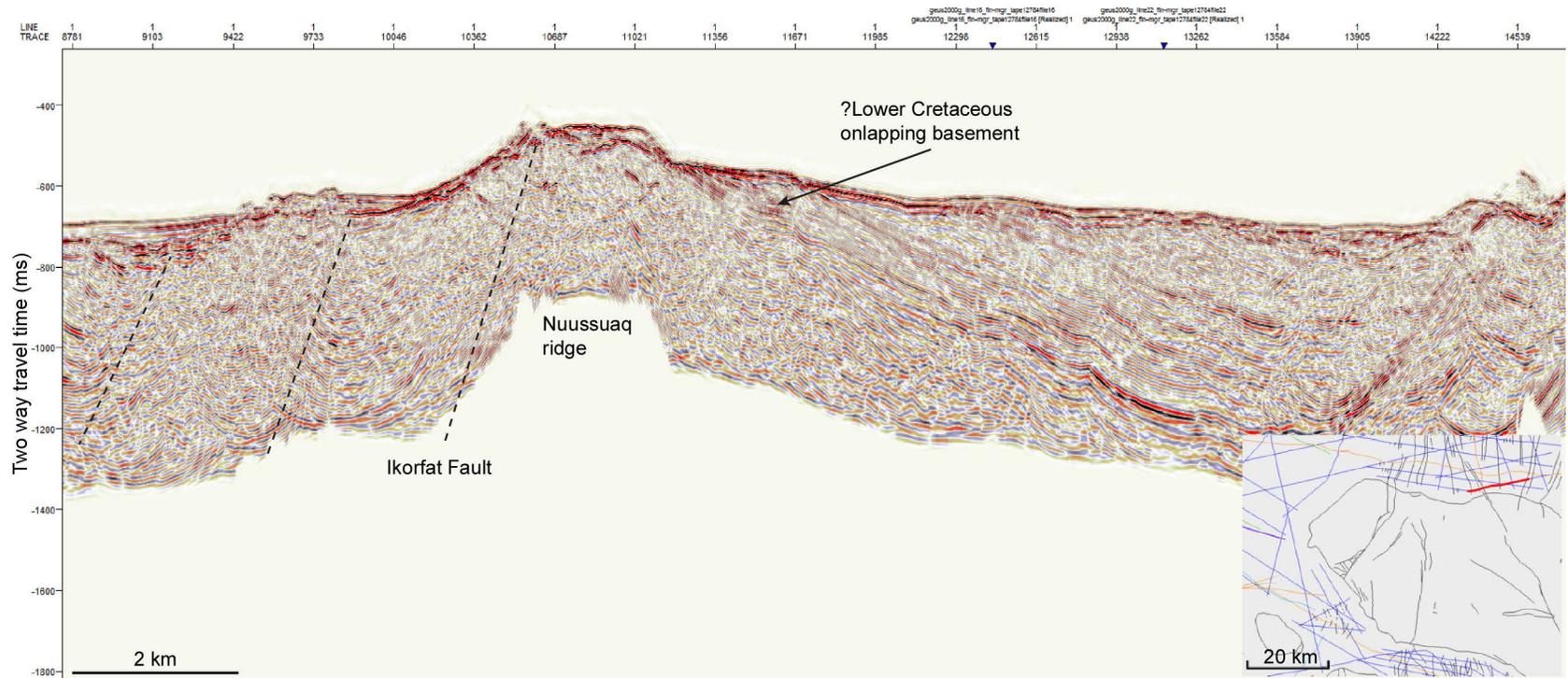
Figure 3.10. *Seismic reflection profile north of Nuussuaq crossing the Ikorfat fault. Note the onlap of ?Lower Cretaceous sediments onto the basement high. Compare to geologic cross section two in Figure 3.7. Red line on map inset shows location of profile.*

West

East
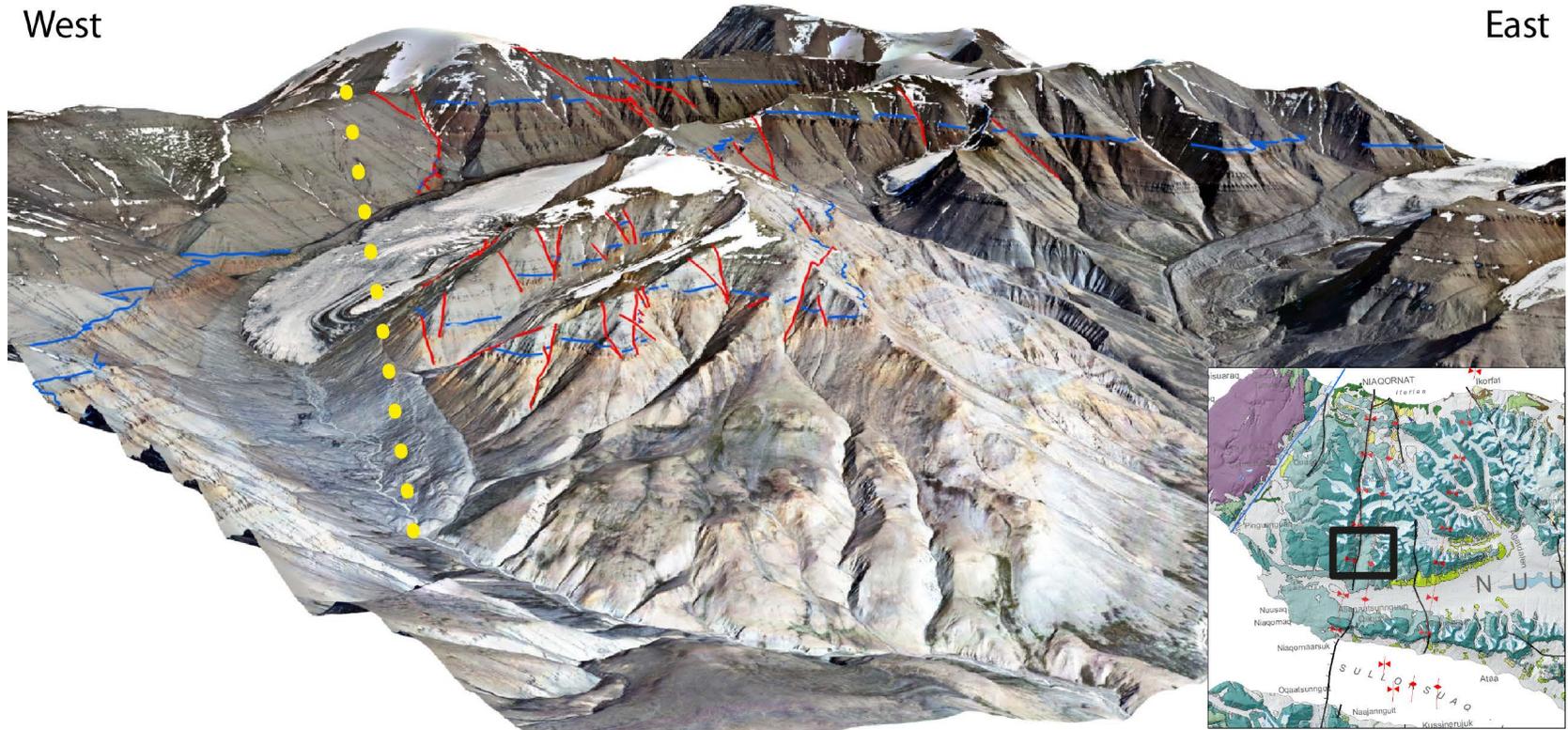
Figure 3.11. *Perspective view of the Qunnilik area on Nuussuaq. The view direction is north and the figure shows a coloured orthophoto draped on a digital terrain model. Blue lines show the outline Tunoqqu Member marker horizon that was mapped while red lines show faults. The yellow dots mark the approximate trace of the Qunnilik Fault. Black box on map inset shows location of the photo. The figure illustrates how the area around Qunnilik in the core of the anticline is also highly faulted.*

East   Disko   West

Kuuganguaq

Nuussuaq

Tunoqqu surface

Sediments

Ikorfat

Itilli fault

20 km
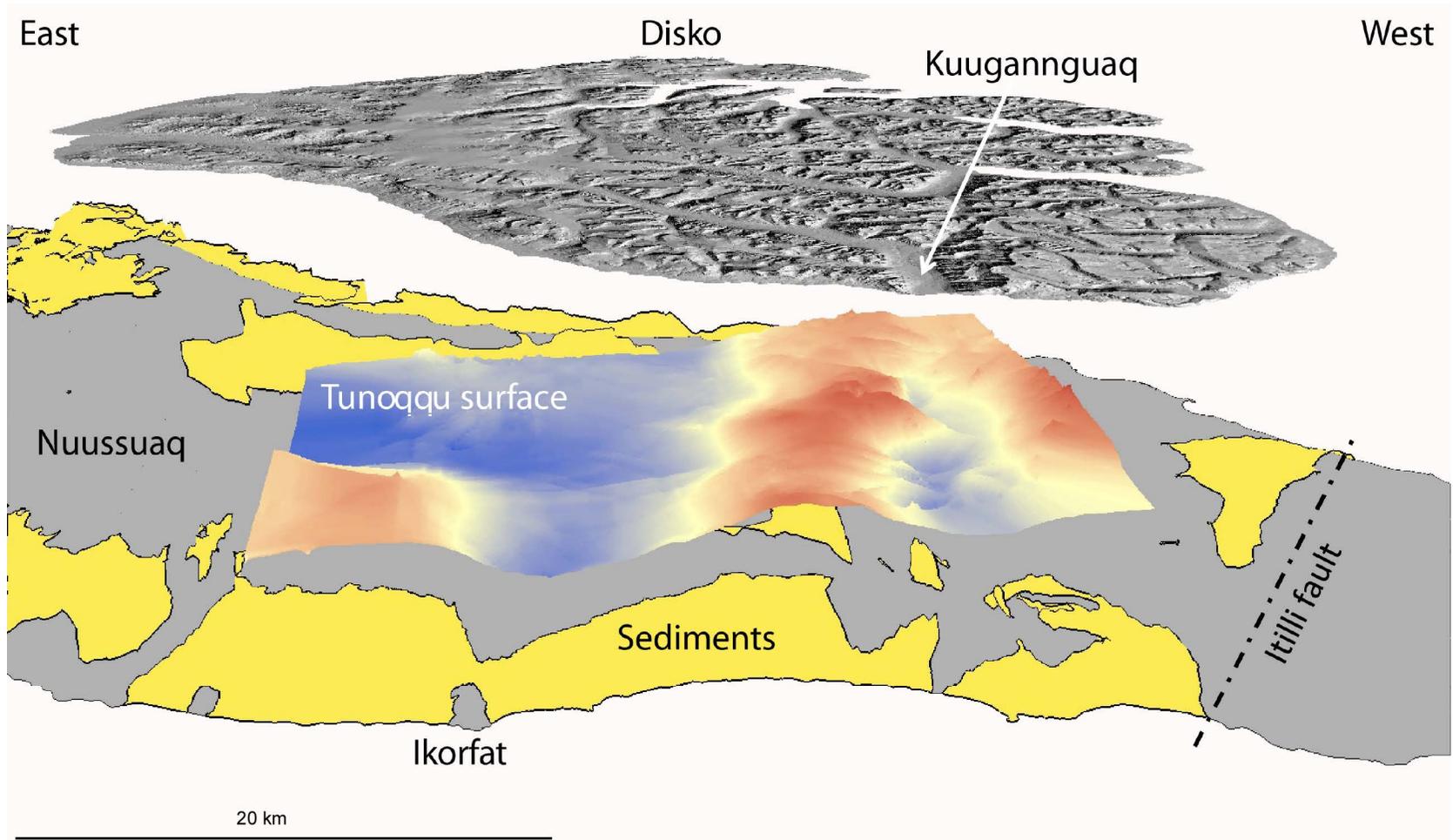
Figure 3.12. *Perspective view of the Tunoqqu Surface on Nuussuaq. The view direction is to the south. Nuussuaq is shown with 4x vertical exaggeration. Yellow coloured polygons show the distribution of sediments on Nuussuaq. The Tunoqqu Surface is an interpolated surface that is based on the photogrammetrically mapped upper limit of the Tunoqqu Member marker horizon on Nuussuaq and Kûgánguaq and Qordlortorssuaq Members on Disko. The surface clearly demonstrates how the once sub-horizontal Tunoqqu Surface now forms an anticline centered on central Nuussuaq. The difference in elevation between the blue colours and red colours is several hundreds of metres.*

Atane Fm
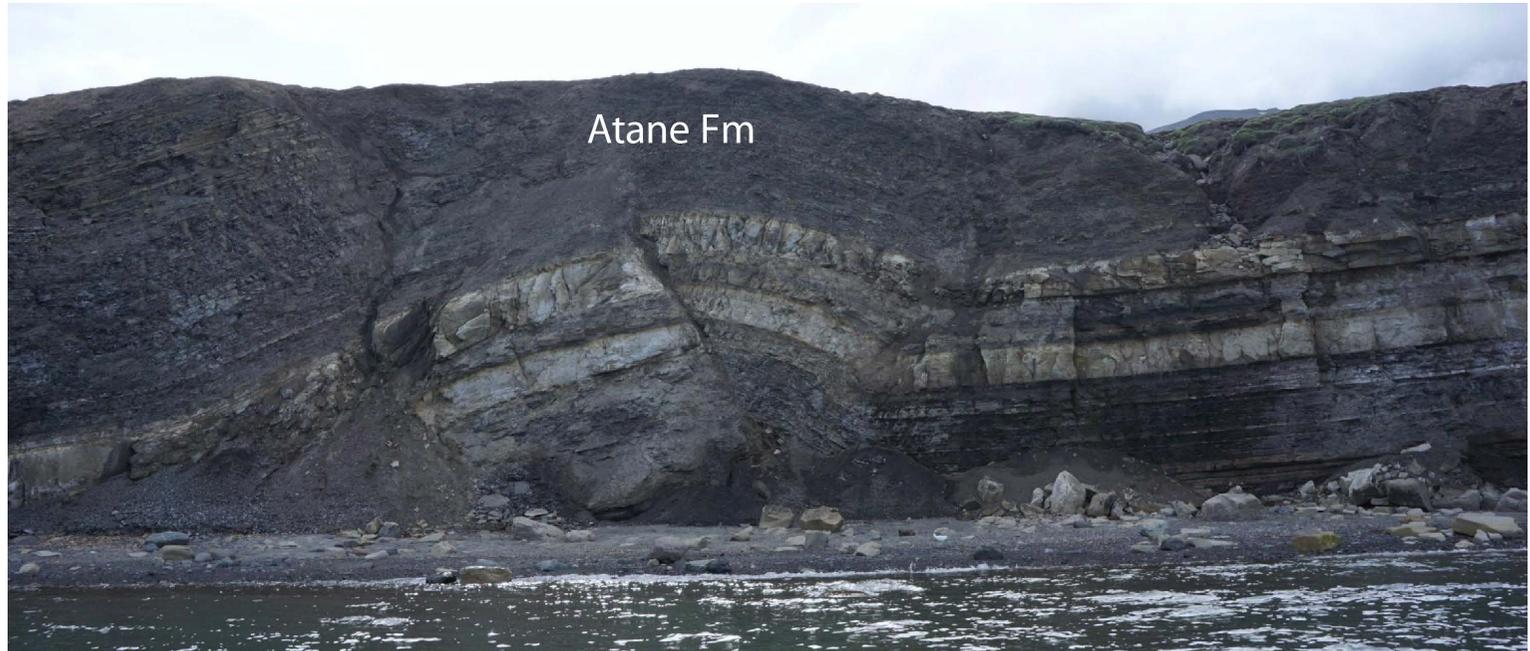
Figure 3.13. *Image from the north coast of Disko around 5 km east of Asuk. The image shows a small reverse fault. There is no clear evidence of deformation of the overlying volcanic rocks higher in the cliff (not shown) which could indicate that the movement on the fault was prior to the deposition of the volcanic rocks or alternatively that the stress related to the compressional movement was absorbed by the volcanic cover without much deformation.*
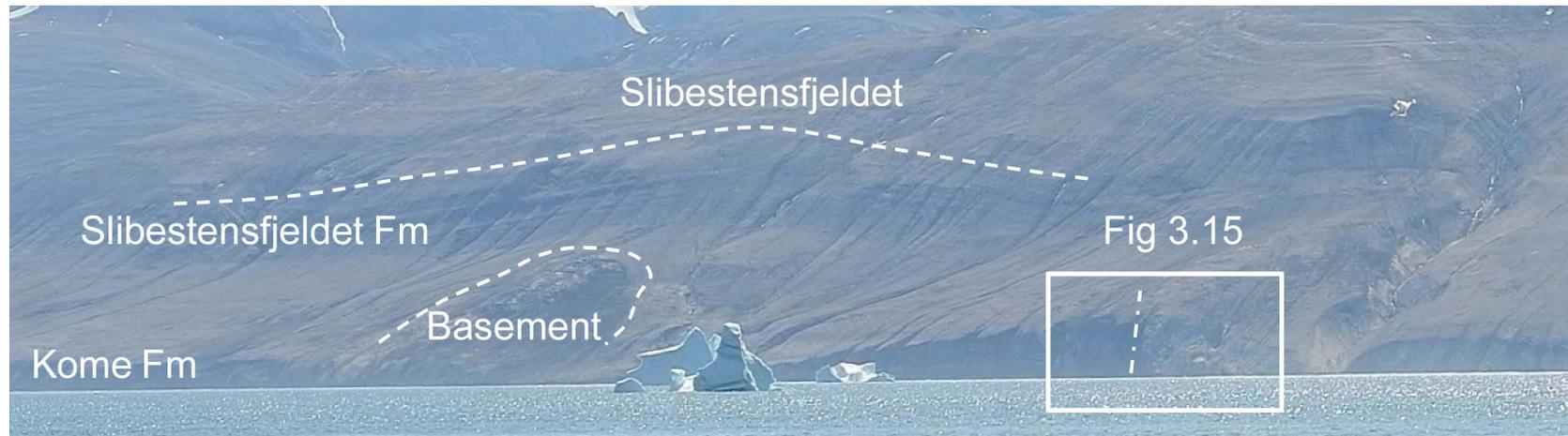
Figure 3.14. *Image showing what could be interpreted as a small inversion structure. The structure is revealed by a small change in dip direction on either side of the basement high exposed in the lower part of Slibestensfjeldet Fm. A larger pre-volcanic fault is observed further to the west as indicated (see also Figure 3.15). The trace of this fault may also be observed in seismic data offshore to the north (Marcussen et al. 2002). The along strike projection of several faults they mapped may intersect the structures here.*
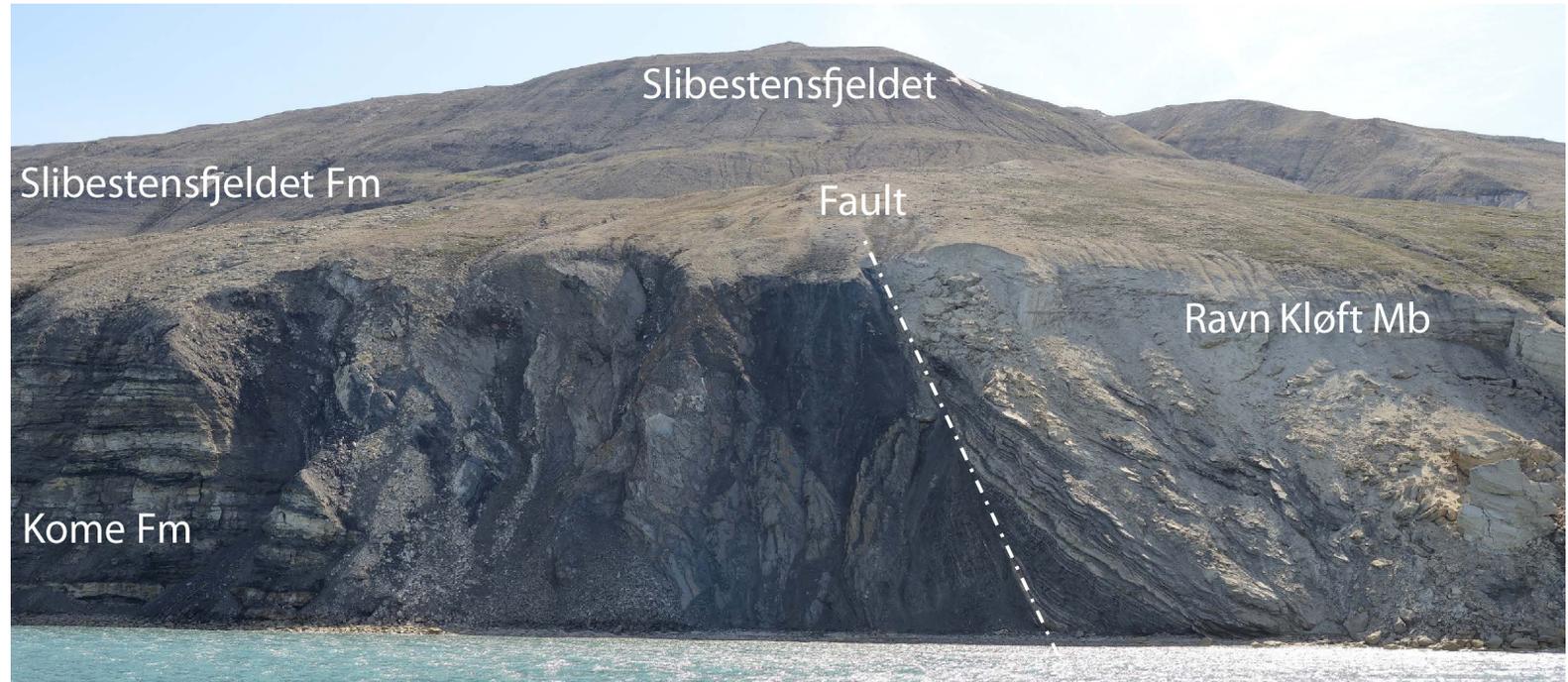
Figure 3.15. *Detail of the fault described in Figure 3.14.*
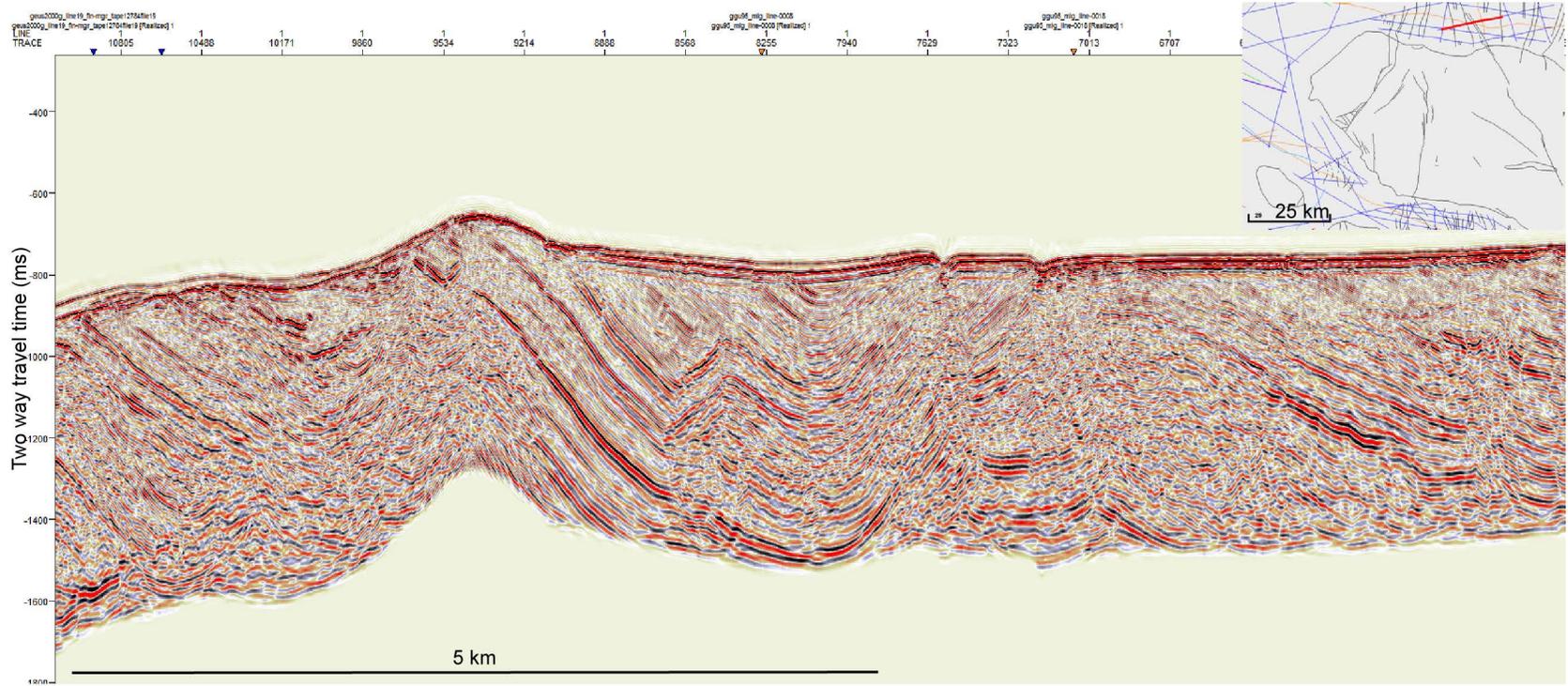
Figure 3.16. *Large syncline structure north of Nuussuaq in offshore seismic reflection data. The eastern limb of appear to merge into a faulted area that could be the northern continuation of the Ikorfat Fault. Red line on map inset shows location of profile.*
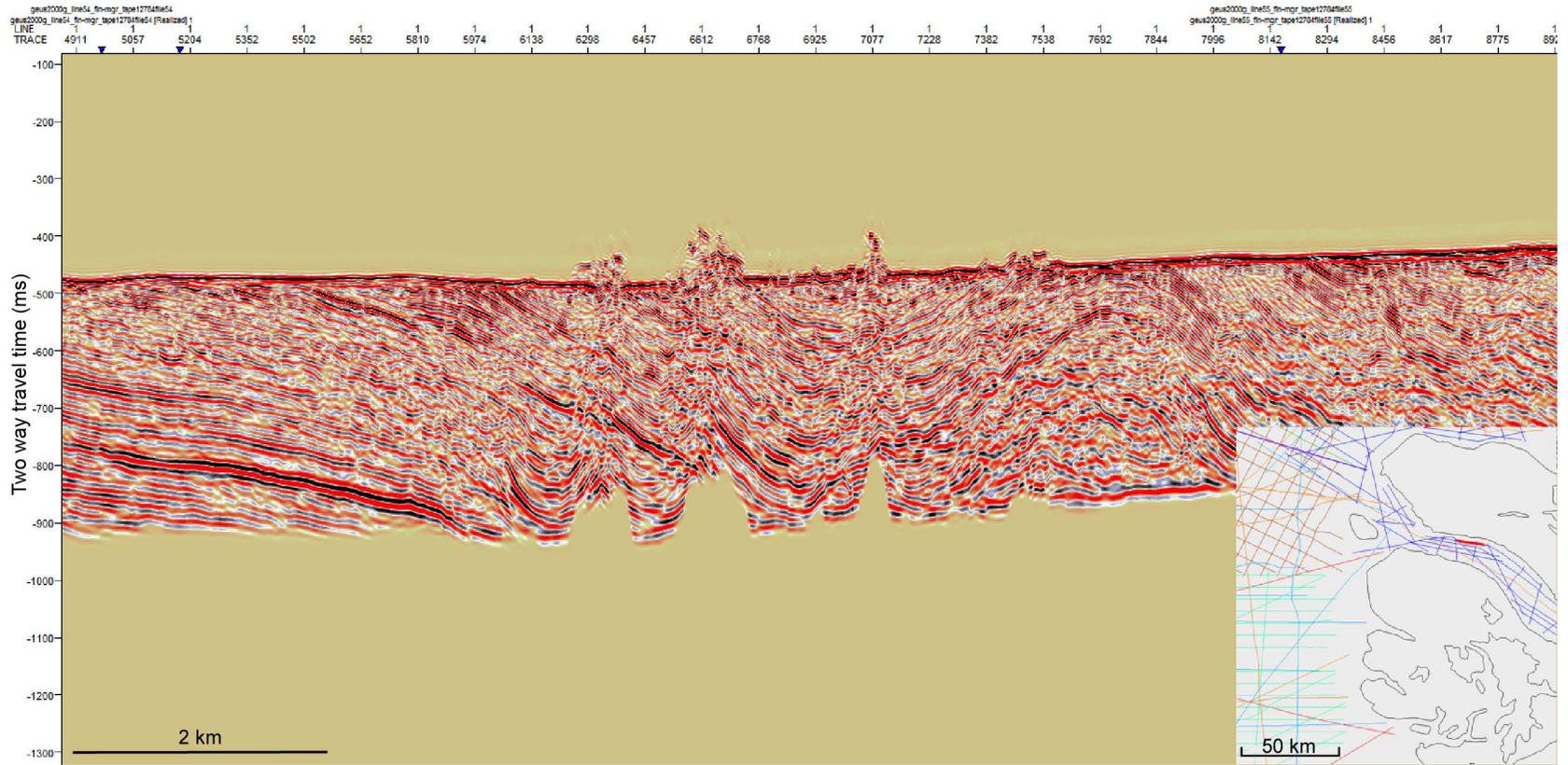
Figure 3.17. *Seismic reflection data from the Vaigat showing folded Cretaceous sediments. Red line on map inset shows location of profile.*
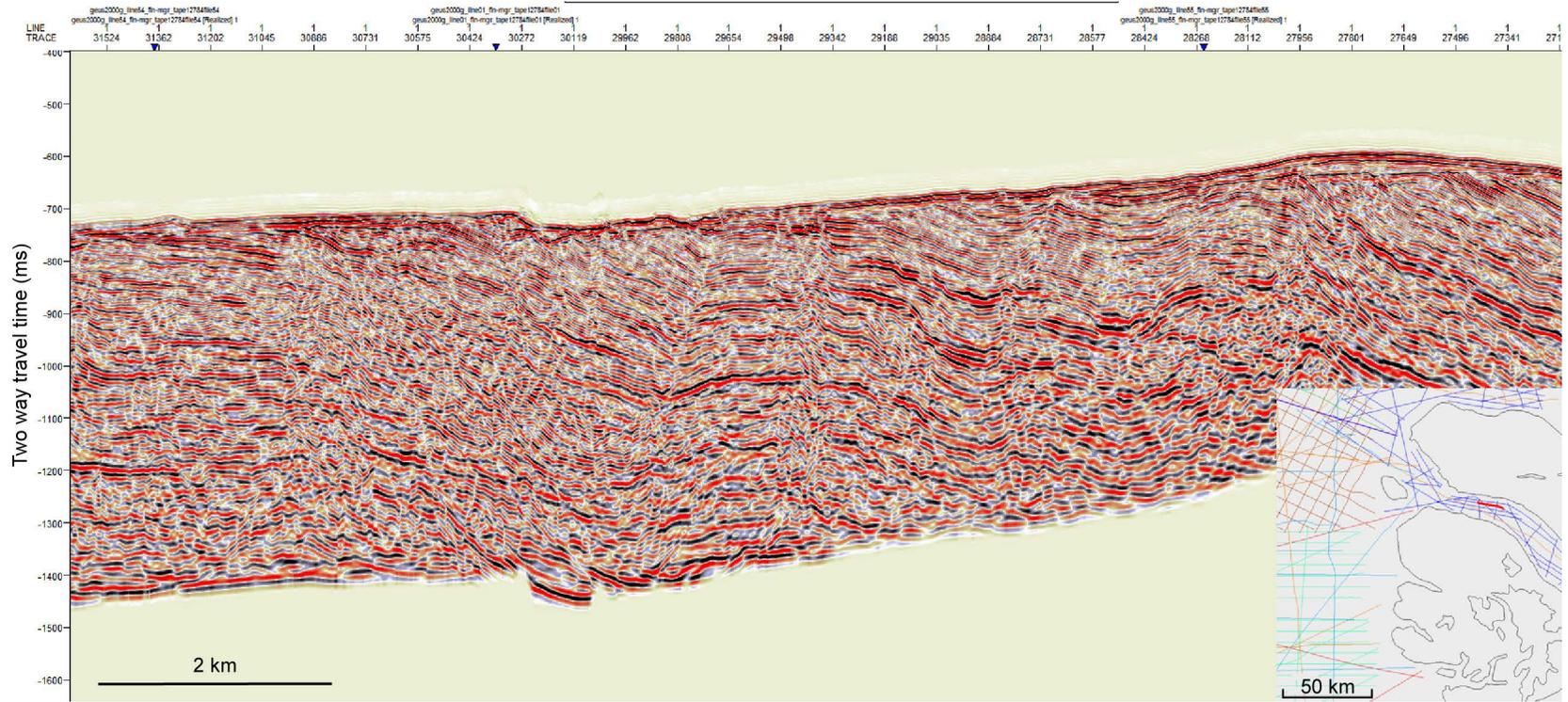
Figure 3.18. *Seismic reflection data from the Vaigat showing folded Cretaceous sediments and several smaller scale reverse faults. Red line on map inset shows location of profile.*
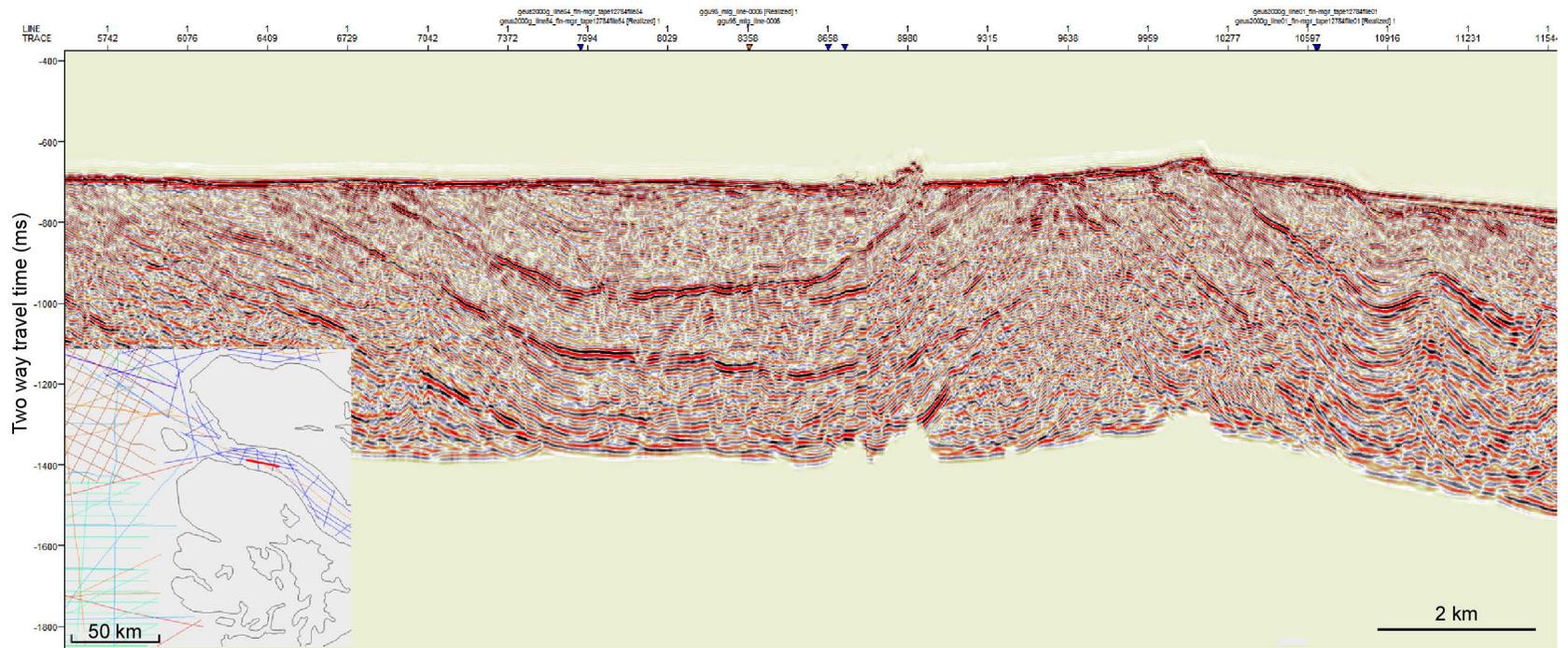
Figure 3.19. *Seismic reflection data from the Vaigat showing a large syncline-anticline structure in the Cretaceous sediments. Red line on map inset shows location of profile.*

4. Sedimentary and volcanic successions of the Nuussuaq Basin

Gunver Krarup Pedersen, Henrik Nøhr-Hansen, & Thomas F. Kokfeldt

4.1   Summary

The sedimentary successions of the Nuussuaq Basin are referred to as the Nuussuaq Group (Dam et al. 2009) and the volcanic successions are referred to as the West Greenland Basalt Group (Clarke & Pedersen 1976, Pedersen 1985, Larsen et al. 2015). The groups are subdivided into 16 formations and 40–50 members (Figures 4.1, 4.2; Dam et al. 2009, Larsen et al. 2015). These papers include references to many of the older studies of the onshore parts of the Nuussuaq Basin. The lithostratigraphy of the offshore area is summarized by Gregersen et al. (2013).

The sedimentary successions are dated mainly on the basis of marine dinoflagellates (Nøhr-Hansen 1996, Nøhr-Hansen et al. 2002, Nøhr-Hansen 2003, Dam et al. 2009, Pedersen & Nøhr-Hansen 2014) and the biostratigraphy of the onshore Nuussuaq Basin is now correlated to the wells offshore Greenland, and to Canadian wells (Fensome et al. 2016, Figure 2.2). Marine invertebrates are generally scarce, but are important in the Danian deposits. Plant macrofossils have been studied in detail (see overview in Dam et al. 2009). The syn-volcanic sediments are dated both biostratigraphically and by their relationship to the volcanic formations. Larsen et al. (2015) presents the radiometric ages of the volcanic successions and shows that the largest volumes of igneous rocks erupted in the late Paleocene (Selandian and Thanetian).

Traces of hydrocarbons have been mapped in western Nuussuaq and five oil types have been identified (Bojesen-Koefoed et al. 1999, 2004; review by F.G. Christiansen). Analyses of the biomarkers indicate that the source rocks include both terrestrial and marine deposits ranging in age from mid-Cretaceous to Paleocene. Most of the hydrocarbon finds have been located in volcanic rocks (hyaloclastites and lavas in the lower part of the volcanic pile), but the available data on the siliciclastic sandstones indicate that these also possess a fair to good porosity. Potential reservoir rocks are discussed in Chapter 5 of this report.

The figures accompanying this chapter include seven maps showing the distribution of the sedimentary formations (Figures 4.4–4.10). Five geological cross-sections have been published by Pedersen et al. (1993, 2002, 2003, 2005, & 2006) and are included in the GIS compilation. A set of schematic diagrams showing the ages of the lithostratigraphic units mapped in the cross-sections are enclosed in the GIS compilation.

This subdivision largely follows the tectonstratigraphic sequences of Dam & Nøhr-Hansen (2001) and Dam et al. (2009, figure 11). The main differences between the TSS-units and the headings in this chapter are:

1. The unconformity between TSS1 and TSS2, i.e., between the Slibestensfjeldet Fm and the Ravn Kløft Mb of the Atane Fm, is included in the section on "Lower Cretaceous" non-marine deposits.

2. The erosional unconformity and the subsequent marine transgression at the base of the Kussinerujuk Mb in northern Disko is described in the section on the mid-Cretaceous marine deposits.

Two phases of incision in the Danian (TSS5, TSS6) are both described in Section 4.9. Descriptions of the sedimentary successions are to a large extent published by Dam et al. (2009), and references within. Newer studies include Pedersen et al. (2013), Pedersen & Nøhr-Hansen (2014), and Fensome et al. (2016).

4.2 The "Lower Cretaceous" succession of non-marine deposits

Albian, and early- to mid-Cenomanian sediments are known from numerous localities. With the exception of the FP93-3-1 borehole, all of these are located in the eastern part of the Nuussuaq Basin. The localities are listed below and are commented upon briefly. The Albian is the uppermost stage of the Lower Cretaceous, and lower- to mid-Cenomanian strata belong formally to the Upper Cretaceous. In the Nuussuaq Basin, however, the Albian to mid-Cenomanian deposits are mainly non-marine and include fluvial, lacustrine, deltaic, and estuarine deposits. A significant change in depositional environments took place in the late Cenomanian. For this reason the lower- to mid-Cenomanian is included in the "Lower Cretaceous" below.

The Precambrian basement, locally deeply weathered, is known from the north coast of Nuussuaq between Kuuk and Ikorfat (Dam et al. 2009, figure 18). Well-exposed boundaries between basement and overlying sediments are few, but the boundary can be inferred from geologic mapping. The crystalline rocks are overlain by non-marine sediments, which are referred to as the Kome, Atane, and Upernivik Næs formations (Table 4.1).

Area	Localities	Contact to basement	Lithostratigraphy	Depos. environment	Age	
North coast of Nuussuaq	Ravn Kløft to Ikorfat		Kingittoq Mb*	Delta plain		Early- to mid-Cenomanian
			Ravn Kløft Mb*	Fluvial to estuarine		late Albian
	Vesterfjeld to Ikorfat (Kussinikassaq)		Slibestensfjeldet Fm	Brackish? water enclosed sea		middle to early late Albian
	Ikorfat	+	Kome Fm	Fluvial to lacustrine	Younger→	late Aptian? early or middle Albian?
	Kuuk Majorallattarfik	+	Kome Fm	Alluvial fan, Floodplain, lacustrine		
East to NE Disko	Kussinerujuk		Kingittoq Mb*	Delta plain		Late Albian–early Cenomanian
	Skansen to Pingu		Skansen Mb*	Fluvial channels		Late Albian–early Cenomanian
	Kuuganguaq valley FP93-3-1	+	Atane Fm	Floodplain		?late Albian to early Cenomanian
SE Nuussuaq	Atanikerluk area		Kingittoq Mb*	Delta plain		middle late Alb–early Cenoman
	E of Saqqaq valley	+	Kome Fm	Fluvial channel		Not dated
Upernivik Næs	Upernivik Næs		Upernivik Næs Fm	Estuarine		middle Alb – middle Cenoman
Qeqertarsuaq	West coast of island	+	Upernivik Næs Fm	Estuarine		as Upernivik Næs

Table 4.1. *Localities with "Lower Cretaceous" sediments, which are interpreted as predominantly non-marine to marginally marine. Members of the Atane Fm are marked by *. See text for further information.*

4.2.1   The Kome Formation

The Kome Fm includes breccias with angular basement clasts and conglomerates overlain by cross-bedded, locally channelized, coarse-grained sandstone, mudstones and thin discontinuous coal beds. Root horizons are frequent and the mudstones commonly contain abundant comminuted plant debris (Schiener 1977, Pulvertaft 1979, Midtgaard 1996b). Fine-grained sandstones with wave-ripples forming upward coarsening successions are common in the Ikorfat area (Midtgaard 1996b, Dam et al. 2009).

The Kome Formation contains macrofossil plants referred to as the Kome Flora (Heer 1883) or to the Ikorfat Flora (Boyd 1998a,b,c, 2000; Dam et al. 2009). Croxton (1978a,b) described a poor assemblage of brackish water dinocysts, spores, and pollen from Majorallattorfik near Kuuk, indicating a middle to late Albian age (Dam et al. 2009). New samples, collected in 2016 at Ikorfat and not yet examined may contribute to the understanding of the difference in palynology between the Kome and the overlying Slibestensfjeldet Fm.

A small outlier of fluvial pebbly sandstones overlies the Precambrian east of the basin boundary fault in the Saqqaq valley (located on geological map 1:250 000; Garde 1994; Garde & Steenfelt 1999). The locality was visited by Pulvertaft (1989a,b), but no material suitable for biostratigraphical studies was found. The age of the sandstones is not established, but the outcrop is tentatively referred to the Kome Formation (Dam et al. 2009).

4.2.2   The Slibestensfjeldet Formation

The Slibestensfjeldet Fm is known only from the north coast of Nuussuaq between Vester-fjeld and Ikorfat, where it overlies the Kome Fm. The boundary between the Kome and the Slibestensfjeldet formations is interpreted as a drowning surface. Just east of Ikorfat (at Kussinikassaq) the formation is dominated by mudstones, which grade into an upward coarsening succession that is erosively overlain by the Ravn Kløft Mb of the Atane Fm. At Vesterfjeld, the Slibestensfjeldet Fm is dominated by fine-grained sandstone with wave-generated structures (Midtgaard 1996a). The sedimentary structures indicate a deposition depth around storm wave-base and deeper.

A series of 24 samples from the 200 m thick section through the Slibestensfjeldet Fm at Kussinikassaq indicates that the palynological assemblages are dominated by spores, pol-len, and charcoal. In addition, the sediments contain the oldest dinocysts known from on-shore West Greenland, represented by a low diversity assemblage of thin-walled cysts. The presence of *Hurlandsia* cf. *rugara,* a few *Nyktericysta davisii* and species of the alga *Tetraporina* support the interpretation of a freshwater depositional environment (Batten & Lister 1988). The abundance of *Pseudoceratium interiorense* and the absence of the pollen species *Rugubivesiculites rugosus* suggest a middle to early late Albian age (Pedersen & Nøhr-Hansen 2014).

The Slibestensfjeldet Fm increases in thickness and becomes increasingly dominated by mudstone from Vesterfjeld toward Ikorfat, indicating a higher rate of subsidence and larger water depths toward the Ikorfat Fault. The palynomorphs indicate a fresh- to brackish water environment, which might be found in a marine embayment with a large influx of fresh wa-ter. Some of the freshwater species reported from the Slibestensfjeldet Formation are also known from Canadian wells in the Hopedale Basin, Labrador shelf (Fensome et al. 2016).

4.2.3   The Ravn Kløft Member, Atane Formation

The Ravn Kløft Mb is a complex unit known only from the north coast of Nuussuaq, where it was studied by Midtgaard (1996b). It includes a large number of sedimentary facies, and overlies an erosional surface with a relief of up to 55 m (Midtgaard 1996b). The member is tripartite, composed of a lower pebbly sandstone unit, a middle unit of mudstones, hetero-liths and fine-grained sandstones with coarsening-upward or fining-upward depositional patterns, and an upper unit of thick-bedded medium- to coarse-grained sandstones inter-bedded with mudstones and heteroliths (Dam et al. 2009). The depositional environment is interpreted as basal fluvial valley fill succeeded by deltaic or tidal estuarine deposits, and overlain by fluvial sandstones, which show an increasing tendency up-section to amalgam-ate and form thick, multi-story sandstone sheets with palaeocurrents toward the NE–N–NW (Midtgaard 1996b, Dam et al. 2009).

The geometry of the Ravn Kløft Mb suggests that it fills a huge incised valley that is related to changes in relative sea level, possibly caused by increased subsidence or eustatic sea level changes. The incision also suggests that large volumes of sediment were transported to offshore areas during the initial phase of valley formation.

Five samples from the lower 30 m of the Ravn Kløft Mb have a palynological assemblage dominated by miospores and charcoal. The low diversity dinocyst assemblage is similar to that of the Slibestensfjeldet Fm. It is represented by the thin-walled brackish water species *Pseudoceratium interiorense, Vesperopsis nebulosa*, *Balmula tripenta*, and *Nyktericysta davisii*. However, the assemblage differs by having reduced numbers of *Pseudoceratium interiorense* and by the common to abundant appearance of *Nyktericysta davisii*. The pollen *Rugubivesiculites rugosus* has its FO at the base of the member. Samples from the upper 300 m of the member yielded very few dinocysts of the species *Vesperopsis nebulosa*. The presence of a few specimens of the megaspore *Balmeisporites glenelgensis* within and at the top of the member, together with a few specimens of *Rugubivesiculites rugosus*, suggests a late Albian age (Pedersen & Nøhr-Hansen 2014).

4.2.4   The Atane Formation in borehole FP93-3-1, NW Disko

In northern Disko the boundary between crystalline rocks and overlying sediments is recorded in cores from the borehole FP93-3-1 in the Kuugannguaq valley. A sedimentological log of the core is shown in figure 19 of Dam et al. (2009). The sediments are considered as part of the Atane Fm, but which member is not clear. The palynomorphs indicate a terrestrial environment in the lower part of FP93-3-1 overlain by brackish water deposits (Pedersen & Nøhr-Hansen 2014).

Twenty-one samples from borehole FP93−3−1 demonstrate that the oldest sediments on northern Disko are of ?late Albian to early Cenomanian age, which is slightly younger than the middle to late Albian sediments of the Kome Fm, which overlies the basement at Majorallatarffik, northern Nuussuaq. The palynological assemblages are dominated by the pollen *Rugubivesiculites rugosus* and the dinocyst *Nyktericysta arachnion* is present in the lower part and becomes common upward, similar to observations from the nearby Kamaffiaraq section through the Kingittoq Mb (Pedersen & Nøhr-Hansen 2014).

4.2.5   The Skansen Member, Atane Formation

The Skansen Mb is known from eastern Disko and is characterized by thick fluvial sandstones overlain by thin units of mudstones locally with thin coal beds. Palaeocurrent measurements from eastern Disko suggest sediment transport directions to the NW (Pedersen & Pulvertaft 1992). The lower boundary of the Skansen Mb is not known. Seismic data south and east of Disko (Chalmers et al. 1999) indicate that the depth to basement exceeds 2 km, suggesting that the Skansen Mb may reach considerable thickness in the subsurface. The Skansen Mb is overlain by the syn-volcanic, non-marine Atanikerluk Fm, and by volcanic rocks of the Rinks Dal Mb of the Maligât Fm. The relationship is shown diagrammatically in figure 131 of Dam et al. (2009).

Macroflora, spores and pollen are known from the Skansen Mb (Koppelhus & Pedersen 1993, Dam et al. 2009). The member is dated on the basis of spores and pollen. At its type locality, a mid-Cenomanian age seems most likely; with a maximum age range of late Albian to Cenomanian for the palynomorph assemblage (Dam et al. 2009).

4.2.6   The Kingittoq Member, the Atane Formation

The Kingittoq Mb is characterized by 10–25 m thick depositional cycles, which include coarsening-upward successions of mudstones, heteroliths and well-sorted sandstones. The mudstones are grey, silty, carbonaceous and may be interbedded with coal beds. The sandstones are friable, and range from fine- to coarse-grained, locally with thin pebble horizons. The ratio between sandstones and mudstones varies between the localities.

Four facies associations are recognized: 1) a delta front association characterized by coarsening upward heterolithic sandstones with wave-generated structures; 2) a distributary channel association characterized by thick, cross-bedded or structureless sandstones; 3) a delta-plain association dominated by mudstones with thin sandstone and coal beds' and 4) a shore-face association with a thin sandstone unit overlying a marine erosional surface. Plant macrofossils, spores and pollen are known from the Kingittoq Mb (Dam et al. 2009, Pedersen & Nøhr-Hansen 2014).

The Kingittoq Mb at Atanikerluk was studied by Lanstorp (1999) in samples from two sections, Tartunaq and Atanikerluk, collected by C. Croxton (C1, C3 and C14 in Croxton 1976, 1978a) and K. Raunsgaard Pedersen (A1–A5), pers. comm). Lanstorp (1999) assigned the spores and pollen assemblages to one biozone, which has two subzones:

Tartunaq (C3/A1, A2, A3) • *Rugubivesiculites rugosus – Retitricolpites georgensis* Assemblage-Zone, *Cycadopites* Subzone (middle-late Albian age).

West of Atanikerluk (A4, A5) • *Rugubivesiculites rugosus – Retitricolpites georgensis* Assemblage-Zone, *Tricolporopollenites* Subzone (early Cenomanian age).

The Kingittoq Mb overlying the Ravn Kløft Mb (North coast of Nuussuaq between J.P.J. Ravns Kløft and Ikorfat; see Dam et al. 2009, figure 22 for location) is not well known. A few samples from the Kingittoq Mb, representing the upper 50 m of the C8 Kussinikassaq section, previously examined by Croxton (1976, 1978a), yielded neither dinocysts nor other palynological marker species; however, an increase in the pollen species *Rugubivesiculites rugosus* through this section may be of stratigraphic value (Pedersen & Nøhr-Hansen 2014).

The Kingittoq Mb at Kussinerujuk was tentatively dated as Cenomanian by D.J. McIntyre (personal communication 1997) based on the record of abundant *Rugubivesiculites rugosus, Parvisacites radiatus* and a small gemmate of undescribed *Rugubivesiculites* species, which is indicative for the Cenomanian in Western Canada (D.J. McIntyre personal communication 1997). From the lowermost part of the section, Nøhr-Hansen subsequently recorded a few specimens of the pollen species *Rugubivesiculites multisaccus*, also suggesting an early Cenomanian age (Singh 1983), as well as the FO of the brackish water dinocyst indicator *Nyktericysta arachnion* in the upper part of the Kingittoq Mb. The presence of *Nyktericysta arachnion* suggests a late Albian age according to Bint (1986); however, the fact that *Nyktericysta arachnion* seems to have a FO above the FO of *Rugubivesiculites multisaccus,* indicates that the FO of *Nyktericysta arachnion* may be a lower Cenomanian marker in West Greenland (Pedersen & Nøhr-Hansen 2014).

Further west, along the south coast of Nuussuaq (Qallunnguaq and Kingittoq), the Kingittoq Mb is younger than at Atanikerluk and includes a larger proportion of delta front deposits where marine palynomorphs are encountered more frequently. These localities occupied a more seaward position within the delta complex relative to Atanikerluk.

4.2.7   The Upernivik Næs Formation

The Upernivik Næs Fm is known from Upernivik Ø, Qeqertarsuaq, and Itsaku (Larsen & Pulvertaft 2000; Dam et al. 2009, figures 35–36). The formation is dominated by sandstones and was divided into four facies associations by Midtgaard (1996b; see also Dam et al. 2009, figure 34). These include: 1) A coarse-grained, poorly sorted sandstone up to 34 m thick with basal channel lags of pebbles (crystalline rocks), mudstone clasts and coalified wood. Cross-bedding indicates westerly palaeocurrents and soft sediment deformation is common. The sandstones are interpreted as deposited in braided fluvial channels. 2) A well-sorted, fine- to medium-grained sandstone with abundant mudstone clasts locally has mud-draped foresets and show bundled lamination. Cross-bedding indicates palaeocurrents to the north. Mud-dominated heteroliths and mudstones contain much comminuted plant debris; bioturbation varies from moderate to intense. The heterolithic, burrowed sandstones are interpreted as estuarine deposits. 3) A very fine- to very coarse-grained sandstones interbedded with mudstones in 3−8 m thick successions. Sandstone dykes are common and gentle folding indicates that they were intruded before or during compaction. These facies are interpreted as coastal plain deposits. 4) A coarsening-upward succession comprising black fissile mudstones, heterolithic mudstones and sandstones, and trough cross-bedded sandstones with comminuted plant debris, which may represent bay-head delta deposits (Midtgaard 1996b).

The Cretaceous boundary fault system is mapped in eastern Svartenhuk and several phases of subsidence, uplift and erosion are identified between the Albian and the late Paleocene (Larsen & Pulvertaft 2000, figure 7). The boundary between the Precambrian crystalline rocks and the Upernivik Næs Fm at Upernivik Næs and western Qeqertarsuaq was described by Rosenkrantz & Pulvertaft (1969). The locality where conglomeratic sandstones are in contact with basement, indicating the presence of a fault escarpment, is shown in figure 3C in Rosenkrantz & Pulvertaft (1969) and in figure 34 in Dam et al. (2009).

Macroplant fossils suggest that the Upernivik Næs flora is contemporaneous with the middle–late Albian and earliest Cenomanian Ravn Kløft flora of Boyd (1998c). The results of a new palynological study of samples from the Upernivik Næs Fm are reported by Pedersen & Nøhr-Hansen (2014). A low diversity dinocyst assemblage from the lower part of the section suggests correlation with the lower part of the Ravn Kløft Mb, indicating a late Albian age. A few specimens of the large species of *Nyktericysta davisii* have been recorded higher up, suggesting an early to middle Cenomanian age for the upper part of the section (Pedersen & Nøhr-Hansen 2014).

4.3 The mid-Cretaceous marine deposits

4.3.1   The erosional unconformity at Kussinerujuk

The erosional unconformity at Kussinerujuk was first described by Pulvertaft & Chalmers (1990). The erosional surface has a marked relief and may be traced from Kussinerujuk eastwards to Asuk (5 km). It separates the Kingittoq Mb (Atane Fm) from the Kussinerujuk Mb (Itilli Fm) (Dam et al. 2009, figures 77–80). The deltaic deposits of the Kingittoq Mb are exposed in gullies at Kussinerujuk (Pulvertaft & Chalmers 1990) and in the coastal cliff at Asuk. Palynological studies indicate a late Albian–early Cenomanian age.

The Kussinerujuk Mb comprises mudstone clast conglomerates interbedded with thin mudstone or sandstone beds. The mudstone clasts are angular to rounded and range from boulder- to pebble size at Kussinerujuk. At Asuk this facies is subordinate and the member is dominated by mudstones interbedded with thinner sandstone beds. The oil-stained sand at Asuk is part of the Kussinerujuk Mb. The Kussinerujuk Mb contains marine dinocysts.

Palynology. McIntyre (1994a,b, personal communication 1997) studied 10 samples from the Kussinerujuk Mb above the unconformity at Kussinerujuk. These samples contain abundant *Rugubivesiculites rugosus* and abundant *Quadripollis krempii*, accompanied, in some samples, by a few specimens of the gemmate undescribed *Rugubivesiculites* sp., which suggests a Cenomanian age. Recent studies of the same section revealed a few dinocysts, including the marine *Isabelidinium magnum*, suggesting a late Cenomanian age; further up the section a moderately diverse marine assemblage with *Cauveridinium membraniphorum, Isabelidinium magnum, Odontochitina operculata, Surculosphaeridium longifurcatum*, and *Trithyrodinium suspectum* indicates a late Cenomanian age (Pedersen & Nøhr-Hansen 2014).

The oil-seep section at Asuk represents 90 m of the Kussinerujuk Mb, dated as late Albian–late Cenomanian based on the study of twenty palynological samples (Nøhr-Hansen 2006; Bojesen-Koefoed et al. 2007). The lower 6 m of the interval is dominated by the pollen *Rugubivesiculites rugosus*. The acritarch or schizosporous algal *Paralecaniella indenta* is common. The brackish water dinocyst indicators *Nyktericysta* sand *Quantouendinium* soccur together with the more marine indicators *Circulodinium* sp., *Odontochitina ancala* and *Oligosphaeridium* sp., *Spiniferites* sp., and *Subtilisphaera kalaalliti*, indicating a ?late Albian/early Cenomanian age. The upper part of the Asuk section is dated as late Cenomanian based on the presence of *Trithyrodinium suspectum, Isabelidinium magnum*, *Isabelidinium* spp., *Palaeohystrichophora infusorioides* and *Surculosphaeridium longifurcatum*, common *Rugubivesiculites rugosus*, and the absence of *Heterosphaeridium difficile* (Pedersen & Nøhr-Hansen 2014).

The palynological data thus indicate that the erosional relief was created and overlain by the Kussinerujuk Mb during the late Cenomanian. This unconformity has not been identified at other outcrops.

4.3.2   A late Cenomanian – early Turonian marine transgression

The marine transgression at the base of the Kussinerujuk Mb (above the unconformity at Kussinerujuk and Asuk) may be co-eval with the globally recognized, late Cenomanian OAE2 (Oceanic Anoxic Event 2). Observations in support of this include:

- a mudstone section within the Ikorfat Fault Zone (samples 358361–366);

- recognition of OAE-2 at Ellesmere Island (Kanguk Fm);

- the succession in the Umiivik-1 well.

Steeply dipping mudstones within the Ikorfat Fault were sampled by F.G. Christiansen on a reconnaissance trip in 1992 (samples 358361–366). The samples contain the oldest marine dinocyst assemblage, thus indicating the oldest known marine transgression on the north coast of Nuussuaq. A Cenomanian to Turonian age is suggested for the six mudstone samples based on the presence of common to abundant *Rugubivesiculites rugosus* pollen. An early or middle Cenomanian age is now suggested for sample 358364 based on the presence of *Palaeohystrichophora infusorioides* and a large specimen of *Nyktericysta davisii* as well as the absence of *Isabelidinium magnum*. This sample was incorrectly referred to as Turonian in Dam et al. (2009, p. 50). Samples 358361–363, and −365 are dated late Cenomanian based on the presence of a few specimens of *Isabelidinium* spp., *Isabelidinium magnum*, *Wrevittia cassidata*, and *Cauveridinium membraniphorum*. Sample 358366 has a diverse assemblage characterized by *Heterosphaeridium difficile, Chatangiella* species, and *Trithyrodinium suspectum*, which suggests a Turonian age (Pedersen & Nøhr-Hansen 2014). The six samples in the flexural dip are overlain by upper Maastrichtian mudstones with ammonites (Birkelund 1965; Kennedy et al. 1999).

Oceanic anoxic events (OAEs) have been studied extensively since their recognition by Schlanger & Jenkyns (1976). The Cenomanian–Turonian (~94 Ma) oceanic anoxic event (OAE2) is one of the largest carbon cycle perturbations in Earth history, resulting in the extensive formation of petroleum source rocks (Lenniger et al. 2014). The black shales in the Kanguk Fm (May Point succession, Axel Heiberg Island) have been suggested to be related to OAE2 based on lithological similarities (high total organic carbon and high hydrogen index), relative stratigraphic position, and broad biostratigraphy. Lenniger et al. (2014) studied the geochemistry and biostratigraphy of the lower 70 m of the Kanguk Fm in the May Point succession and concluded that the papery shales were deposited in an anoxic environment. The very significant organic-carbon burial was synchronous with OAE2 and was likely driven by a globally enhanced nutrient flux. It is possible that similar depositional environments may have existed elsewhere in the Arctic (Lenniger et al. 2014).

The Umiivik-1 well was drilled in 1995 and is fully cored to a depth of 1200 m. The sand-streaked mudstones constitute the type section of the Umiivik Mb of the Itilli Fm. Due to the thermal influence from igneous intrusions no palynomorphs are preserved below 540 m (?late Turonian; see Dam et al. 1998). The prime objective of Umiivik-1 was to document oil-prone source rocks in mid-Cretaceous strata. The most likely candidate was a Cenomanian–Turonian marine source rock, supported by data on the Kanguk Fm at Ellesmere Island (Núñez-Betelu 1994, Lenniger et al. 2014). The lower boundary of the Itilli Fm was not reached in the well.

The boundary between the Upernivik Næs Fm and the Umiivik Mb of the Itilli Fm is not exposed, but the contrast in sedimentary facies between the two formations is striking. The Upernivik Næs Fm contains thick sandstone units and is interpreted as fluvial to estuarine. Its age is interpreted as late Albian to mid-Cenomanian (Pedersen & Nøhr-Hansen 2014). The mudstones of the Umiivik Mb are interpreted as deposition from low-density and high-density turbidity currents in a base-of-slope and basin-floor fan environment (Dam et al. 1998). Their age is interpreted as late Cenomanian and younger. It thus seems probable that a late Cenomanian–early Turonian marine transgression separates the Upernivik Næs Fm from the Itilli Fm.

Between the late Cenomanian–early Turonian transgression and the early Campanian tectonic phase (angular unconformity), two depositional environments co-existed in the Nuussuaq Basin. Deltaic deposits of the Atane Fm (Qilakitsoq Mb) crop out in southern and central Nuussuaq, whereas deep-water marine deposits of the Itilli Fm are known from Svartenhuk Halvø and Itsaku, and from western Nuussuaq see also Dam et al. (2009, figure 16). The members of the Itilli Fm are described below in section 4.5 on the Upper Cretaceous deep-water marine deposits.

4.3.3   The Qilakitsoq Member of the Atane Fm

The Qilakitsoq Mb is exposed from Paatuut and westward to the Kuuganguaq–Qunnilik Fault (outcrops at Paatuut, Ataata Kuua, including cores from the borehole GGU 247801), Tupaasat, Nuuk Qiterleq, Nuuk Killeq and Alianaatsunnguaq). The Qilakitsoq Mb is also exposed along the north slope of the Aaffarsuaq Valley from east of Ilugissoq, Qilakitsoq and Tunoqqu to Kangersooq and from boreholes 400701–704 in the Agatdal valley (Dam et al. 2000, 2009; Figure 4.6). The Qilakitsoq Mb includes the same facies associations as the Kingittoq Mb (Section 4.2.6), but in different proportions. In the Qilakitsoq Mb the delta front deposits are thicker, and the shore-face association is well developed (Dam et al. 2009, figures 60–61). The sedimentary facies indicates more marine conditions, but the diversity and density of dinocysts, spores, and pollen are very low in 21 delta-front mudstone samples from borehole GGU–247801 (Pedersen et al. 2013). However, the presence *Chatangiella granulifera*, *Heterosphaeridium difficile*, and *Spinidinium* cf. *echinoideum* in the lower part, *Chatangiella mcintyrei* and *Spinidinium* cf. *echinoideum* in the middle to upper part, and by the presence of *Rugubivesciculites* spp., *Heterosphaeridium difficile*, *Laciniadinium arcticum*, and *Spinidinium* cf. *echinoideum* in the upper part indicate an early Coniacian to early Santonian age or younger (Pedersen et al. 2013). David J. McIntyre examined 24 samples from the Paatuut area, with few dinocysts but good assemblages of fern spores and conifer pollen, although few species are age-diagnostic. The flora indicates a probable Campanian age based on the presence of *Hazaria sheopiariae*, *Hamulatisporis amplus*, and single specimens of *Azonia cribrata* and *Radialisporis radiates*, although the absence of any *Aquilapollenites* species may suggest that the sediments are not younger than early Campanian (D.J. McIntyre personal communication 1997, 1999). Lanstorp (1999) also suggested a late Santonian–early Campanian age for his *Pilosisporites* sA – *Hazaria sheopiarii* Assemblage –Zone (PH) described from the Paatuut area and supported by the record of the molluscs *Sphenoceramus steenstrupi* (de Loriol) and *S. patootensis patootensis* (de Loriol), which indicate a late Santonian to earliest Campanian age (Rosenkrantz 1970; Tröger 2009).

4.4 The Early Campanian unconformity

An angular unconformity separates the Atane Fm (Qilakitsoq Mb) from the Itilli Fm (Aaffarsuaq Mb) in various sections long the north slope of Aaffarsuaq (between Qilakitsoq and Tunoqqu, and in Kangersooq) (Dam et al. 2000). The strata of the Atane Fm dip to the NE, whereas the overlying Itilli Fm is almost horizontal (Dam et al. 2000, figure 21; Dam et al. 2009, figure 84). This angular unconformity indicates a tectonic phase that is dated to the early Campanian (Dam et al. 2000). The sections at Tunoqqu and in the ravines between Tunoqqu and Qilakitsoq are probably the best outcrops for dating the tectonic unconformity. The deposition of the Itilli Fm reflects a regional transgression following the early Campanian tectonic phase.

A study of the sparse palynofloras in the Qilakitsoq Mb revealed *Heterosphaeridium difficile* and *Spinidinium* cf. *echinoideum*, suggesting an early Coniacian–early Santonian age of the Atane Fm (Nøhr-Hansen 1996). The Agatdal section shows that deposition of the Atane Fm continued to the late Santonian (Dam et al. 2000). The overlying Affarsuaq Mb of the Itilli Fm, at Tunoqqu, contains *Aquilapollenites* spp., which indicates an early–middle Campanian age (Nøhr-Hansen 1996; Dam et al. 2000). A new record of *Alterbidinium ioannidesii*, together with *Aquilapollenites* spp indicates an age not younger than early Campanian (Pearce 2010). This age is supported by the inoceramids *S. steenstrupi* and *S. patootensis patootensis*, but not by the few and poorly preserved ammonites. Early Campanian is a probable maximum age for the Aaffarsuaq Mb of the Itilli Fm (Pedersen & Nøhr-Hansen 2014).

It is interesting that one sample from the upper part of the Atane Fm at Tunoqqo contains *Aquilapollenites* sp. This indicates that only a short time interval is missing at the boundary between the Atane and Itilli formations. In other sections the boundary between the two formations is clearly erosional with large parts of the succession removed (Pedersen & Nøhr-Hansen 2014). The early Campanian unconformity has been traced regionally (Gregersen et al. 2013).

Despite the regional extent of the early Campanian unconformity, it is not exposed along the south coast of Nuussuaq or on Disko, nor is the Itilli Fm recognized here, except for the Kussinerujuk Mb in northern Disko. This suggests that these areas (northern Disko–southern Nuussuaq) had a different history of tectonic subsidence/uplift and erosion than central Nuussuaq. In northern Nuussuaq, the unconformity may be present below sea level between Ikorfat and Niaqornat. The exception is below a small outcrop of marine mudstones with a Maastrichtian ammonite fauna (Birkelund 1965, Kennedy et al. 1999), a short distance east of the Ikorfat Fault.

4.5   The deep-water marine deposits of the Itilli Formation

The Campanian–Maastrichtian deep-water marine deposits of the Itilli Fm are known from central Nuussuaq, northern Nuussuaq west of Ikorfat, the Itilli valley, and the GRO-3-well. However, only uppermost Santonian to lower Campanian and lower Campanian deposits are present in the offshore wells Qulleq-1 and Ikermiut-1. The Itilli Fm is represented by the Umiivik, Anariartorfik, and Aaffarsuaq members.

Area	Localities	Lithostratigraphy	Depos. environment	Age	
North coast Nuussuaq	Kangilia, Annertuneq	Kangilia Fm	Unconfined slope Submarine canyon		late Maastrichtian–Danian
		Annertuneq Cgl. Mb	Submarine canyon	↑	?late Maastrichtian
		Itilli Fm, Umiivik Mb	Basin-floor fan		late Campanian older parts of mb not exposed
Western Nuussuaq	Itilli valley GRO#3	Itilli Fm, Anariartorfik Mb	Fault-controlled slope	?Coniacian–Early Maastrichtian	
Central Nuussuaq	Tunoqqu	Itilli Fm, Aaffarsuaq Mb	Channelized footwall fan		early–middle Campanian
	Agatdal valley	Atane Fm, Qilakitsoq Mb	Delta	↑	late Santonian
	Tunoqqu				early Coniacian–early Santonian

Table 4.2. *Outcrops of the Upper Cretaceous–Lower Palaeogene deep-water marine deposits in Nuussuaq. For further information, see text.*

The Umiivik Mb is known from two separate geographical areas. In the Svartenhuk area, it is known from outcrops, five shallow wells, GGU 400708–712, and the deep Umiivik-1 well (Dam et al. 2009, figure 73). The age of the member ranges from late Cenomanian(?)–early Turonian to early Campanian. In Northern Nuussuaq the Umiivik Mb is known from outcrops between Ikorfat and Niaqornat, and in the deep GANT-1 well, as well as in several shallow boreholes: GGU 400701–704 (Agatdal), GGU 400705–707 (Annertuneq), and FP94-11-02, FP94-11-04 and FP94-11-05 (see Dam et al. 2009, figure 92). Here a late Campanian–Maastrichtian age for the Umiivik Mb is indicated by ammonites and palyno-stratigraphy (Birkelund 1965, Nøhr-Hansen 1996). As discussed above in Section 4.3.2, the Itilli Fm is also represented by a succession of steeply dipping mudstones in the Ikorfat Fault. This outcrop was mentioned by Rosenkrantz & Pulvertaft (1969, figure 3A) and five samples were collected by F.G. Christiansen during reconnaissance field work in 1992 (discussed above). These samples indicate a Cenomanian–Turonian age and suggest that a complete Cenomanian to late Campanian mudstone succession may be present in the subsurface between Ikorfat and Niaqornat.

The Umiivik Mb is interpreted as deposition from low-density and high-density turbidity currents, debris flows, slumping and fall-out from suspension. Deposition of the mudstones and intercalated mudstones and sandstones took place in a base-of-slope and basin-floor fan environment. The succession in the GANT-1 well, which is situated close to the K–Q Fault, reflects a fault-controlled base-of-slope environment with major and minor distributary feeder channels, small turbidite lobes and interdistributary channels (Dam et al. 2009, 95).

The Anariartorfik Mb is known from the Itilli Valley and from deep GRO-3 well in western Nuussuaq (Dam et al. 2009, figures 66–70). The succession in GRO-3 at 1440–3000 m depth is older than the Campanian. The member is exposed in river sections in the Itilli Valley, where the repeated alteration of sandstones and mudstones is documented (Dam et al. 2009, plate 2). Deposition of the Anariartorfik Mb took place in a fault-controlled slope environment (Dam & Sønderholm 1994). Most of the channelized amalgamated turbidite sandstone beds were deposited from high-density turbidity currents in confined low-sinuosity channels. The thinly inter-bedded sandstones and mudstones were deposited

from traction currents and from fall-out processes within waning low-density turbidity currents, probably in an inter-channel slope environment. Where present, the chaotic mudstone beds always underlie undisturbed channel sandstones. This suggests that the channels were initially excavated by retrogressive slumping of unstable sediments on the slope followed by channel excavation by scouring (Dam & Sønderholm 1994, Dam et al. 2009).

Palynomorphs in the GRO-3 well indicate Campanian and Maastrichtian age for the uppermost 700 m of the Anariartorfik Mb (Dam et al. 2009). The thickness of the member is not known, as base of the member was not reached in the GRO-3 well. It is possible that the more than 1500 m of pre-Campanian deposits may date back to the late Cenomanian. Samples from the Itilli Valley, as well as samples from the lower part of GRO-3, cannot be dated as the organic material is degraded due to thermal maturation (Dam et al. 2009).

The Aaffarsuaq Mb is exposed in the Kangersooq valley in stream sections on the north slope of the Aaffarsuaq valley between Qilakitsoq and Tunoqqu and in 1–2 outcrops on the south slope of the Aaffarsuaq valley. The member is characterized by amalgamated sandstone and rip-up mudstone and sandstone clast conglomerate units alternating with thinly interbedded sandstones and mudstones, dark, sand-streaked mudstones, and chaotic beds of homogeneous mudstone commonly cut by sandstone dykes and syn-sedimentary faults (Dam et al. 2000).

The thick units of amalgamated sandstone and conglomerate beds are interpreted as deposition mainly from gravity flows in a channelized, footwall fan system. Deposition of the amalgamated sands was confined to major turbidite channels. The intervening thinly interbedded sandstone and mudstone units were deposited mainly from low-density turbidity currents confined to minor channels. The sand-streaked, mudstone-dominated units were deposited by waning low-density turbidity currents in an interchannel slope setting. The contorted beds probably formed by downslope displacement of semi-consolidated sediment. Downslope failure may have been associated with seismic activity (Dam et al. 2009).

The Aaffarsuaq Mb contains ammonites, inoceramids and locally a rich flora of palynomorphs. The fossils indicate an early–middle Campanian age (Nøhr-Hansen 1996; Dam et al. 2000).

4.6 The late Maastrichtian uplift and submarine erosion

Large erosive valley systems are a characteristic feature of the latest Cretaceous and Early Paleocene of the Nuussuaq Basin. Three phases of erosion are recognized (Table 4.3). Submarine canyons formed at the base of the Kangilia and Agatdal formations, whereas the Quikavsak Fm represents the fluvial fill of incised valleys (Dam 2002). which is a characteristic feature. The latter are interpreted as sequence boundaries (see Wilgus et al. 1988) and the incision is likely a response to thermal uplift related to the arrival of a mantle plume that preceded the volcanic activity (Dam & Nøhr-Hansen 2001). A very thick volcanic succession formed within a relatively short period of time (Larsen et al. 2015).

Age	Enviroment	Locality/area	Formation below	Valley fill	Description
Danian	Deep marine	Agatdal valley GRO#3 well	Kangilia Fm	Sandstone and mudstone Agatdal Fm	4.9.2
Danian	Fluvial	Paatuut–Tupaasat South Nuussuaq	Atane Fm, Qilakitsoq Mb	Pebbly sandstones Quikavsak Fm	4.9.1
Danian?	Deep marine	Ataata Kuua South Nuussuaq	Atane Fm, Qilakitsoq Mb	Mudstone and conglomerates Kangilia Fm	4.6 4.7.3
Maastrichtian	Deep marine	Kangilia North Nuussuaq	Itilli Fm, Umiivik Mb	Conglomerate and sandstone Annertuneq Cgl Mb	4.7.2
Late Cenomanian	Marine	Asuk–Kussinerujuk North Nuussuaq	Atane Fm, Kingittoq Mb	Mudstone, sandstone, congl. Kussinerujuk Mb	4.3.1
?middle Albian	Estuarine	Ravn Kløft North Nuussuaq	Slibestensfjeldet Fm	Mostly sandstones Ravn Kløft Mb	4.2.3

Table 4.3. *Overview of valley erosion in the Nuussuaq Basin in the Cretaceous and earliest Paleocene. The two older erosive events are described above.*

Marine incised valleys with a considerable relief define the lower boundary of the Kangilia Fm (Dam et al. 2009). In northern Nuussuaq, the valleys are eroded into the Itilli Fm and are outlined by the Annertuneq Conglomerate Mb. In southern Nuussuaq at Ataata Kuua, a valley is eroded into the Atane Fm (Dam et al. 2009, figure 15). The submarine canyon at the base of the Kangilia Fm at Ataata Kuua has a minimum relief of 250 m (Dam et al. 2009, figure 15), illustrating the considerable erosion into the Qilakitsoq Mb (Atane Fm) in the ?early Danian (Dam & Nøhr-Hansen 2001). The width of the canyon is not known. Its steep slope indicates that erosion followed a listric fault. The canyon and its fill (the Kangilia Fm) was described in detail by Dam & Nøhr-Hansen (2001, p. 194–97).

It is likely that this erosional unconformity was expressed as a regression in areas closer to the Maastrichtian shoreline. However, sediments of this age are not known from the eastern part of the basin Figure 4.8, where a major unconformity separates the Lower Cretaceous from the Paleocene (Dam et al. 2009, figure 16).

4.7 The deep-water marine deposits of the Kangilia Formation

The Kangilia Fm is 75–400 m thick and is known from southern Nuussuaq (Ataata Kuua, Ivisaanguit, Tupaasat; Figure 4.8), central Nuussuaq (Agatdal valley), northern Nuussuaq between Ikorfat and Niaqornat, the Tunorsuaq valley, western Nuussuaq (GRO-3), and at Itsaku, Svartenhuk Halvø. The Kangilia Fm has one member, the distinctive Annertuneq Conglomerate Mb, which defines the base of the formation where the conglomerate is present. The overlying part of the Kangilia Fm is not assigned to a member. The classic sections for studies of this deep-water marine succession are those at Kangilia and Annertuneq at the north coast of Nuussuaq, where the top of the Umiivik Mb is truncated by the Annertuneq Conglomerate Mb of the Kangilia Fm.

The palynology of several sections from the Annertuneq/Kangilia area spanning the uppermost Cretaceous and lower Paleocene has been described previously (Nøhr-Hansen 1996; Nøhr-Hansen & Dam 1997; Nøhr-Hansen et al. 2002). The Itilli Fm is dated as late

Campanian. The Kangilia Fm is late Maastrichtian to Danian in age (Nøhr-Hansen & Dam 1997, Pedersen & Nøhr-Hansen 2014). The K/T boundary is located within the Annertuneq Conglomerate Mb at Kangilia, and above the conglomerate at other localities (Dam et al. 2009) (Table 4.2).

4.7.1   The Annertuneq Conglomerate Member

The Annertuneq Conglomerate Mb is a 85–140 m thick unit (Figure 4.3) exposed between Niaqorsuaq and Kangilia on the north coast of Nuussuaq. It is also known from the GANT-1 well. The clast-supported conglomerate, with pebble- to boulder-sized clasts, is dominated by quartz or quartzitic sandstones (Dam et al. 2009). These lithologies indicate a provenance of the clasts outside the Nuussuaq Basin, in contrast to the intraformational clasts in the Aaffarsuaq Mb. The Annertuneq Conglomerate Mb is interpreted as deposition from debris flows and high density turbidity currents. The considerable increase in the thickness of the member in the GANT-1 well, compared to the exposures at Kangilia and Annertuneq, suggests that deposition took place in a major submarine canyon and that the GANT-1 well is situated in a more axial position (Dam et al. 2009).

4.7.2   The mudstones of the Kangilia Formation

Most of the Kangilia Fm consists of dark grey marine mudstones with thin sandstone beds. The mudstones are interpreted as deposited from waning, low-density turbidity currents or by dilute turbidity currents in an unconfined slope setting (Dam et al. 2009).

The dinocysts flora suggests a late Maastrichtian to Danian age for the Kangilia Fm on the north coast of Nuussuaq and a Danian age in the central part of Nuussuaq. These ages are supported by several groups of fossils (see Dam et al. 2009, p. 109–110).

4.7.3   The Kangilia Formation at Ataata Kuua

The Kangilia Fm constitutes an overall upward fining succession with a conglomeratic unit, which represents deposition in a turbidite channel. The clast composition is equal to that of the Annertuneq Conglomerate Mb. The Kangilia Fm at Ataata Kuua is interpreted as a transgressive highstand system (Dam & Nøhr-Hansen 2001). During the Danian, the Kangilia Fm at Ataata Kuua was truncated by an incised valley filled by the Quikavsak Fm (Section 4.9.2).

4.8 Potential source rocks

Hydrocarbons are found in the Nuussuaq Basin as minor oil stains, intensive oil stains or as seepage of oil, especially in the areas west of the Kuugannguaq–Qunnilik (K–Q) Fault (Figure 4.11). The finds are numerous in western Nuussuaq, but minor stains are also known from the north coast of Disko, Hareøen, Ubekendt Ejland, Schades Øer and Svartenhuk Halvø (mapped in Bojesen-Koefoed et al. 1999, figure 2). These authors identified five oil

types based on organic chemistry and biomarker analysis (Table 4.4). Some offshore occurrences are listed by Knutsen et al. (2012).

		Potential source rocks		
Oil name	Type	Known distribution	Age	Possible source rock
Potentially wide distribution				
Marraaat	'high-wax' oil 'deltaic'	Western Nuussuaq	Latest Cretaceous or younger	Most likely the Eqalulik Fm based on GRO#3 results; possibly also Paleocene mudstones of the the Kangilia Fm
Itilli	'low-wax' oil 'marine'	W of Itilli Fault Zone	Late cretaceous, Cenomanian-Turonian?	Marine mudstone similar to Canadian Kanguk Fm; the Itilli Fm?
Only known from restricted areas				
Eqalulik	moderate wax, unusual type	GANE#1 well; local area W Nuussuaq	Santonian or older	Lacustrine or lagoonal deposits
Niaqornaarsuk	'high-wax'	S. Nuussuaq, close to Kuugannguaq Fault	Campanian	Marine mudstone w terrigeneous influx, the Itilli Fm?
Kuugannguaq	'high wax' oil 'terrigeneous'	N. Disko, close to Kuugannguaq fault	Santonian or older	The Atane Fm?

Table 4.4 *Oil types and potential source rocks, data from onshore areas in the Nuussuaq Basin from Bojesen-Koefoed et al. (1999).*

Three of the oil types are only known from very restricted areas, and it is possible that they were generated in response to locally favourable conditions. The Marraat and Itilli oil types are known from several occurrences. The Itilli oil type is interpreted as originating from source rocks that potentially have a wide distribution (Bojesen-Koefoed et al. 2004).

A plot of vitrinite reflectance data shows that the samples from the GRO-3 well were buried to depths of 2000–5000 m, whereas samples from localities east of the K–Q Fault only show a burial to 1000–2000 m (Pedersen et al. 2006, figure 9). These data indicate that generation of hydrocarbons east of the K–Q Fault would depend on the presence of pre-Cretaceous sediments in source rock facies. The stratigraphic distribution maps (Figures 4.4–4.10) and the geological cross-sections (in the GIS compilation) show that the Cretaceous to Paleocene marine mudstones that are most likely to include source rock facies occur west of the K–Q Fault in southern Nuussuaq, and west of the Ikorfat Fault Zone in northern Nuussuaq. Consequently both depositional environments and subsidence suggest that potential source rocks are most likely to be present in western Nuussuaq.

4.9 The Danian phases of uplift, incision, deposition, and deepening

Dam & Nøhr-Hansen (2001) and Dam et al. (2009) distinguished two phases of uplift and incision during the Danian, most clearly seen in the two generations of fluvial incision in the

Quikavsak Fm. These phases are correlated to phases of submarine canyon incision (the Agatdal Fm).

4.9.1   The Quikavsak Formation, fluvial fill of incised valleys

The Quikavsak Fm was thoroughly described by Dam (2002), who documented two stages of fluvial erosion and deposition separated by a phase of lacustrine deposition. The formation has three members, the Tupaasat Mb, the Nuuk Qiterleq Mb and the Paatuutkløften Mb (Dam et al. 2009, figures 97–111). The Quikavsak Fm is up to 180 m thick, and is exposed in a series of outcrops along the south coast of Nuussuaq (Figure 4.9). The lower boundary of both the Tupaasat and Paatuutkløften members is strongly erosive (Dam et al. 2009, figures 97–112). The formation is dated as Danian from its stratigraphic position between the Kangilia Fm and the overlying syn-volcanic Eqalulik Fm of Danian to Selandian age (Dam et al. 2009).

4.9.2   The Agatdal Formation, fill of a submarine canyon

The Agatdal Fm includes marine mudstones and sandstones with a rich fauna of invertebrate fossils, which were a main target for the Nûgssuaq Expeditions (1938–1968) led by A. Rosenkrantz (see Dam et al. 2009, p.15–17). The macrofossils are indicative of relatively shallow-water, marine depositional environments, such as a lower shore-face or inner shelf environment (Petersen & Vedelsby 2000). In contrast, the sedimentary facies are interpreted as deposition in a deep-water slope environment. The Agatdal Fm is interpreted as the fill of a major submarine canyon (Dam et al. 2009, plate 3), and it is suggested that this canyon may have continued to western Nuussuaq, where comparable facies occur in the GRO-3 and GANE-1 wells.

4.9.3   The late Danian transgression

In an outcrop at the western slope of Ataata Kuua (below point 1010 m) the fluvial sandstones of the Quikavsak Fm (the Paatuutkløften Mb) are overlain by tidal-estuarine bioturbated sandstones. These are followed by 10–15 m of shore-face sandstone with a rich fauna of marine trace fossils and tuffaceous, marine mudstones, which are referred to as the marine, syn-volcanic Eqalulik Fm (Dam & Nøhr-Hansen 2001, figure 12; Dam et al. 2009, figure 108). This section demonstrates a marine transgression and a rapid deepening that followed a period of uplift that resulted in incision at the base of the Quikavsak Fm. In areas where the Eqalulik Fm overlies deep-water marine deposits of the Kangilia and Agatdal formations the marine transgression is not as clearly expressed in the sedimentary facies as it is in the area around Ataata Kuua and Paatuut.

The foreset-bedded hyaloclastites of the Naujannguit Mb (Vaigat Fm), which prograded eastwards above the Eqalulik Fm, has foresets that are up to 600 m thick. This indicates that they were deposited in a basin up to 600 m deep. Rapid vertical movements are interpreted as related to the mantle plume (Dam et al. 1998, Dam & Nøhr-Hansen 2001).

4.10   The syn-volcanic sedimentary deposits

4.10.1   The Eqalulik Fm

The Eqalulik Fm can be mapped below the volcanic Vaigat Fm in western and central Nuussuaq (Figure 4.10). In the exposures along the south coast of Nuussuaq between Nuusap Qaqqarsua and Paatuut, the Eqalulik Fm is overlain by foreset-bedded hyaloclastite breccias which prograded eastwards, overlain by subaerial lava flows (geological section 1, included in the GIS compilation). East of Paatuutkløften the Eqalulik Fm is not well documented, and from Kingittoq and eastwards the syn-volcanic mudstones are referred to as the non-marine Atanikerluk Fm (Koch 1959, Pedersen et al. 1998, Dam et al. 2009).

In the Sikillingi area, the volcanic breccias and hyaloclastites of the Anaanaa Mb overlie the Eqalulik Fm. In western Nuussuaq, the boundary between the Agatdal Fm and the Eqalulik Fm is located in the type section (cores from GANE-1 and GANE-1A), while the reference section in GANK-1 demonstrates the boundary between the Kangilia Fm and the Eqalulik Fm. The cores from these wells also represent the upper boundary between the Eqalulik Fm and the Anaanaa Mb of the Vaigat Fm (Dam et al. 2009, figures 118–122). The Eqalulik Fm varies in thickness from 218 m in the GANK-1 well to 100–160 at the north coast of Nuussuaq, and 10–20 m in central Nuussuaq (Dam et al. 2009).

In the Agatdal valley the basal part of the Eqalulik Fm is referred to as the Abraham Mb (Dam et al. 2009, figure 114). The Abraham Mb is stratigraphically important because the tuff beds can be shown to derive from a graphite-rich eruption from a crater at Ilugissoq in the Aaffarsuaq valley (Pedersen & Larsen 2006). This allows a chemical/petrological correlation between the Abraham Mb and the Asuk Mb of the volcanic Vaigat Fm.

The upper boundary of the Eqalulik Fm is diachronous, reflecting the progressive eastward progradation of the hyaloclastite fans. However, the biostratigraphic resolution is in most cases not good enough to resolve this diachronism. The macrofauna indicates an Early Danian age (Rosenkrantz 1970; Floris 1972; Henderson et al. 1976). New dinocyst and nannoplankton data indicate an NP4 or possibly base NP5 zone age (latest Danian–early Selandian; Nøhr-Hansen et al. 2002). The volcanic rocks of the Anaanaa Mb (Vaigat Fm) close to the basal part of the Eqalulik Fm, belong to magnetic Chron C27N (Danian) (Figure 4.2).

4.10.2   The Atanikerluk Formation

The Atanikerluk Fm is composed of non-marine syn-volcanic sediments, i.e., sediments coeval with the Ordlingassoq Mb of the Vaigat Fm and with the lower Rinks Dal Mb of the Maligât Fm (Dam et al. 2009, figure 131). The Atanikerluk Fm has been subdivided into five members: the Akunneq, Naujât, Pingu, Umiussat and Assoq members (Figure 4.3), which are interpreted as deposited in fluvial to lacustrine environments (Koch 1959; Pedersen et al. 1998; Dam et al. 2009).

Three lacustrine drowning surfaces may be recognized:

- the oldest, located at the lower boundary of the lacustrine Naujât Mb on Nuussuaq, probably corresponding to the lower boundary of the Akunneq Mb on Disko. In the Saqqaq valley and at Kingittoq the old, erosional topography of the Cretaceous sediments is preserved below the drowning surface (Dam et al. 2009, figure 130);

- an intermediate surface located at the base of the lacustrine Pingu Mb on Disko, corresponding to a position within the Naujât Mb on Nuussuaq;

- the youngest, located at the base of the lacustrine Assoq Mb both in eastern Nuussuaq and eastern Disko. The outcrops of these mudstones are relatively small, and the mudstones are frequently seen to include invasive lava flows.

The Atanikerluk Fm is up to 500 m thick in a composite section, but individual outcrops reach thicknesses from 200–400 m (Dam et al. 2009, figures 126 & 128). The Atanikerluk Fm is dated by dinocysts, pollen or plant macrofossils. It is also constrained by magneto-stratigraphic and radiometric dating of the correlative volcanic units. A maximum age for the formation is obtained from the underlying Eqalulik Fm (late Danian). A minimum age is provided by the subaerial lava flows of the Rinks Dal Mb, which is 61.2 ± 0.4 m.y (Selandian using the timescale of Gradstein et al. (2012) and overlies the Assoq Mb. (Larsen et al. 2015)

4.10.3   Intrabasaltic sediments (not included in the Nuussuaq Group)

Locally sediments occur below or within the overlying Niaqussat Mb in eastern Nuussuaq. Intrabasaltic sediments in western Nuussuaq are referred to as the Ifsorisoq Mb, which is part of the Paleocene volcanic Svartenhuk Fm (Figure 4.2). Eocene intrabasaltic sediments, the Aumarûtigssâ Mb of the Hareøen Fm, have a limited extent. A resinite-rich coal bed has yielded very well preserved pollen, indicating a remarkable diversity of the family Fagaceae in the Eocene of West Greenland (Grímsson et al. 2015).

4.11   The volcanic development in West Greenland

The depositional environment at the onset of volcanism around 62 Ma involved a marine embayment that stretched from an open sea to the NW toward the south and SE, where the coast was delineated by the Disko gneiss ridge and an active delta system. To the E–NE was a gneissic highland. Deposition of the volcanic rocks initiated in northwestern Nuussuaq and propagated eastwards with time, simultaneous to subsidence taking place in the sedimentary basin. Exposures of younger lavas of Eocene age are restricted to the westernmost part of Nuussuaq peninsula, west of the Itilli fault, and on Hareøen.

4.12   The picritic eruptions of the Vaigat Formation

The earliest volcanism in the Nuussuaq basin is represented by the Vaigat Fm, which forms a shield-like structure centered on western Nuussuaq and northern Disko, reaching up to 1.6 km in thickness and wedging out further eastward and southward. The greatest thick-

nesses are reached north of Nuussuaq (on Ubekendt Ejland), where more than 5km of volcanic rocks accumulated. In total, the Vaigat Fm is estimated to have a total volume of 10,000 km^3 (Larsen & Pedersen 2009). The Vaigat Fm is subdivided into three members, the Anaanaa, Naujánguit and Ordlingassoq members, of which the former two are contemporaneous to the marine mudstones of the Eqalulik Fm and the latter is synchronous with the non-marine mudstones and sandstones of the Atanikerluk Fm (Dam et al. 2009; see above). The Anaanaa Mb is dated to 62.5–62.2 Ma and corresponds to Chron C27N, whereas the remaining of Vaigat Fm and the overlying Maligât Fm that all are reversely magnetized and erupted during C26R (62.2–59.2 Ma). The Vaigat Fm is dominated by picritic units, of which around 1/3 were erupted as foreset-bedded hyaloclastites under submarine conditions and the rest as subaerial lavas (Sørensen 2011). Some examples of mass flows, including re-deposited hyaloclastites and blocks of oxidized subaerial lavas, can also be found, e.g., at Nuusaq on the south coast of western Nuussuaq.

The earliest Anaanaa Mb is present only in the western part of Nuussuaq east of the Itilli valley, where exposures however are relatively sparse. The stratigraphy of the lowermost Vaigat Fm is consequently based on cores from four drill holes that show three discernible units, including a lower (unnamed) olivine-micro-phyric unit, overlain by the plagioclase-phyric Niaqornaq unit and the contaminated Marraat unit. The overlaying Naujánguit Mb, present in western Nuussuaq and northern Disko, contains several contaminated units of which three have obtained (sub)member status (Nuusap Qaqqarsua, Nuuk Killeq and Asuk Mbs) and constitute several recognizable marker horizons that have been useful in establishing the volcanic stratigraphy. Most distinct of these is the Asuk Mb that includes strongly contaminated basaltic andesites and andesites, some of which contain native iron or graphite reflecting the interaction with underlying reducing sediments. Also noticeable is the Tunoqqu (Nuussuaq), Kûgánguaq (Disko) and Qordlortorssuaq (Disko) members. They formed toward the end of the second Naujánguit Mb volcanic cycle and are believed to be closely related in time. They formed an approximately coherent sub-horizontal surface, the Tunoqqu surface, which at the time of formation covered more than 3100 km^2 on Disko and Nuussuaq (Sørensen 2011). The Tunoqqu surface is now found segmented into areas of different elevation and structural trends as a result of later tectonic deformation (Chapter 3).

The overlying Ordlingassoq Mb extended the Vaigat Fm to eastern Nuussuaq and northern Disko and marks a transitional shift from marine to non-marine environments, as the advancing volcanic front closed the gateway to the sea turning the embayment into a freshwater lake. The Ordlingassoq Mb mostly consists of uncontaminated picrites, but also includes crustally contaminated, iron-bearing units in northern Disko (Stordal), as well as examples of enriched alkaline picrites and basalts grouped under the Manîtdlat Mb. The Ordlingassoq Mb is dated to 61.3 ± 0.5 Ma and terminates the Vaigat Fm. The lavas of the Vaigat Fm were erupted locally, as witnessed by identified eruption sites such as craters and feeder dykes.

4.13   Eruption of the Maligât Formation

The Maligât Fm was dated to 61.2 (± 0.4)–60.2 (± 0.5) Ma and has a total volume of 20,000 km^3. The Maligât Fm is centered on Disko where it makes up more than 1700 m of volcanic stratigraphy, being thickest in western Disko. Eastward on Disko, the lavas of the Maligât

Fm becomes thinner as they interfinger with lake sediments and deltaic sands. In the north they onlap onto the Vaigat Fm. The volcanic eruption style shows a temporal and W–E development from early submarine lavas and hyaloclastites, over intrusive lavas in contact with wet sediments (forming 'sills'), to subaerial lava flows that finally covered much of the basinal area and lapped onto the gneiss highland in the east (geological cross sections 2 and 5, included in GIS compilation). The Maligât Fm marks a shift from submarine to mainly subaerial style of eruptions and also marks a shift from more frequent, smaller eruptions (typically a few meters in thickness) characterizing the Vaigat Fm, to rarer but more voluminous lava flows, up to 10–30 m (or more) thick. This shift in flow morphology results in the characteristic 'trap' morphology of the flood basalt province characteristic of the Maligât Fm. With the Maligât Fm, the focus of volcanism shifted to west of Disko. The eruption sites for the Maligât Fm lavas are rarely identified, but are believed to have been centered west of, or in western Disko where the succession is thickest (Larsen & Pedersen 2009). Formally, the Maligât Fm is divided into four main members, the Rinks Dal, Nordfjord, Niaqussat Mbs and Sapernuvik Mb. The Rinks Dal Mb includes 1400 m of monotonous basalts that have been subdivided based on geochemical variations (Larsen & Pedersen 2009). In the middle part of the Rinks Dal Mb, a distinctive unit of Ti-rich basalts has been identified and is referred to as the Akuarut unit. The Skarvefjeld unit stands out chemically from the remaining of the Rinks Dal Mb lavas. The overlying Nordfjord Mb is volumentrically minor but compositionally diverse, and includes mildly alkaline compositions (hawaiites) as well as crustally contaminated evolved rocks (including andesites, dacites and rhyolites). The Niaqussat Mb contains mildly contaminated picrites and basalts as well as highly contaminated andesites and dacites. The overlying Sapernuvik Mb comprises the three youngest, uncontaminated Paleocene lava flows and is preserved in a local area in western Disko.

4.14 Svartenhuk and Naqerloq formations

The earliest lavas of the Svartenhuk Fm include the Tunarsuak Mb, which occurs on Svartenhuk Halvø where it is intercalated with quartzo-feldspathic and volcaniclastic sediments. These lavas are dated to 60 Ma and are broadly coeval, but not co-genetic, with the uppermost Maligât Fm. The overlying Nuuit and Skalø members are dated to 58 Ma and are clearly younger than the Maligât Fm. The widespread distribution of these three members on Svartenhuk Halvø suggests a westward continuation in the offshore areas (Larsen et al. 2015).
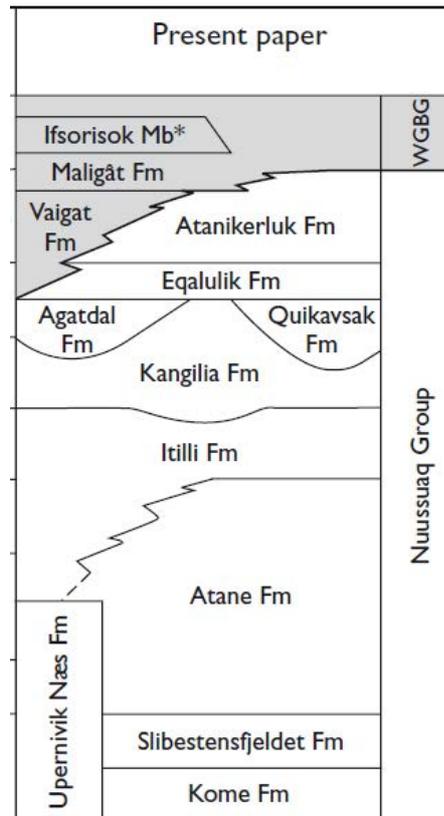
Figure 4.1. *Schematic overview of the formations within the Nuussuaq Group and the boundary between the Nuussuaq Group and the West Greenland Basalt Group (Clarke & Pedersen 1976). No vertical scale is implied. The pre-volcanic formations range from the Lower Cretaceous Kome Fm to the Danian Agatdal and Quikavsak formations, and the Upper Danian to Selandian syn-volcanic sediments constitute the Eqalulik and Atanikerluk formations. The figure is from Dam et al. (2009, figure 13).*

Figure 3. Stratigraphic scheme for the volcanic rocks in the Nuussuaq Basin. Based on Hald & Pedersen (1975) for Disko and Nuussuaq, Hald (1976) for Hareøen and western Nuussuaq, Larsen (1977a) for Ubekendt Ejland, and Larsen & Grocott (1991) and Larsen & Pulvertaft (2000) for Svartenhuk Halvø. Tunuarsuk Member to Naqerloq Formation correspond to the mapped β₁– β₄ basalt units in Larsen & Grocott (1991), which will be described elsewhere. S.Q – Sarqâta qáqâ central complex; l. – lower; m. – middle; u. – upper; yellow – sediments with a quartzo-feldspathic component; brown – purely volcaniclastic sediments; wavy lines – unconformities. Narrow black and white columns at the right side of some lithological columns are palaeomagnetic directions, with magnetochrons indicated, from Riisager & Abrahamsen (1999), Riisager et al. (1999, 2003), Schmidt et al. (2005) and unpub. data by P. Riisager. Radiometric ages (Ma) with two digits after the decimal point are from this work, and ages with one digit after the decimal point are from Storey et al. (1998) and Larsen et al. (2009). The age for the Anaanaa Member is not radiometric but based on its normally magnetized character. Note that the vertical 'age scale' is not equidistant (compare Fig. 9 for an equidistant age scale).

Figure 4.2. *The lithostratigraphical subdivision of the volcanic successions within the onshore parts of the Nuussuaq Basin. The figure is from Larsen et al. (2015) and shows also the radiometric ages of the formations. The papers cited by Larsen et al. in the caption to the figure are not included in the reference list of this report.*

Figure 4.3. *Simplified logs through the formation and members of the Nuussuaq Group from the Nuussuaq Basin (drawn from Dam et al. 2009: figure16). Please note that the vertical scale indicates time, not thickness. Two major transgressive surfaces, and erosional unconformities discussed in the text are indicated.*
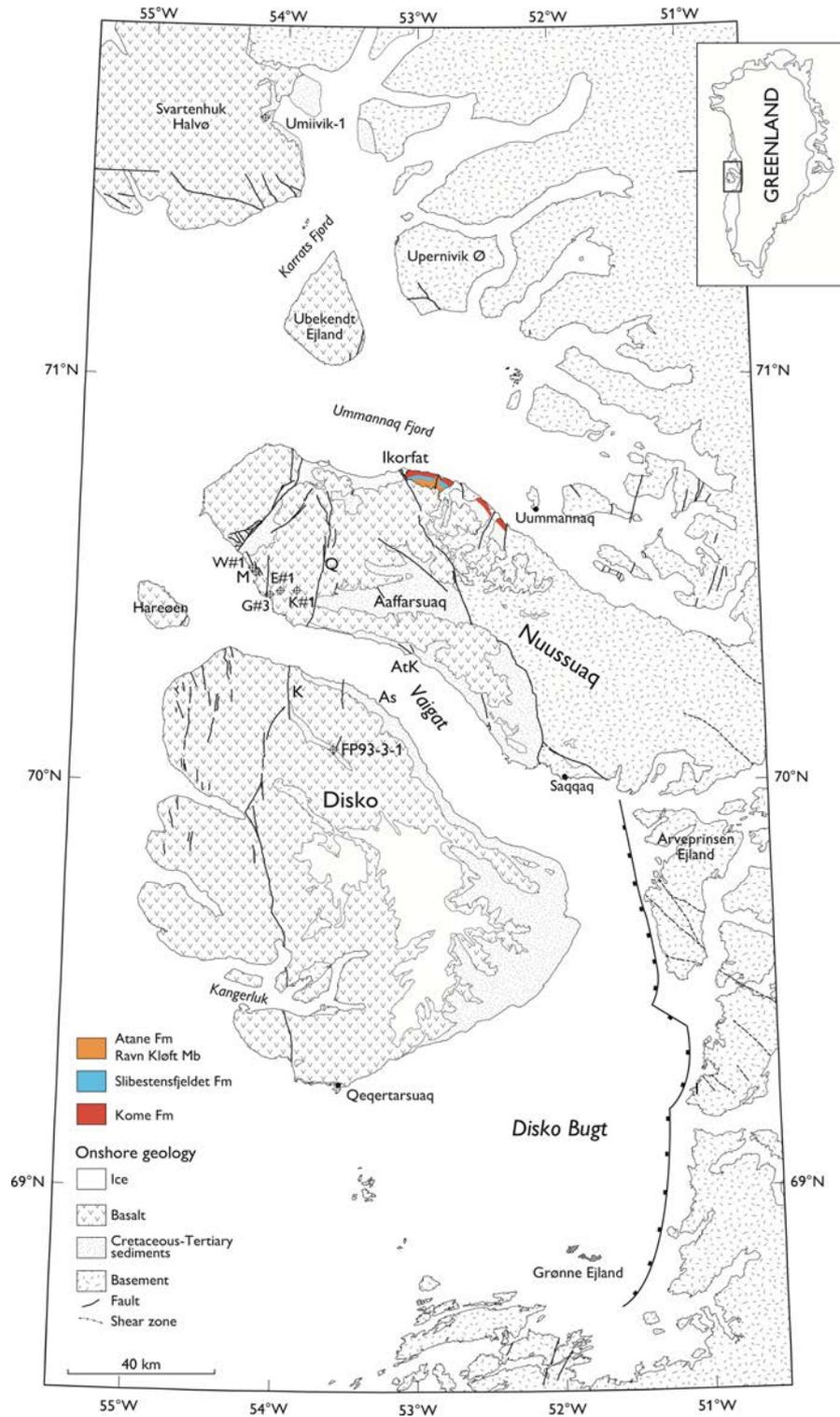
Figure 4.4. *Map showing the known distribution of the Kome Fm, the Slibestensfjeldet Fm, and the Ravn Kløft Mb of the Atane Fm. These formations are discussed in section 4.2.*
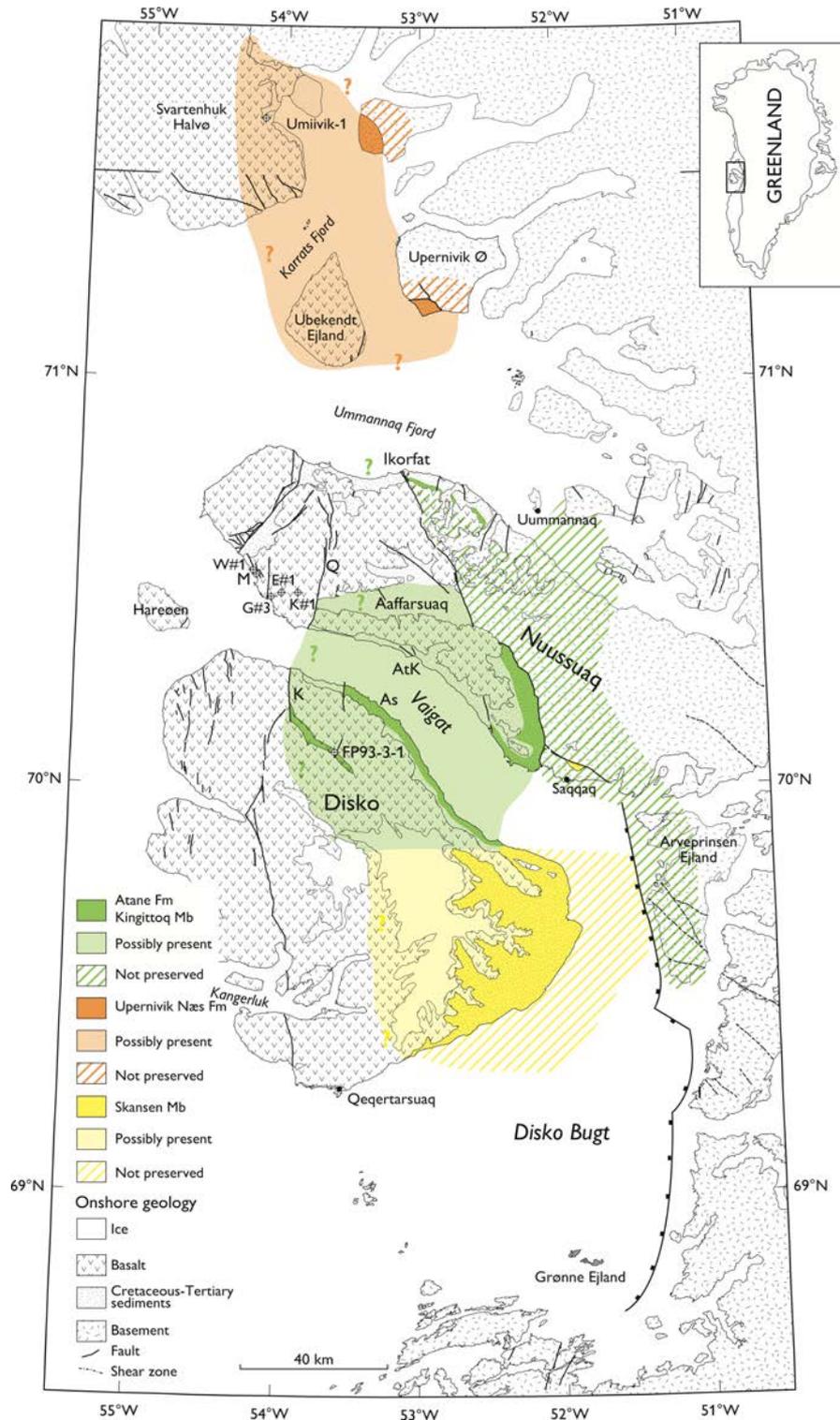
Figure 4.5. *Map showing the distribution of the Skansen Mb and the Kingittoq Mb of the Atane Fm, and the Upernivik Næs Fm. The known distributions are shown in dark colours, the possible distribution in pale colours. The hatching indicates area where the lithostratigraphic units are not preserved. Note added in proof: The yellow hatched area should be pale yellow.*
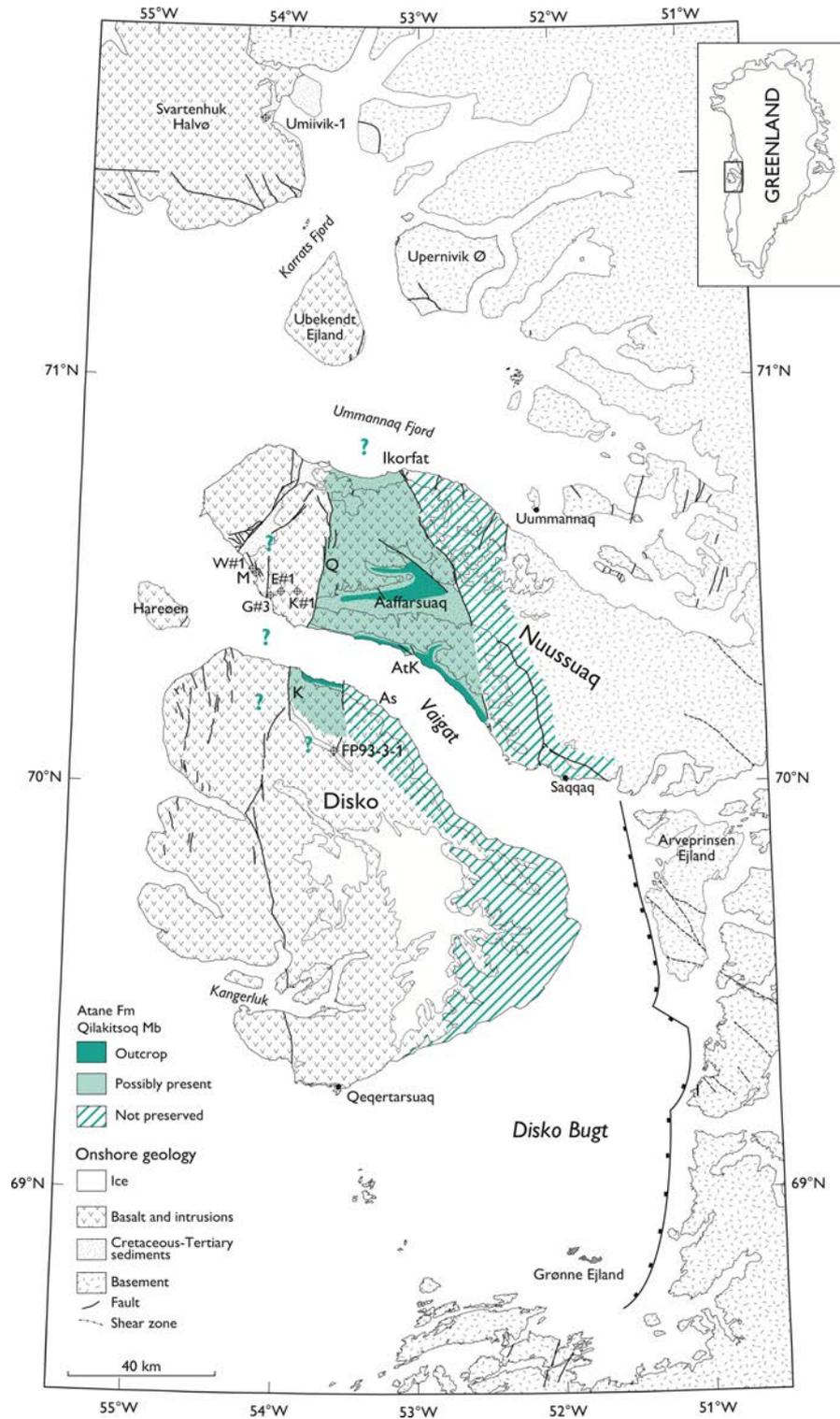
Figure 4.6. *Map showing the distribution of the Qilakitsoq Mb of the Atane Fm. The known distribution is shown in dark colours, the possible distribution in pale colours. The hatching indicates area where the member is not preserved.*
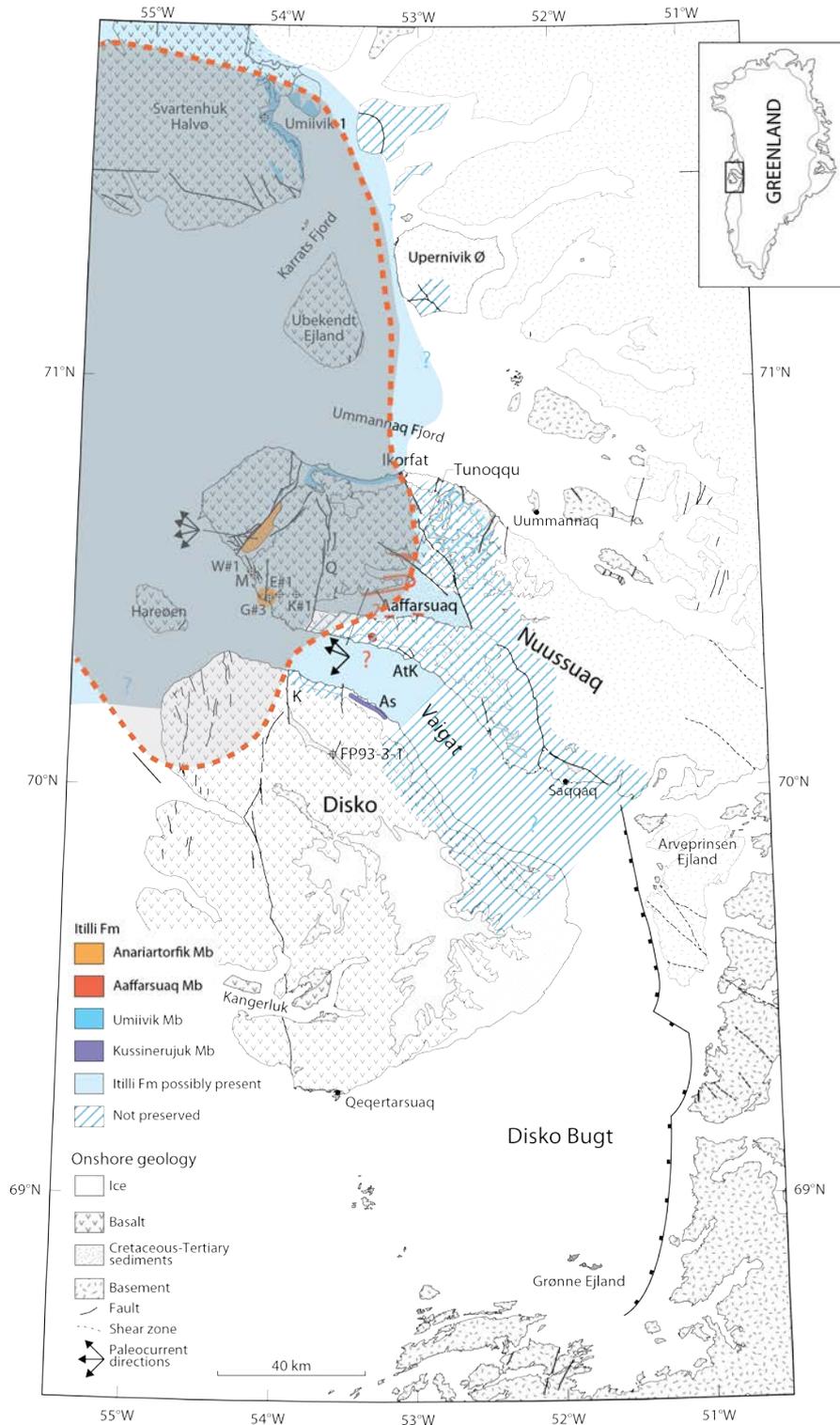
Figure 4.7. *Map showing the distribution of the Kussinerujuk Mb, the Umiivik Mb, the Aaffarsuaq Mb, and the Anariartoftik Mb of the Itilli Fm. The known distributions are shown in dark colours, the possible distribution in pale colours. The hatching indicates area where the lithostratigraphic units are not preserved. Grey shaded area outlined in dashed orange is possible distribution of source rock from the Itilli Fm.*
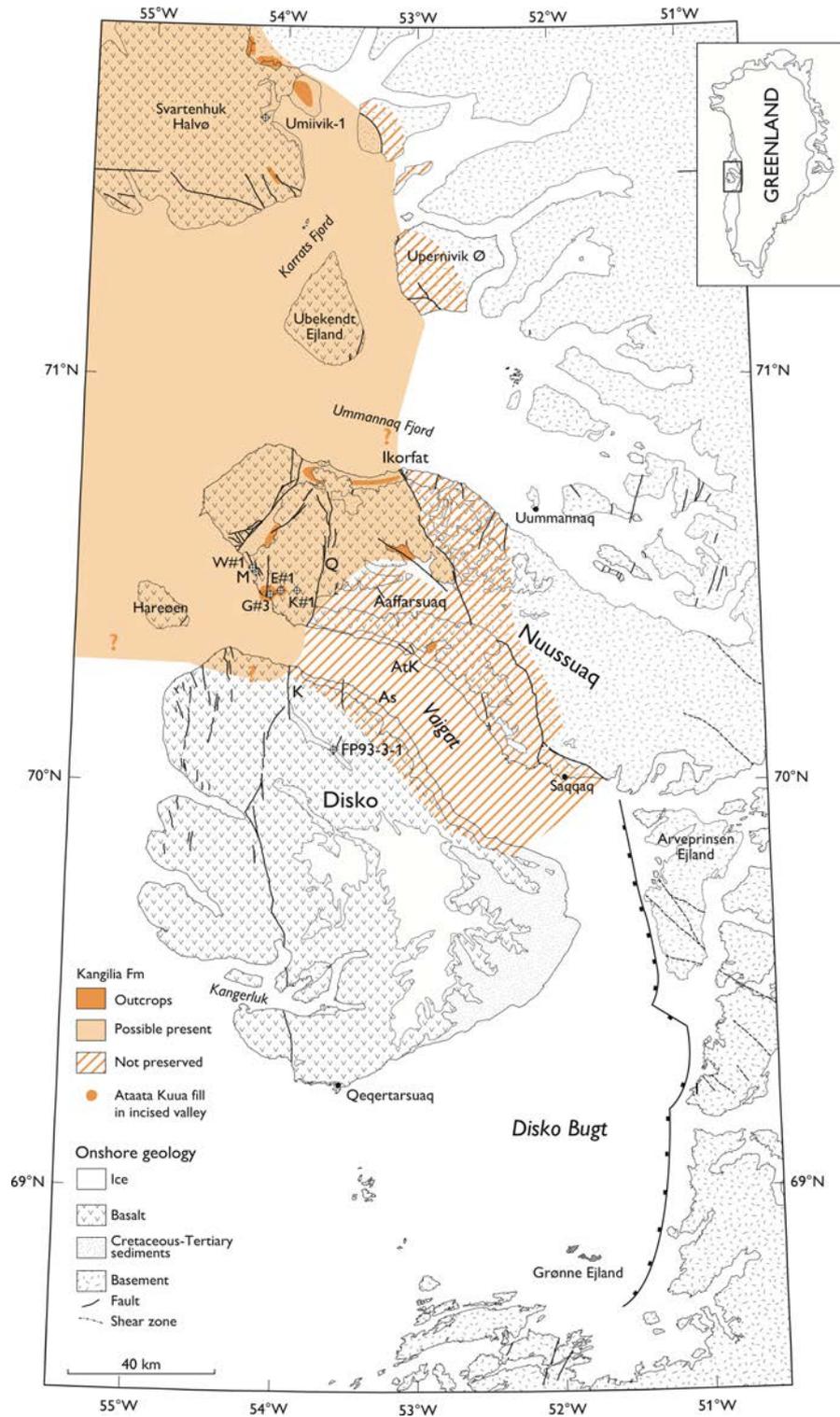
Figure 4.8. *Map showing the distribution of the Kangilia Fm. The known distribution is shown in dark colours, the possible distribution in pale colours. The hatching indicates area where the formation is not preserved.*
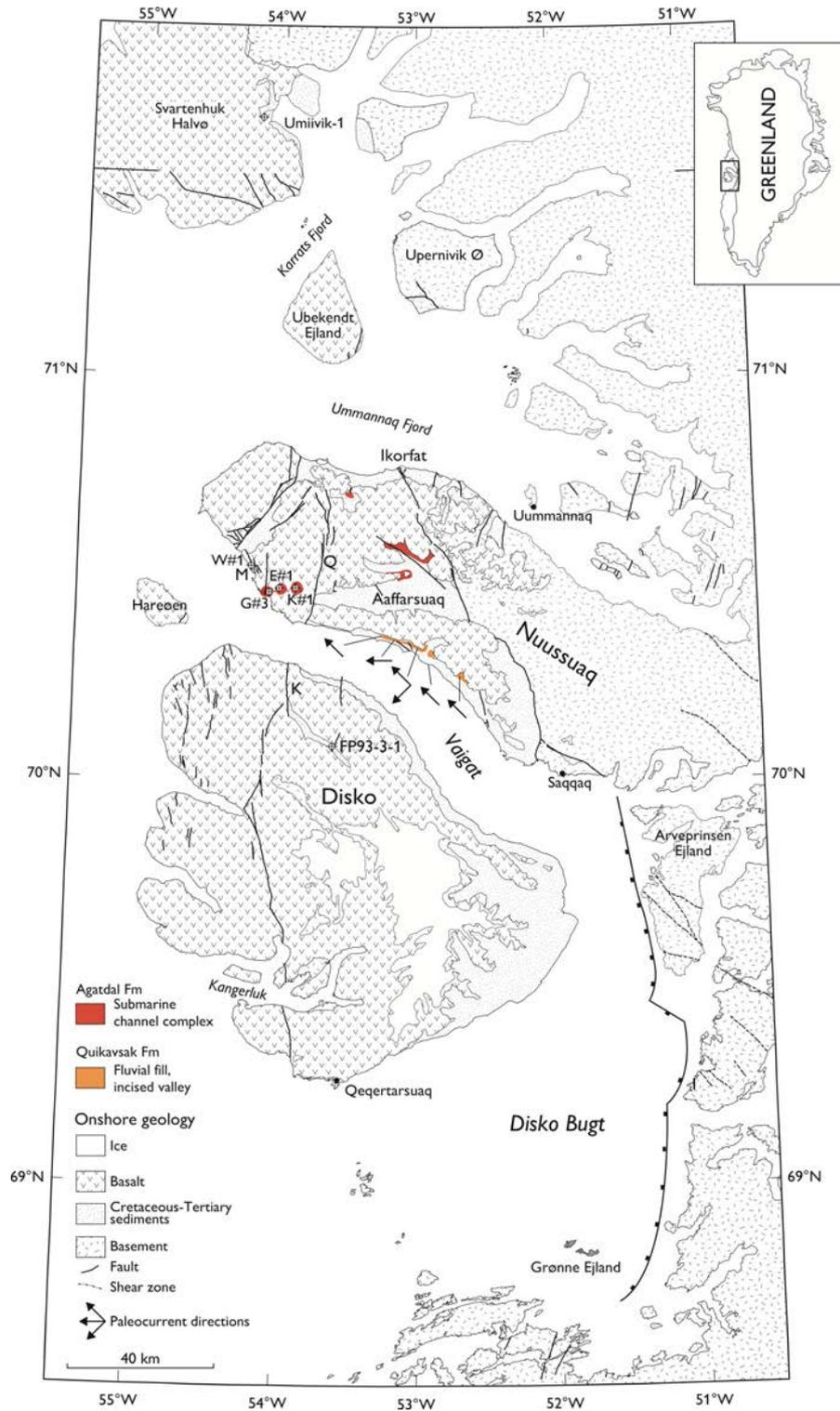
Figure 4.9. *Map showing the distribution of the Quikavsak Fm and the Agatdal Fm. The known distributions are shown in dark colours.*
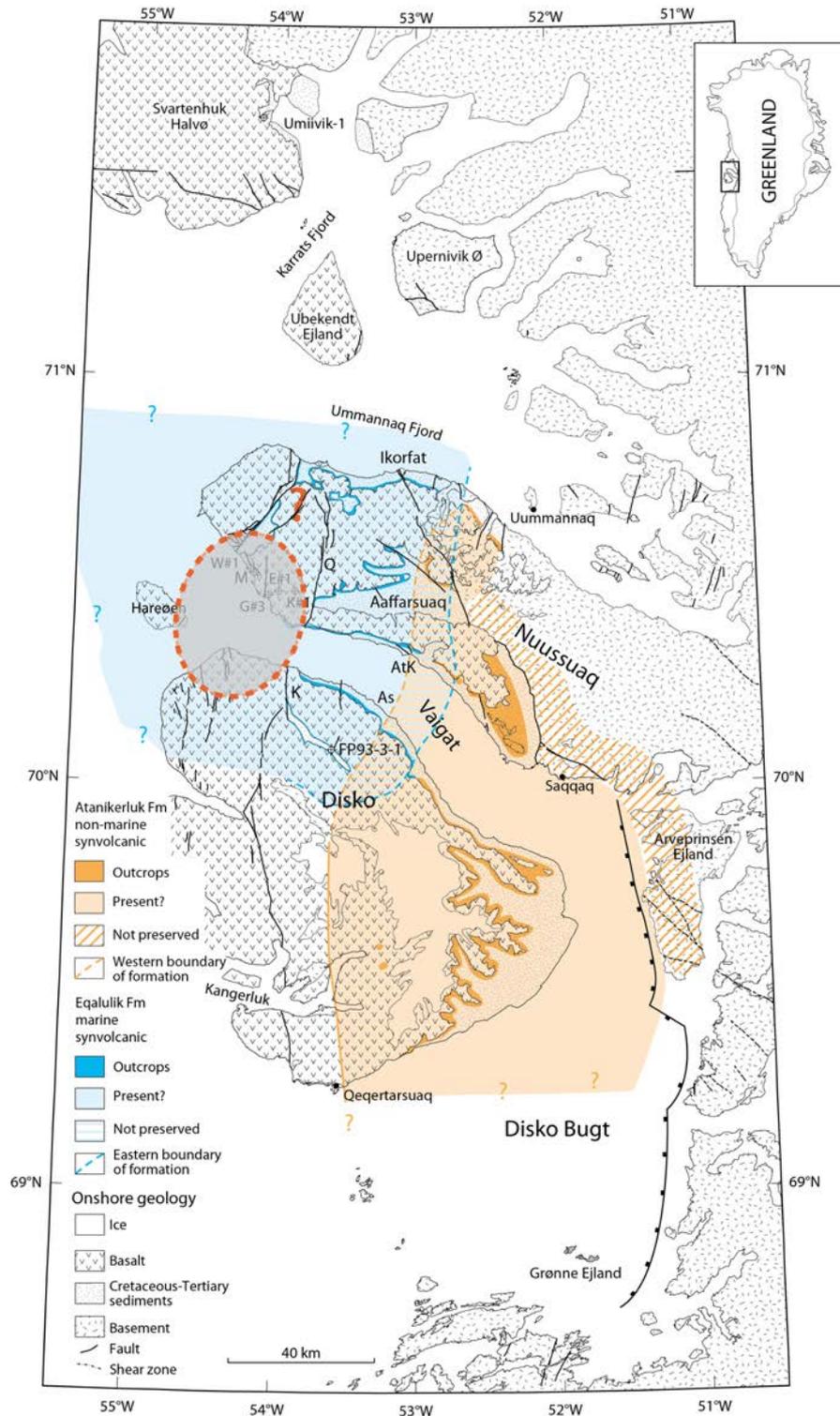
Figure 4.10. *Map showing the distribution of the Eqalulik Fm and the Atanikerluk Fm. The known distributions are shown in dark colours, the possible distribution in pale colours. The hatching indicates area where the formations are not preserved. Grey shaded area outlined in dashed orange is possible distribution of source rock from the Eqalulik Fm.*
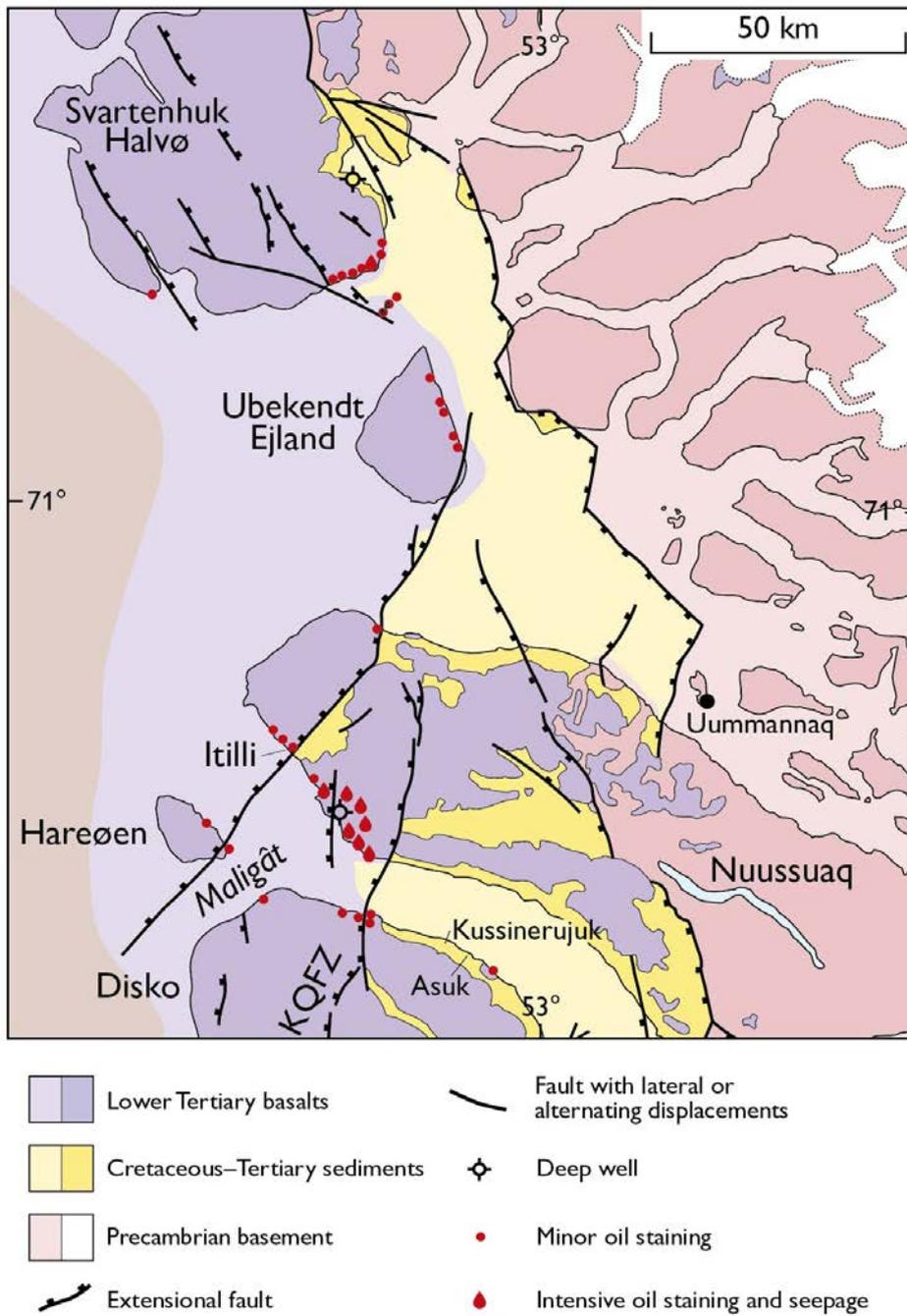
Figure 4.11. *Map showing occurrences of oil seepage and staining onshore West Greenland (from Bojesen-Koefoed et al. 2007).*

Figure 4.12. *(A) Vitrinite reflectance data from the GRO-3 well, barehole 247801 (ataata Kuua), and the coals from Ataa, Paatuut and Saqqaqdalen plotted against depth (corrected for exhumation). The data form a very well-constrained VR-trend for the area . It is seen, that the stata from the Atane Formation (all symbols except circles) were buried to depth of 1000–20000m and that they probably are immature with regard to generation of hydrocarbons. (B) On a semi-log plot, the VR data define a straight line cutting the surfacw at c. 0.2%Ro, as would be expected for correctly determined VR values. Data from Shekhar et al. (1982) and Bojesen-Koefoed et al. (1997). Figure from Pedersen et al. (2006).*

Figure 4.13. *Foreset-bedded hyaloclastites (Anaanaa Mb) in the western part of Nuussuaq.*

5. Petrophysical properties of key units

Niels H. Schovsbo & Morten L. Hjuler

5.1 Introduction

This chapter presents an overview of the reservoir properties of various formations in the Disko–Nuussuaq area based on analyses of key wells and outcrops. The aim is to outline the main porosity–permeability trends for the reservoirs and to present the net/gross ratio of the formations. In addition, suggestions for relevant future work on core material and cuttings in order to improve the reservoir evaluation are presented.

5.2 Wells and localities included

Six wells have been included in this review of reservoirs from the Disko–Nuussuaq area (Figure 5.1). The wells represent hydrocarbon exploration wells, mineral exploration wells, coal exploration wells and scientific wells. Most data are summarised by Sønderholm & Dam (1998). Outcrop data from 13 localities including 15 formations are used as a valuable supplement to the reservoir distribution and quality evaluation in the area. With respect to the outcrops, the systematic descriptions presented by Dam et al. (2009) are used as input for the evaluation.

5.3 Reservoir description

Reservoir parameters for the formations investigated are presented in Table 5.1. Parameters include: formation thickness, gross sand thickness, mudstone thickness, coal thickness, thickness of volcanics/hyaloclastites and the ratio of gross sand thickness/ formation thickness (the net/gross ratio). If available, information on grain size, hydrocarbon shows, and average porosity (core or log-derived) are included in Table 5.1.

For outcrops and wells, information of thicknesses and grain size was evaluated based on Dam et al. (2009). Following Dam et al. (2009), non-reservoir sections were defined as muddy to silty and heterolithic lithologies. Reservoir sand has been defined as sand beds with less than 15% clay content.

When available, mean porosities for the formations are provided. The porosity values were derived from core data and each porosity value represents the arithmetic mean of a formation. In the wells investigated, sampling was not necessarily performed with a fixed (and high density) sampling rate, which is otherwise mandatory when sampling in exploration wells. Thus, some sandstone beds were not sampled systematically. Variations in sampling procedure will impact on the resulting arithmetic mean, which should be taken into consideration when porosities are evaluated.

In the GRO-3 and Marraat-1 wells, new wireline log interpretations were performed in order to identify the vertical lithology distribution and assess the thickness of the accumulated

gross sand and net sand intervals. The well log-based mean porosities of these wells were calculated from porosity values with a porosity cut-off of 10% applied. Thus, porosities < 10% were excluded from the calculated mean in reservoir sections.

In this study, the reservoir section was defined as a rock interval with low clay content since these minerals are known to impact negatively on the reservoir performance. Typical clean reservoirs were defined as reservoir rock with less than 30% clay volume (Vshale). Since clay minerals tend to incorporate radioactive elements such as K, and Th a Vshale index curve was constructed from the gamma log and used as guide in selecting the reservoir rocks. XRD data was not available for calibration of the Vshale index. Instead, Vshale was used as reservoir qualifier with clean sand defined as having a Vshale of 0% and a Vshale of 100% was assumed to occur in the most gamma ray active parts of the mudstone. Thus, a shale cut-off of 30% was used to separate reservoirs from non-reservoirs (See Tables 5.2 & 5.3). In the volcanic sequence of Marraat-1, this approach could not be used and, as a substitute, a gamma ray cut-off of 10 API was used to differentiate between reservoirs and non-reservoirs (Table 5.4). A porosity cut-off of 10% net reservoir thickness was estimated (Table 5.5).

It should be stressed that the assumption that the gamma ray can be used as proxy for clean sand interval may not be true and thus that the above method should always be validated by independent means. In a case study for the Atane Formation, Pedersen et al. (2013) showed that the gamma ray curve could not be used to discriminate between sandstone and mudstone lithologies due to the presence of potassium feldspars in the sandstone and abundance of kaolinite clay in the mudstone. Under such circumstances other wire-line log tools such as neutron porosity and sonic logs should be applied. In this study, lithological information gained from cores and cuttings has been used to validate the wireline log interpretations.

Applying the shale cut-off provides an averaged porosity that is typically 6–15% higher compared to the average porosity when no shale cut-off is applied. Thus, using the shale cut-off provides a more realistic estimate of the averaged formation porosity and a more realistic basis for estimating the reservoir parameters of a potential reservoir, which is likely to occur only in the most porous part of the formation (Tables 5.1 & 5.2).

Grain sizes depend on facies and vary widely within the formations. Porosity is theoretically nearly grain size independent and depends more on the sorting and on the diagenesis that the rock has experienced. The permeability, on the other hand, is highly dependent on grain size with the highest permeabilities occurring in the more coarse-grained rock types. In addition, permeability will be lowered in poorly sorted rock types and where fibrous pore filling cement occurs. In general, coarse to pebbly grain sizes are common in channel facies and fine to very fine grain sizes are typical in distal turbidite rocks. In the wells analysed, channel facies have the highest porosities and permeabilities, whereas the turbidite facies have the lowest porosities and permeabilities.

Information on hydrocarbon (HC) shows is included when available. No systematic review of HC show occurrence has been performed since this was not the scope of this study. However, we do note that gas shows and oil shows tend to be associated with the highest permeabilities and porosities, as seen in the GANE-1 well. Whether this trend is a general feature and directly applicable to other wells is currently unknown.

T" œble 5.1. *Overview of reservoir properties in formations encountered in wells and outcrops. See Chapter 4 for detailed stratigraphy and lithology.*

Coordinates	UTM X	UTM Y	Well name	Outcrop name	Formation	Member	Petroleum system element	Formation m TVD	Volcanics m	Hyaloclastite Gross m	Hyaloclastite Net m	SAND Gross m	SAND Net m	Mudstone m	Coal m	Intrusive m	N/G hyaloclastite	N/G sandstone	Sandstone thickness divided w. mudstone thickness	Sandstone grain size	Porosity Formation %	Porosity Gross %	Porosity Net %	Hydrocarbon shows
			FP94-11-04		"Intrusive complex"		Reservoir/seal	106	0	0	0	0	0	0	0	106	0.00	0.00	-	-	-	-	-	
			FP94-11-04		Itilli		Reservoir/source rock	235	0	0	0	120	-	115	0	0	0.00	0.51	1.04	-	-	-	-	Gas
			FP93-3-1		Atane	Umiivik	Reservoir	62	0	0	0	33	-	29	0	0	0.00	0.53	1.14	m	-	-	-	
71°36.70'N, 54°02.52'W			Umiivik-1		Itilli	Umiivik	Reservoir/source rock	1200	0	0	0	21	-	910	0	240	0.00	0.02	0.02	vf	-	-	-	
			Gant-1		Kengilia	Annertuneq Conglomerate	Reservoir	156	0	0	0	113	-	43	0	0	0.00	0.72	2.63	m-m(p)	-	-	-	
			Gant-1		Itilli	Umiivik	Reservoir/source rock	646	0	0	0	133	-	491	0	22	0.00	0.21	0.27	f-c	-	-	-	Oil
	608683.0	7820083.0	Gro-3		Vaigat		Reservoir/seal	265	265	265	-	0	0	0	0	0	1.00	0.00	-		-	-	-	
			Gro-3		Eqalulik		Reservoir	120	2	2	-	14	5	100	0	4	0.02	0.12	0.14		5	11	24	
			Gro-3		Agatdal		Reservoir	295	45	0	0	148	68	102	0	0	0.00	0.50	1.46		6	9	12	
			Gro-3		Kengilia		Reservoir	241	0	0	0	134	16	83	0	20	0.00	0.56	1.61		4	6	11	
			Gro-3		Itilli	Anariartorfik	Reservoir/source rock	2040	0	0	0	458	23	1531	0	51	0.00	0.22	0.30		1	4	13	
			Gane-1/1A		Vaigat	Annaanaa	Volcanics	497	471	469	-	0	0	0	0	0	0.94	0.00	-		14	-	-	Oil
70°28.25'N, 54°00.40'W			Gane-1/1A		Eqalulik		Reservoir	100	0	0	0	40	-	60	0	0	0.00	0.40	0.67		5	-	-	
			Gane-1/1A		Agatdal		Reservoir	106	0	0	0	71	-	18	0	9	0.00	0.67	3.94		11	-	-	Gas/oil
			Gank-1		Vaigat	Annaanaa	Volcanics	80	80	80	-	0	0	0	0	0	1.00	0.00			-	-	-	Oil
			Gank-1		Eqalulik		Reservoir	235	0	0	0	20	-	193	0	12	0.00	0.09	0.10		-	-	-	Oil
			Gank-1		Kengilia		Reservoir	67	0	0	0	0	0	50	0	0	0.00	0.00	0.00		-	-	-	Oil
			Ganw-1		Vaigat		Reservoir/seal	800	800	671	-	0	0	0	0	0	0.84	0.00	-		-	-	-	
			Marraat-1		Vaigat		Reservoir/seal	450	450	216	80	0	-	0	0	0	0.48	0.00	-		10	10	17	Oil
70°19.87'N, 52°55.18'W			GGU 247.801 (Ataata Kuua well)		Atane	Qilakitsoq	Reservoir	566	0	0	0	306	-	230	30	0	0.00	0.54	1.33	f-c	17	-	-	
70°38.60'N, 52°21.83'W				Majorriallattarfik	Kome		Reservoir	115	0	0	0	75	-	38	2	0	0.00	0.65	1.97	f-vc	-	-	-	
71°09.88'N, 52°54.52'W				Upernivik Næs	Upernivik Næs		Reservoir	560	0	0	0	475	-	85	0	0	0.00	0.85	5.59	f-c	-	-	-	
					Atane	Kingittoq	Reservoir	82	0	0	0	65	-	15	2	0	0.00	0.79	4.33	f-m	-	-	-	
70°46.20'N, 53°03.37'W				Ikorfat	Atane	Ravn Kløft	Reservoir	365	0	0	0	300	-	55	10	0	0.00	0.82	5.45	m-c	-	-	-	
					Slibestensfjeldet		Reservoir	35	0	0	0	23	-	11	1	0	0.00	0.66	2.09	vf-f	-	-	-	
				Pingunnguup Kuua	Itilli		Reservoir/source rock	680	0	0	0	230	-	450	0	0	0.00	0.34	0.51	f-c	-	-	-	
70°36.35'N, 54°13.79'W				Ukalersalik	Itilli		Reservoir/source rock	370	0	0	0	160	-	210	0	0	0.00	0.43	0.76	f-c	-	-	-	
70°36.35'N, 54°13.79'W				Anariartofik	Itilli	Anariartorfik	Reservoir/source rock	710	0	0	0	100	-	602	0	8	0.00	0.14	0.17	f-c	-	-	-	
70°09.77'N, 52°31.38'W				Kingittoq	Atane	Kingittoq	Reservoir	490	0	0	0	345	-	115	30	0	0.00	0.70	3.00	f-c	-	-	-	
70°27.97'N, 53°27.13'W				Qilakitsoq	Atane	Qilakitsoq	Reservoir	485	0	0	0	320	-	150	15	0	0.00	0.66	2.13	f-c	-	-	-	
				Ataata Kuua	Kangilia		Reservoir	150	0	0	0	60	-	90	0	0	0.00	0.40	0.67	f-c	-	-	-	
69°15.27'N, 52°40.65'W				Tupaasat	Quikavsak	Tupaasat	Reservoir	83	0	0	0	83	-	0	0	0	0.00	1.00	-	c-peb	-	-	-	
69°15.27'N, 52°40.65'W				Patuutkløften	Quikavsak	Patuutkløften	Reservoir	145	0	0	0	143	-	2	0	0	0.00	0.99	71.50	c-peb	-	-	-	
69°47.13'N, 52°02.12'W				Pingu	Atanikerluk		Reservoir	420	0	0	0	321	-	86	2	13	0.00	0.76	3.73	m-c	-	-	-	
69°47.13'N, 52°02.12'W				Pingu	Atane	Skansen	Reservoir	62	0	0	0	60	-	0	2	0	0.00	0.97	-	m-c	-	-	-	
70°03.63'N, 52°13.53'W				Nuugaarsuk	Atanikerluk		Reservoir	350	0	0	0	260	-	90	1	0	0.00	0.74	2.89	m-c	-	-	-	

5.4 Well log-derived porosity, reservoir thickness and shale volumes

Well	Formation	Rock type	Formation thickness (m)	Mean Porosity (%)	Reservoir thickness (m)
	Vaigat	Volcanic	265	-	-
	Eqalulik	Clastic	120	10.8	14.1
GRO-3	Agatdal	Clastic	295	9.0	148.1
	Kangilia	Clastic	241	5.7	134.3
	Itilli	Clastic	2040	3.7	458.1

Table 5.2. *Gross reservoir thickness and mean porosity of the GRO-3 well using a shale cut-off (Vshale) of 30%.*

Well	Formation	Rock type	Formation thickness (m)	Mean porosity (%)	Reservoir thickness (m)
	Vaigat	Volcanic	265	-	-
	Eqalulik	Clastic	120	24.2	5
GRO-3	Agatdal	Clastic	295	12.3	68
	Kangilia	Clastic	241	11.0	16
	Itilli	Clastic	2040	13.5	23

Table 5.3. *Net reservoir thickness and mean porosity of the GRO-3 well using a shale cut-off of 30% and a porosity cut-off of 10%.*

Well	Formation	Rock type	Formation thickness (m)	Logged interval (m)	Mean Porosity (%)	Reservoir thickness (m)
Marraat-1	Vaigat	Volcanic	450	346	10.1	106

Table 5.4. *Gross reservoir thickness and mean porosity of the Marraat-1 well based on the logged interval. As shale cut-offs cannot be used in volcanic rocks, a gamma ray cut-off of 10 API was applied to provide an assessment of porosity.*

Well	Formation	Rock type	Formation thickness (m)	Logged interval (m)	Mean Porosity (%)	Reservoir thickness (m)
Marraat-1	Vaigat	Volcanic	450	346	16.5	118

Table 5.5. *Net reservoir thickness and mean porosity of the Marraat-1 well based on the logged interval. As shale cut-offs cannot be used in volcanic rocks, a gamma ray cut-off of 10 API was applied to provide an assessment of porosity. Afterwards a porosity cut-off of 10% was applied.*

5.5 Clastic reservoir thickness

In Figure 5.2, the thickness of the formation is compared with the thickness of the sand within the formation. In the diagram, the pure sand prone formations plot along the 1:1 line whereas shale dominated formations plots with a low ratio. In the Disko–Nuussuaq area, formations with high sand ratios are found in many different settings, ranging from fluvial-deltaic, e.g., the Atane Formation, to slope settings such as the Agatdal Formation (Table 5.1). The only unit with general low ratios (<0.5) is the Itilli Formation, which includes clay dominated organic rich strata (Figure 5.2). It is important to note, however, that despite the low net/gross ratio, the formation typically consists of more than 100 m of sand interbedded with shale.

5.6 Porosity and permeability relationships for reservoirs

To illustrate the main trends of the key reservoirs in terms of porosity and permeability core analysis data from the GANE-1, GANT-1 and the Marraat-1 wells are presented in Figure 5.3. Currently, the core analysis database for the Disko–Nuussuaq area is not representative for the total variation seen in the reservoirs. At this stage, the database is only used to point out the main development and controls on the reservoir properties.

The lavas and the hyaloclastites in the GANE-1 and Marraat-1 wells define two almost mutually exclusive trends within the porosity versus log permeability diagram (Figure 5.3). The Marraat-1 lava flows typically plot with 0–18% porosity and with 0.01 to 10 mD permeability. The porosity-permeability parameters are positively correlated and thus define a relatively low permeability trend in Figure 5.3. Few samples plot away from the trend line, mostly having higher permeabilities than defined by trend B. These samples are interpreted to have enhanced permeabilities due to fractures.

Generally, the hyaloclastites in the GANE-1 well plot with much lower porosities compared to the lavas from the Marraat-1 well. The porosities generally range between 0–10%. The permeabilities mostly range from 0.01 to 20 mD. The two parameters are positively correlated and define two trends in Figure 5.3. For the hyaloclastites few samples plot away from trend A, both with higher and lower permeabilities as expected from trend A. The deviations away from the general trend line are interpreted to reflect the presence (higher permeabilities) or absence (lower permeabilities) of micro-fractures in the sample.

Compared to these two trends mentioned above and highlighted in Figure 5.3, the sandstone lithologies analysed in the GANE-1 and GANT-1 wells generally plot with intermedi-

ate porosities and permeabilities (Figure 5.3). In the two wells, two main groupings can be identified. The bulk of the samples plot with porosities in the range 5–19% and permeabilities between 0.05 and 10 mD whereas a minority of the samples plot with porosities in the range 0–10% and permeabilities between 0.5 and 30 mD (Figure 5.3).

The two groupings possibly reflect differences in grain size and/or diagenetically induced deterioration of the permeabilities. However, the amount of micro fractures in the rock may also play a role. The trend expressed by the bulk group of samples is interpreted to reflect matrix porosities that tend to be related to porosity in a positively correlated manner.

5.7 Key reservoir units

The key siliciclastic reservoirs in the Disko–Nuussuaq area include the Cretaceous Atane Formation, the late Maastrichtian–early Palaeocene Kangilia Formation, the Cretaceous Itilli Formation, and the Palaeocene Agatdal Formation. In addition, important reservoir units include the volcanoclastic sequence as seen in the Marraat-1 well. Below are some of the main parameters governing the petrophysical properties of these key units. For the sedimentological and stratigraphic details see chapter 4.

5.7.1   Atane Formation

In parts of Disko, the formation consists of thick alluvial flood plain deposits of medium- to coarse-grained sheets. Toward the north-west the floodplain sandstones grade into delta front and delta plain deposits. In the Ataata Kuua well, the porosity of the sandstones unit range up to 25%, with mean values around 17% (Figure 5.4).

The Atane Formation attains a thickness up to 800 m (Dam et al. 2009). In the Ataata Kuua well the formation is 566 m with a net/gross ratio of 50% (Table 5.1). Typical reservoir beds are between 5–15 m thick and consist of laterally extensive sand sheets. Regional distribution of porosities and permeabilities are poorly known as are the main diagenetic controls on reservoir quality. In the cores study made on parts of the Ataata Kuua well (Pedersen et al. 2013; Appel & Joensen 2014) the porosity varies between 5–25% with mean values of 17% in the sands (Figure 5.4). Permeabilities vary between 0.5–150 mD (Appel & Joensen 2014).

5.7.2   Itilli Formation

The Itilli Formation is estimated to be in excess of 2.5 km thick (Sønderholm & Dam 1998). The formation is dominated by mudstones but thinly interbedded sandstones occur. Beds up to 50 m thick and 1–2 m wide of channelized sandstones deposited in a slope apron setting occur (Sønderholm & Dam 1998). The turbidites and channel sandstones are medium-grained to very coarse-grained. Representative porosity and permeability samples are lacking. Close to the Itilli fault, porosities range up to 10% and permeabilities are less than 1 mD which probably reflect localised hydrothermal circulation and enhanced diagenesis (Sønderholm & Dam 1998).

In the GRO-3 well, more than 2200 m of Itilli Formation was drilled (Figure 5). The accumulated sandstone thickness is about 480 m with individual beds reaching thicknesses up to 100 m (Table 5.2, Figure 5.5, Sønderholm & Dam 1998). The average porosity of all reservoir units is 3.7% porosity with a shale cut-off 30% applied. About 23 m of sandstone has a porosity of more than 10% (Table 5.3).

5.7.3   Kangilia Formation (Conglomerate Member)

The Kangilia Formation is mudstone dominated in most parts of the study area but in Nuussuaq a submarine canyon conglomerate-sandstone unit referred to as the conglomerate member occurs (Sønderholm & Dam 1998). In the GANT-1 well, this member has porosities in the range 5.7–17.5 % and has permeabilities up to almost 219 mD (Sønderholm & Dam 1998) suggesting that locally this unit could be of importance as reservoir. The thickness varies between 67 m and 241 m with a net to gross ratio of up to 72% (Table 5.1).

In the GRO-3 well, the Kangilia Formation is 241 m thick (Figure 5.6). The upper and middle parts of the formation consists almost exclusively of mudstone, only one bed of igneous intrusive breaks the lithological monotony. 11 m of continuous sandstone dominates the lower part of the formation and average porosity is 5.7%. Of this, 16 m of sandstone has a porosity higher than 10%.

5.7.4   Agatdal Formation

Reservoir properties of the Agatdal Formation are presented in Figure 5.7. The lower 20 m of the formation in the GANE-1 well includes thickly bedded coarse-grained to very coarse-grained sandstone beds deposited in a channelized canyon environment. The porosities range from 6.4–20.6 % and permeabilities are up to 10 mD. In the GANE-1 well, the porosities show a general decreasing trend with decreasing depths below 660 m. In the lower part of the well, in the Agatdal Formation, gas bearing coarse to pebbly sands tend to have higher average values than none-gas bearing sections.

In the GRO-3 well, the Agatdal Formation is 295 m thick (Figure 5.8), consisting of sandstone, mudstone and frequent layers of tufa. With an accumulated thickness of 148 m, sandstone dominates the lithology, with the main concentration in the lower part of the formation. Numerous sandstone layers of varying thickness are distributed across the entire formation. Single sandstone beds reach thicknesses up to 30 m and the average porosity of the sandstones is 9.0%. When a porosity cut-off of 10% is applied the accumulated sandstone thickness is reduced to 68 m and average porosity increases to 12.3%.

5.7.5   Vaigat Formation

In the GRO-3 well, the Vaigat Formation is 303 m thick and composed entirely of hyaloclastites (Figure 5.9). 265 m has been logged. It was not possible to estimate effective porosity (PHIE).

In the Marraat-1 well, 450 m of the Vaigat Formation was drilled, but only the uppermost 346 m was logged. No shales were observed (Dam & Christiansen 1994), but by considering volcanic rocks with gamma ray readings close to background radiation, it was possible to establish an alternative expression for Vshale and estimate PHIE (Figure 5.10). Thus, a gamma ray cut-off of 10 API was applied. Most of the section logged exhibits low gamma ray readings. However, the uppermost 45 m exhibits high gamma ray readings often exceeding 200 API and may include radioactive mineralizations where porosity cannot be estimated. An average density of 3.0 g/cm^3 was assumed for the volcanic units using data from Dam & Christiansen (1994). PHIE was calibrated to porosity measurements performed on cores from the uppermost 90 m. The average PHIE is 10.3% for the 346 m logged with no gamma ray and porosity cut-offs applied. With a gamma ray cut-off of 10 API, the accumulated sand thickness is 216 m and the average PHIE is 14.3%. With the further application of a porosity cut-off, the reservoir thickness is 80 m and the average PHIE is 17.3ß%.

5.8 Knowledge gaps

A systematic analysis of porosity and permeabilities in the wells cored will be highly relevant to improve our understanding of the reservoir quality. The analysis should be associated with a description of petrophysical rock types. The porosity and permeability analysis will also benefit if this is done in combination with spectra core gamma scanning and density scanning of cores where no wireline log acquisition was performed (e.g., scientific and/or mineral exploration wells).

For further characterisation of the porosity and permeability trends, documentation of the pore size distribution by means of Hg-injection data will be needed.

Calibration of log derived porosities and Vshale values to core data such as porosity and mineral content (by XRD) will be relevant. In wells where only cuttings are available, the wire-line log interpreted lithologies and petrophysical interpretation can be strengthened by analysis of element composition, mineralogy, and grain density.

A systematic review of hydrocarbon show occurrences and the associated lithologies in the wells will be relevant to identify possible reservoir units and carrier beds.

5.9 Summary

The key reservoir units in the Disko–Nuussuaq area include the Atane Formation, the Kangilia Formation, the Itilli Formation, the Agatdal Formation and the volcanoclastic sequence. The reservoirs reflect a broad range of facies ranging from fluviatile/deltaic to deep slope setting.

The reservoir properties of the units are poorly known and no overall model for reservoir quality distribution can be made. Based on existing core data, selected key trends are defined that may help in an early exploration phase to assign *a prior* reservoir quality properties.

The hyaloclastite sequence in the GANE-1 well defined a low porosity but relatively high permeability trend. This suggests that this unit has very poor sealing properties and should be regarded as a reservoir. The permeability is interpreted to reflect the presence of micro-fractures. Lava flows, as seen in the Marraat-1 well, have very low permeabilities despite rather high porosities and could constitute potential seal for hydrocarbon accumulations.

Reservoir units with relatively low net/gross ration are considered to be positional units for stratigraphical traps. In such cases reservoir units may pinch out in interbedded shaly parts of the formation. This is notably seen in the Itilli Formation, which despite net to gross ratios between 10–80%, has several 100 m of sandy beds.
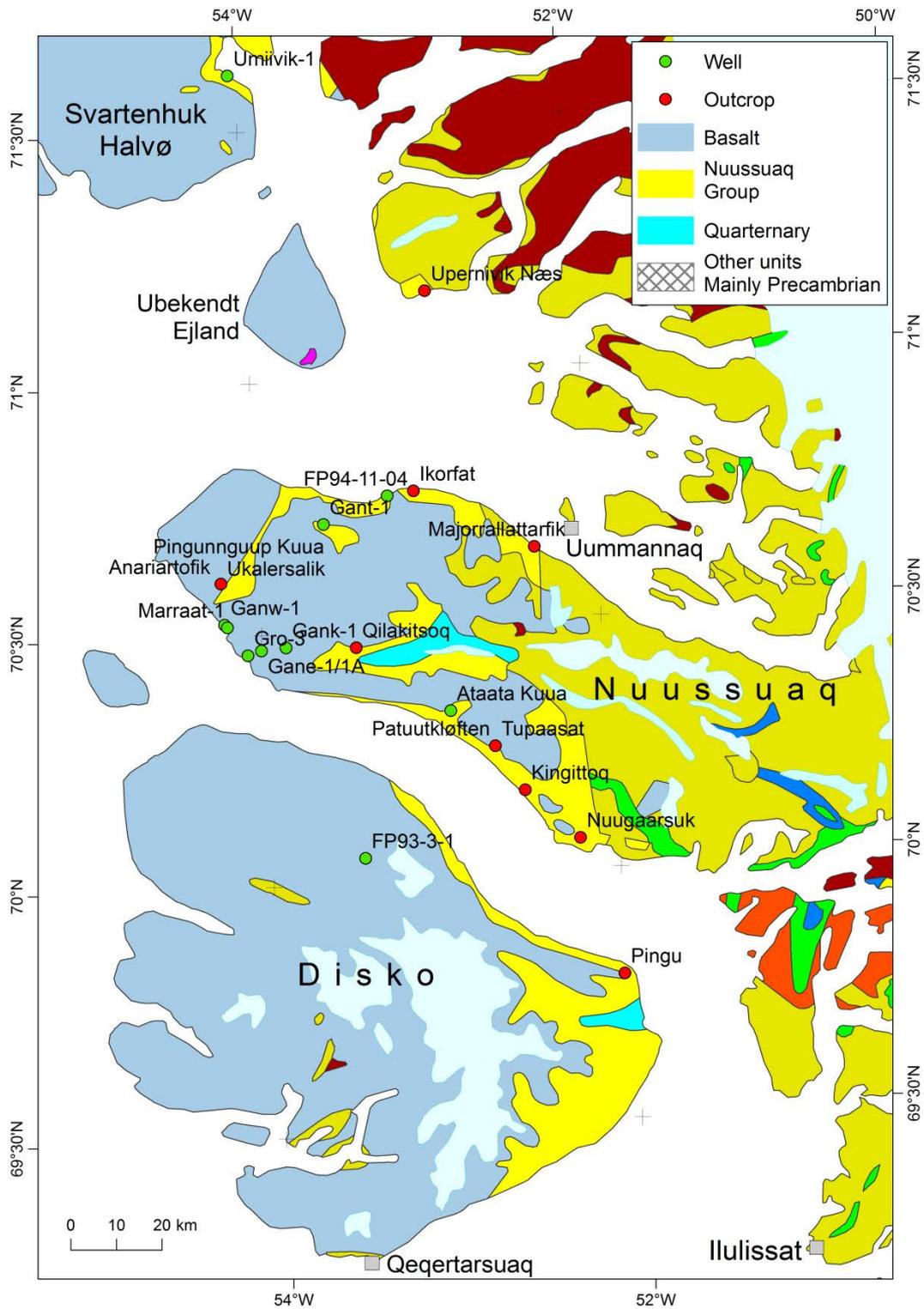
Figure 5.1. *Locality map showing wells and outcrop localities included. The outcrop locality at Ataata Kuua shares coordinates with the Ataata Kuua well on the map. Also Pingunnguup Kuua, Anariartofik and Ukalersalik share coordinates.*

GEUS
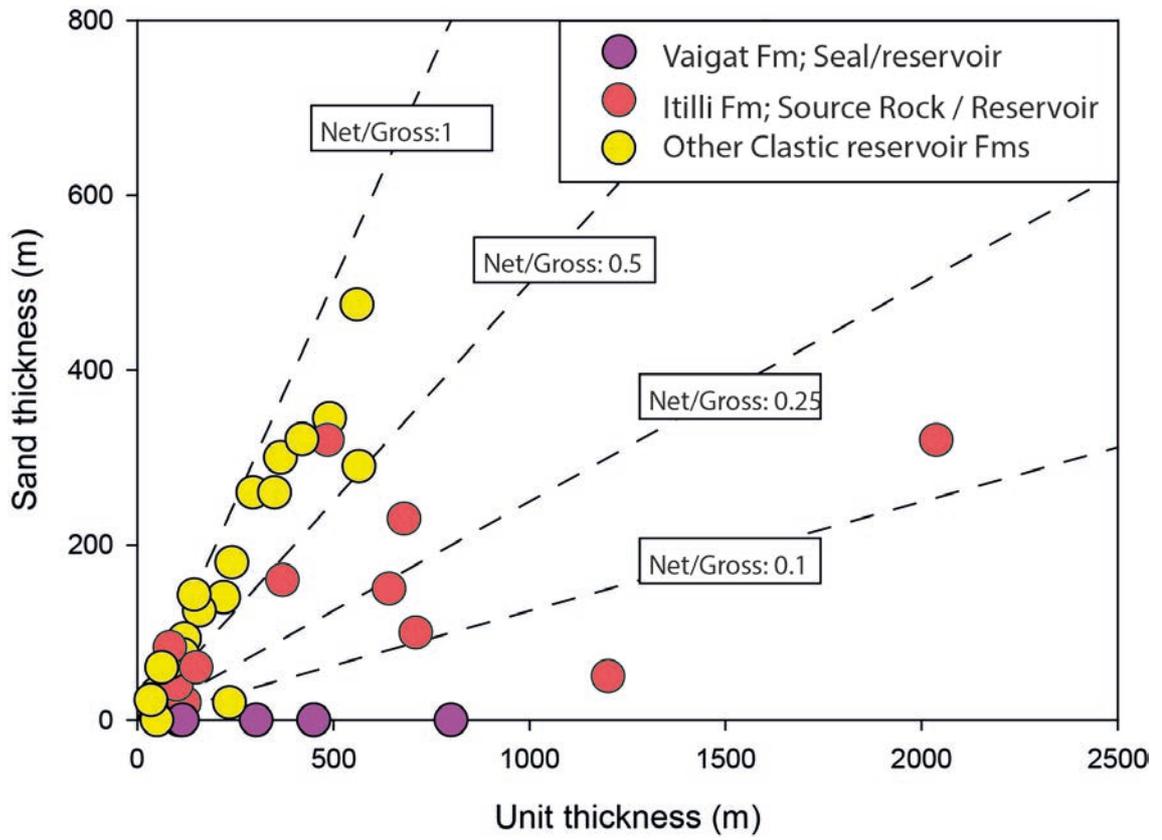
Figure 5.2. *Formation thickness versus sand thickness for wells analyzed and siliciclastic outcrops in the Disko–Nuussuaq area. Data from Table 5.1.*
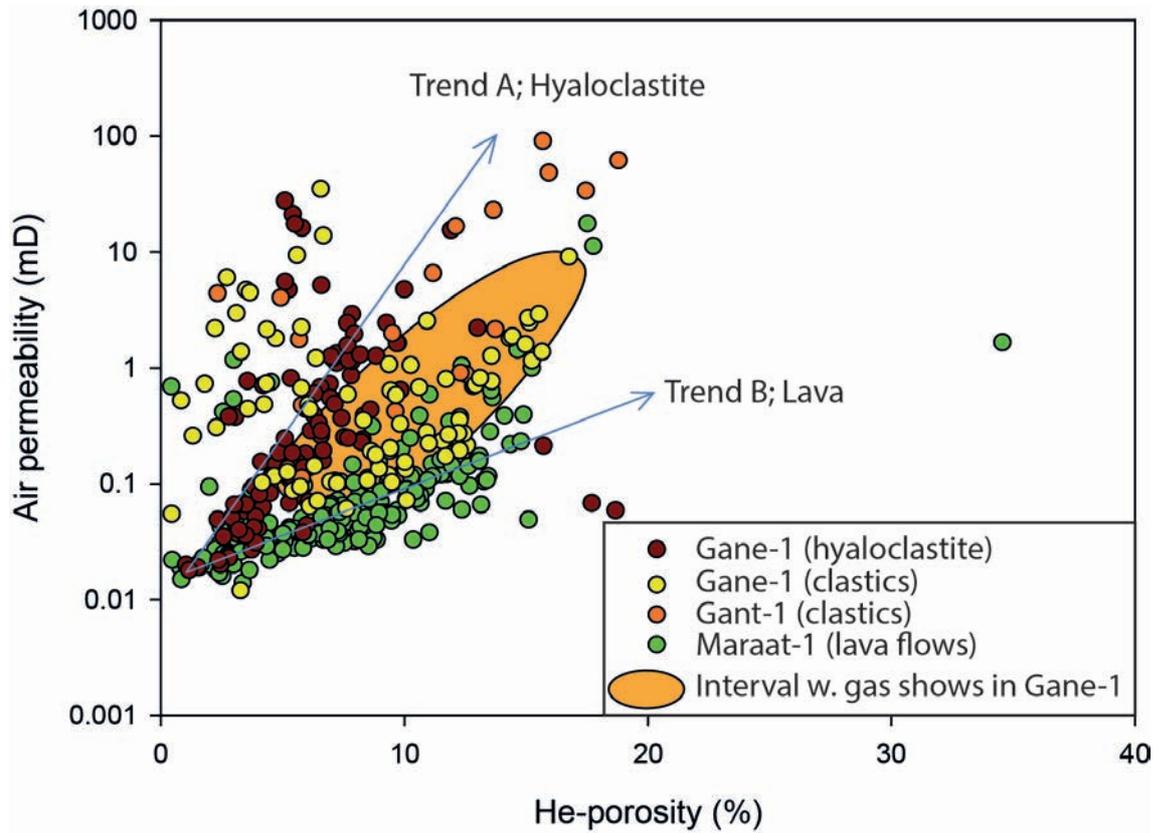
Figure 5.3. *Porosity and permeability relationships for selected wells. Core data from Andersen (1996) and GEUS' core laboratory database. In the GANE-1 well, the lower part of the Agatdal Formation contains gas shows which in Figure 3 are highlighted with orange fill.*
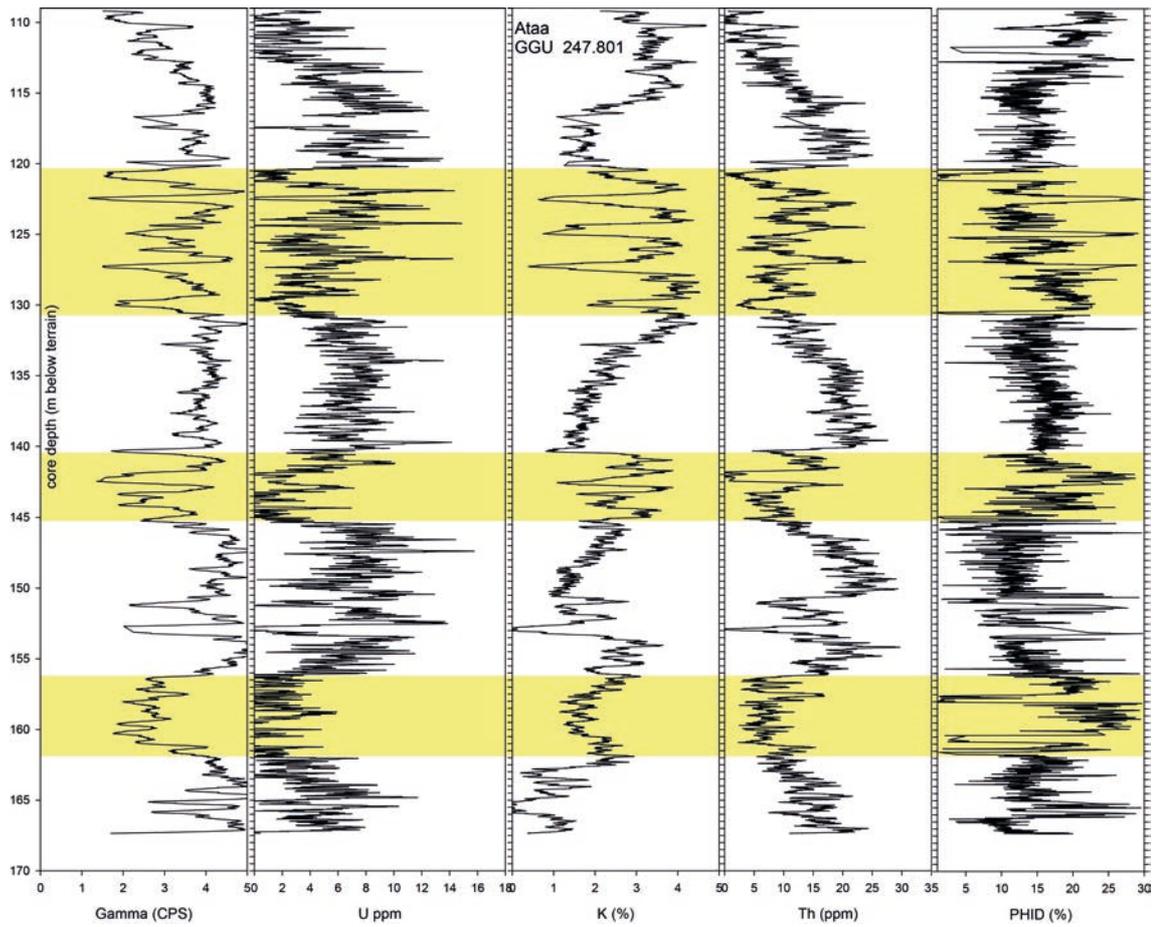
Figure 5.4. *Spectral gamma and density score scanning logs through a representative section in the Atane Formation from the Ataata Kuua well. Legend: yellow sandstone units. Based on Pedersen et al. (2013) and Appel & Joensen (2014).*
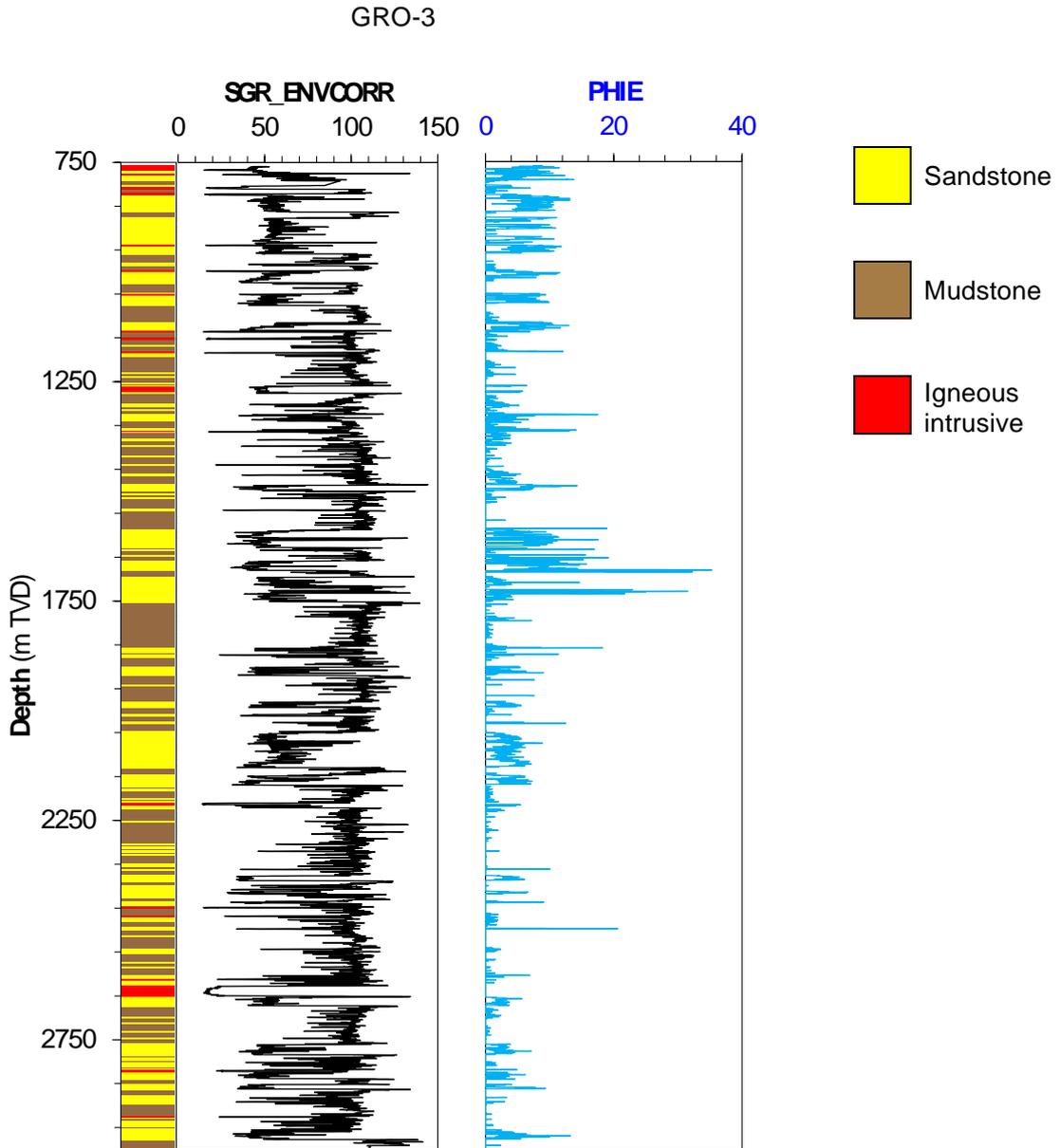
GRO-3

Figure 5.5. *Petrophysical log interpretation of the Itilli Formation in the GRO-3 well showing lithology, the environmentally corrected spectral gamma ray log (SGR_ENVCORR) and estimated effective porosity (PHIE).*
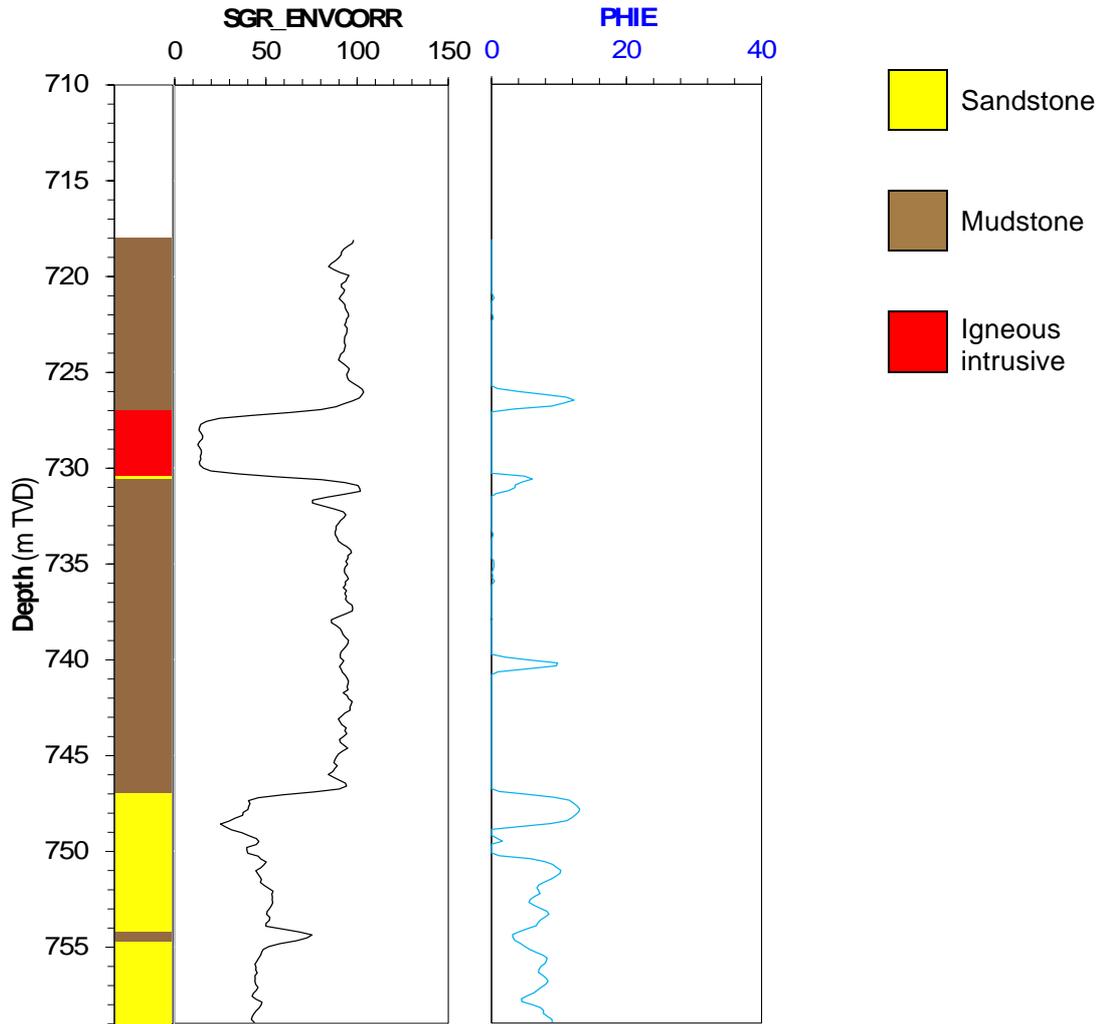
Figure 5.6. *Petrophysical log interpretation of the Kangilia Formation in the GRO-3 well showing lithology, the environmentally corrected spectral gamma ray log (SGR_ENVCORR) and estimated effective porosity (PHIE).*
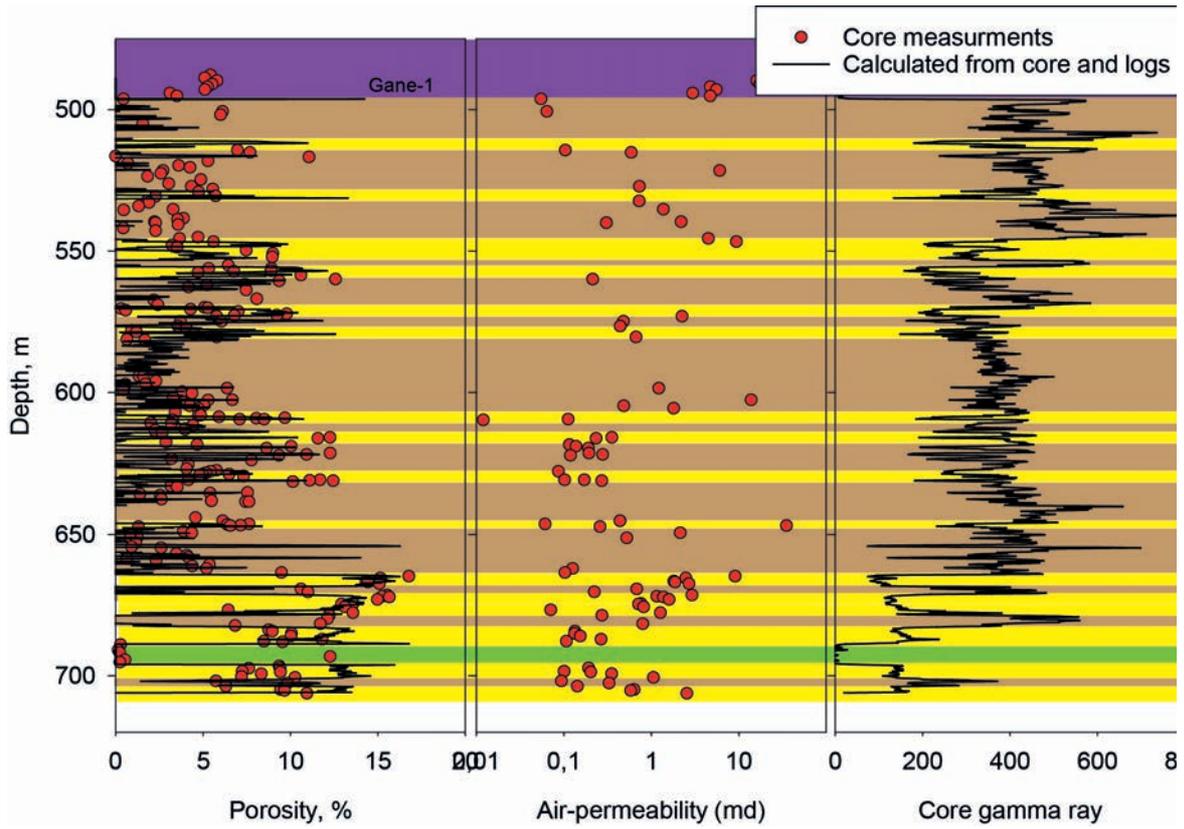
Figure 5.7. *Core analysis and core gamma for GANE-1/1a well. The Agatdal Formation between TD-600 m and Eqalulik Formation between 600–500 m. Legend green: intrusive rock, Yellow sandstone, brown: mudstone, purple: lava. The porosity curve is calculated from core and log data. Gas shows and oil shows were recorded during drilling of the section below 660 m. Core data from Andersen (1996).*
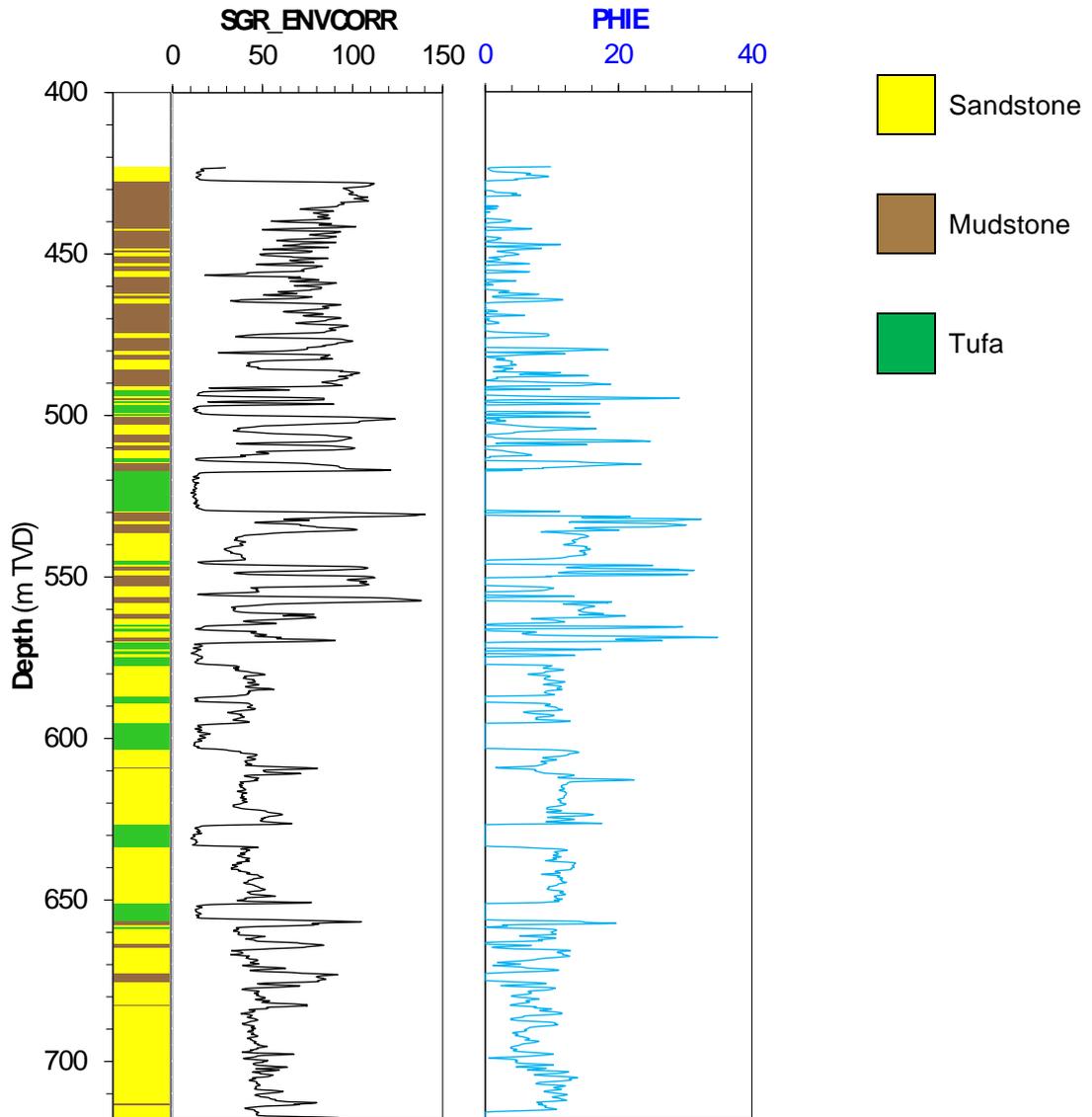
Figure 5.8. *Petrophysical log interpretation of the Agatdal Formation in the GRO-3 well showing lithology, the environmentally corrected spectral gamma ray log (SGR_ENVCORR) and estimated effective porosity (PHIE).*
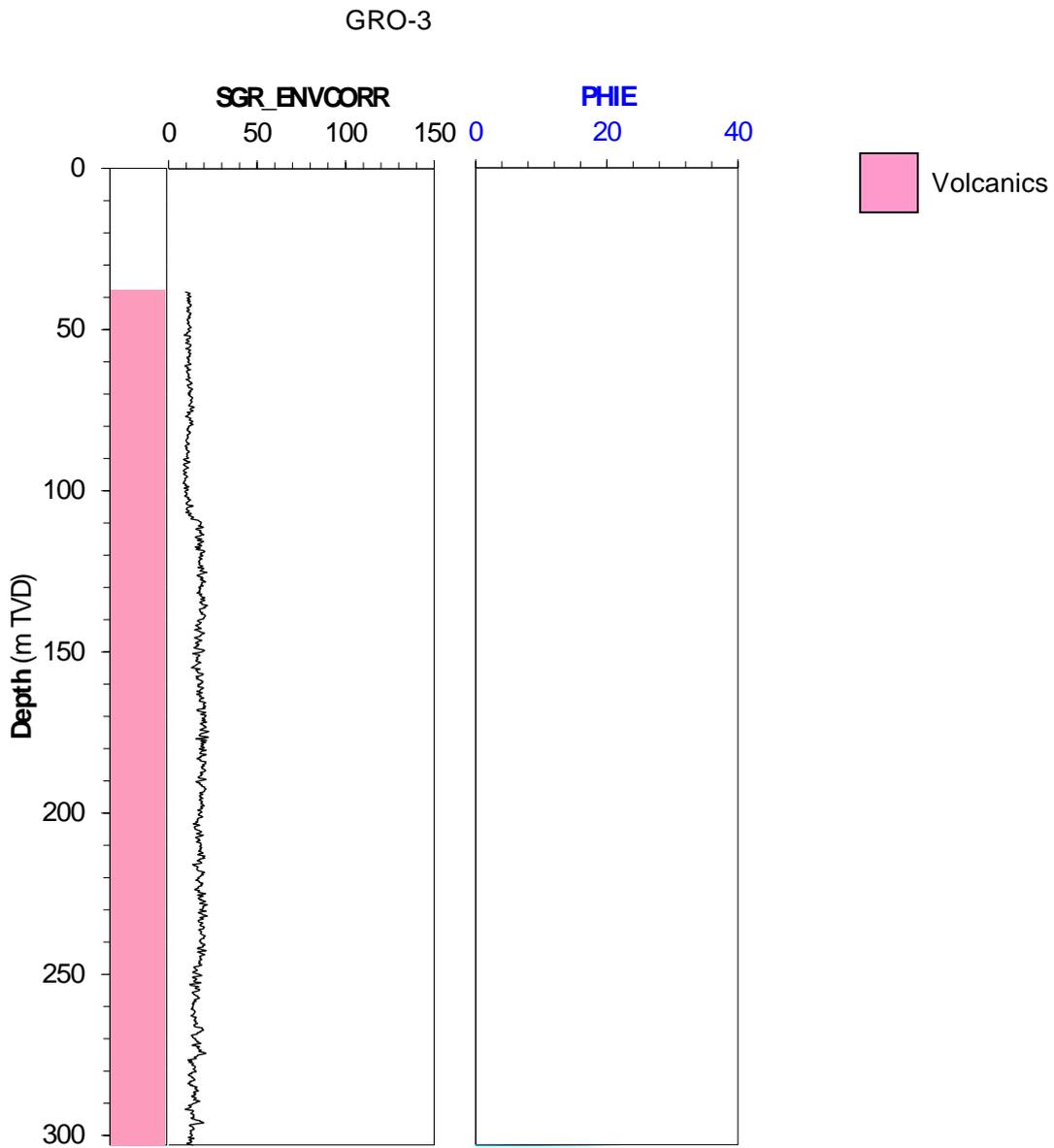
Figure 5.9. *Petrophysical log interpretation of the Vaigat Formation in the GRO-3 well showing lithology and the environmentally corrected spectral gamma ray log (SGR_ENVCORR). It was not possible to estimate effective porosity (PHIE).*
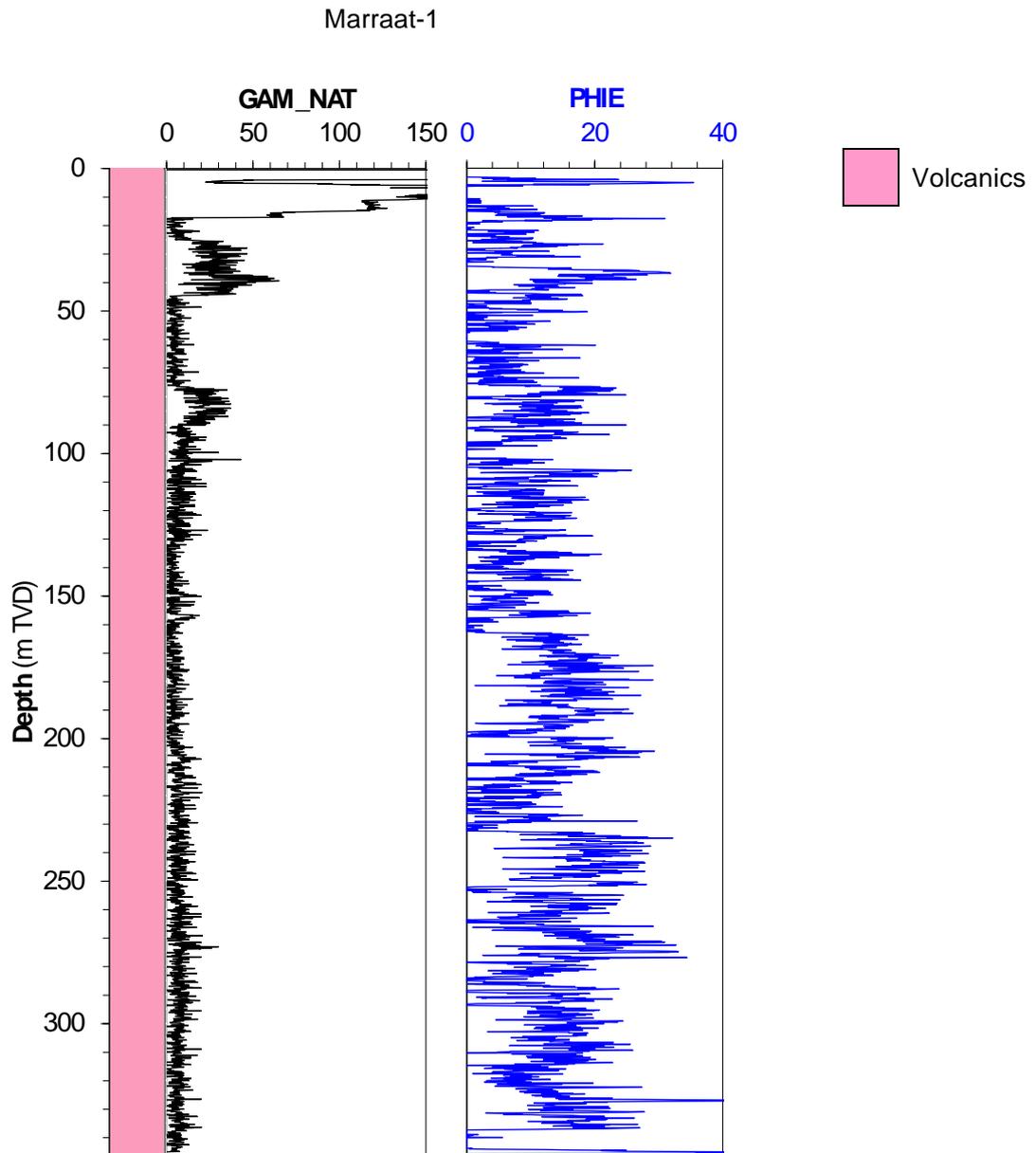
Figure 5.10. *Petrophysical log interpretation of the Vaigat Formation in the Marraat-1 well showing litholo-gy and the natural gamma ray log (GAM_NAT) and effective porosity (PHIE).*

6. Sediment composition and provenance

Christian Knudsen

6.1 Introduction

204 sediment samples have been analyzed for their major- and trace-element composition. The samples represent different lithologies spanning from sandstone, siltstone, shale to pyroclastic rocks. The samples are from outcrop as well as from the two onshore wells GRO-3 and Umiivik-1. The aim of the chemical analysis is to generate an overview of the compositional variations among the sediments. The chemical analysis was performed at ACT Labs in Canada using a combination of total fusion ICP-MS and Neutron activation techniques.

In a profile at Itsaku, samples collected in a profile covering the Upernivik Næs Formation, The Kangilia Formation and the Eqalulik Formation have been analyzed both for their chemical composition as well as their mineralogical composition and texture using Qem-scan. The analysis was performed by SGS Laboratories.

Detrital zircon grains from recent stream sediments have been analyzed for their age using Laser Ablation ICP-MS at GEUS (Scherstén et al 2007 and Scherstén & Sønderholm 2007). These data provide a comprehensive database for establishing fingerprints of the potential source terrains for the Cretaceous and Paleocene sandstones in the Disko–Nuussuaq area. In addition, a large number of detrital zircon grains in outcrop sandstone samples and samples from the GRO-3 onshore well have been analyzed for their detrital zircon age distribution patterns.

6.2 Geochemistry

The Atane Formation represents a major delta system with fluvial channels, lakes and swamps on a delta plain, a prograding marine delta front and marine shore-face deposits, whereas the sandstones of Upernivik Næs Formation were deposited in braided fluvial channels. On Figure 6.1 it can be seen that the samples from the Atane and Upernivik Næs Formations have fairly high contents of silica as compared to the Itilli, Kangilia and Eqalulik Formations due to a higher quartz content in Atane and Upernivik Næs Formations.

Atane and Upernivik Næs Formations also fall on a different trend as compared to the other formations on Figure 6.2. This higher K/Al ratio indicates a high content of K-feldspar in the Atane and Upernivik Næs Formations, a feature that they share with the samples from the Kangilia Formation (outcrop) where there is a very high content of K-feldspar.

In the Itsaku section (Figure 6.3) the Upernivik Næs Formation shows covariation between Fe_2O_3 and CaO with LOI (Loss on Ignition) indicating the presence of siderite to ferric do-lomite and calcite cement. LOI is also coupled to CaO in the Kangilia and Eqalulik for-mations, probably caused by calcite cementation. The geochemical profile on Figure 6.3

shows a significant increase in the content of K_2O from the Upernivik Næs Formation to the Kangilia Formation, indicating a further increase in the content of K-feldspar followed by a sharp decrease in the Eqalulik Formation where other feldspars dominate. The content of elements such as P, Ti, Th, Ce and Zr increases in Kangilia Formation indicating increasing content of heavy minerals such as apatite, ilmenite, zircon and monazite when entering into the Kangilia Formation, a content that decreases again in Eqalulik Formation. The content of elements such a Co, V, Ni and Cr is high in the Kangilia Formation and even higher in Eqalulik Formation which probably is a sign of influx of material derived from the mafic volcanics.

6.3   Mineralogy and textures

The Upernivik Næs Formation is rich in K-feldspar (Figure 6.4) as indicated by the geochemistry and the sand can be classified as sub-arkose to arkose. The grain-size varies from fine- to coarse-grained and kaolin is a common phase filling the pore-space. Carbonate cements are also found as mentioned above. Both calcite and ferric dolomite can be seen on Figure 6.4. The porosity is better in the more coarse-grained sections. Towards the top of the formation, the content of muscovite increases and the content of kaolinite decreases. Kaolinite may be related to a deeply eroded hinterland and the change may suggest a change in the source to less altered basement.

The Kangilia Formation, as noted above, is very rich in K-feldspar clasts (Figure 6.5). Muscovite and biotite clasts are common in the basal part and form a fabric (Figure 6.5). Higher in the section, the muscovite and biotite is less common and chlorite clasts are abundant, probably representing altered mafic volcanic input. The general impression is that the sediment is immature. It should be noted that there are carbonate (calcite) clasts present in the upper part as well.

In the Eqalulik Formation (Figure 6.6), quartz only constitutes a minor proportion of the clastic material and chlorite particles dominate. Calcic plagioclase is also common, indicating that a mafic source is near as these minerals do not travel very far. The clasts are angular, there are rock-fragments, and the sediment is very immature. There are two types of carbonate clasts: calcite and ferric dolomite.

The mineral distribution in the Itsaku section is summarized in Figure 6.7 and 6.8 where it can be seen that the Upernivik Næs Formation is dominated by kaolinite cement in the lower part and carbonate cement becomes more common toward the toThe content of muscovite increases towards the top of the formation and the content is high in the basal part of the Kangilia Formation together with biotite. These minerals were probably derived from weathering of basement cropping out not so far away.

6.4   Provenance of sandstone in the Disko Bay Region

Detrital zircons from stream sediments in the basement areas to the east of the Disko–Nuussuaq region have been analyzed and the results summarized in Figure 6.9. The detrital zircon age distribution patterns are dominated by a peak around 2780 Ma. This peak is

slightly shifted towards younger ages to the north, which may be an effect of the Paleopro-terozoic Nagsugtoqidian metamorphic event. Paleo-Archean zircons are common in the Archean block whereas Paleoproterozoic zircons occur north of the Nagsugtoqidian front (Figure 6.9). It can further be noted that a minor peak at around 2.900 Ma becomes more prominent just east and north of the Disko–Nuussuaq region.

The detrital zircon age distribution patterns for the Cretaceous sandstones are shown on Figure 6.10. These patterns are dominated by the 2780 peak as is expected from the sedi-mentological model suggesting that the sandstones were deposited in a large fluvio-deltaic system by rivers draining a proto Greenland (Figure 6.10). As the number of zircons ana-lyzed both from the present day drainage and Cretaceous sands is very high, and the sta-tistics are therefore reliable. Thus, even small differences between the sandstone and the probable source are worth paying attention to. The higher abundance of the Paleoprotero-zoic 1900 Ma population is explained by the local geology (Figure 6.9). However, the 3200 and 3000 Ma ages are over represented in the sandstones as they are not as common in the area and thus may represent transport from a remote source. Further, it can be noted that there are small but significant populations of zircons with ages around 1500 Ma and 1100 Ma. Such ages are not known from West and South Greenland but are common in the Caledonian Orogenic Belt in East Greenland, which may be the ultimate source. These zircons may have worked their way to West Greenland by re-working and re-deposition of sediments over a long period of time (Anfinson et al. 2012). An alternative explanation could be that these ages were derived from the Grenville Orogenic Belt in Labrador (Scherstén & Sønderholm 2007).

In the Itsaku profile in the Svartenhuk area, a major change in the sediment provenance is indicated by the detrital zircon age distribution patterns in the Upper Cretaceous and Paleocene deposits (Figure 6.11) The top of the Upernivik Næs Formation shows increas-ing content of 1870 Ma zircons, suggesting a change in the source terrain (Scherstén & Sønderholm 2007). In the Kangilia and the Eqalulik formations, the zircons are almost en-tirely derived from this 1870 Ma source, which is probably the Prøven Granite situated just north of the Itsaku section or the Cumberland Batholith of the same age found on Baffin Island. The immature character of the Kangilia Formation mentioned above is in good ac-cordance a short tranportation distance of the sediment. This change in provenance indi-cates that the Prøven Granite was unroofed at the time of formation of the Kangilia For-mation (Maastrictian) and that the transport direction changed from west directed to south (Scherstén & Sønderholm 2007).
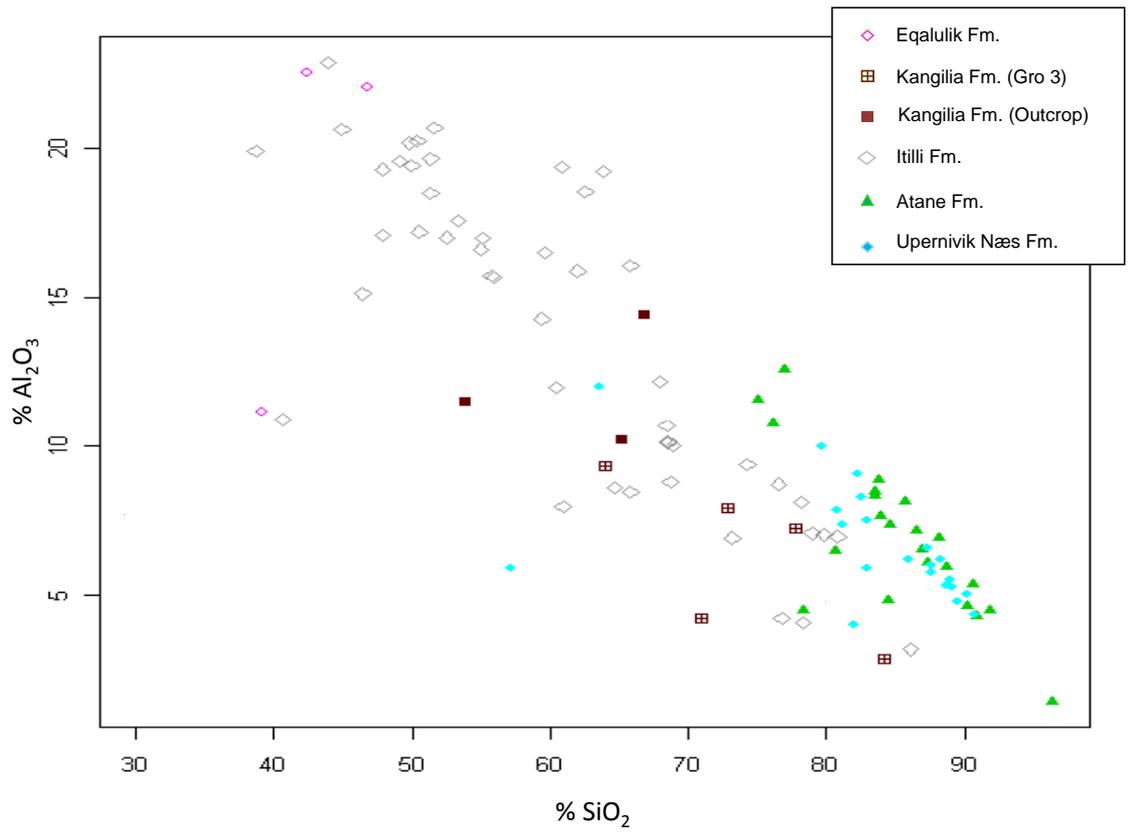
Figure 6.1. *Al$_2$O$_3$ versus SiO$_2$ in sand and mudstones from the Disko Bugt area.*
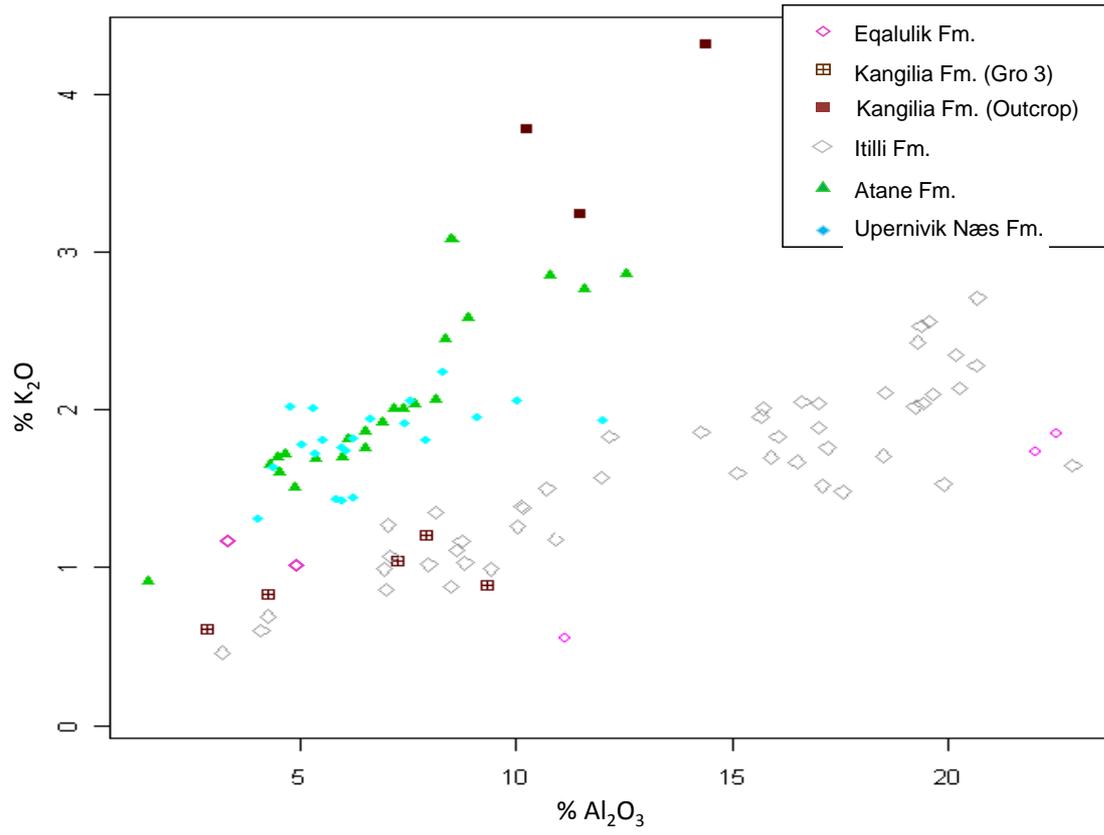
Figure 6.2. *K₂O versus Al₂O₃ in sand and mudstones from the Disko Bugt area.*
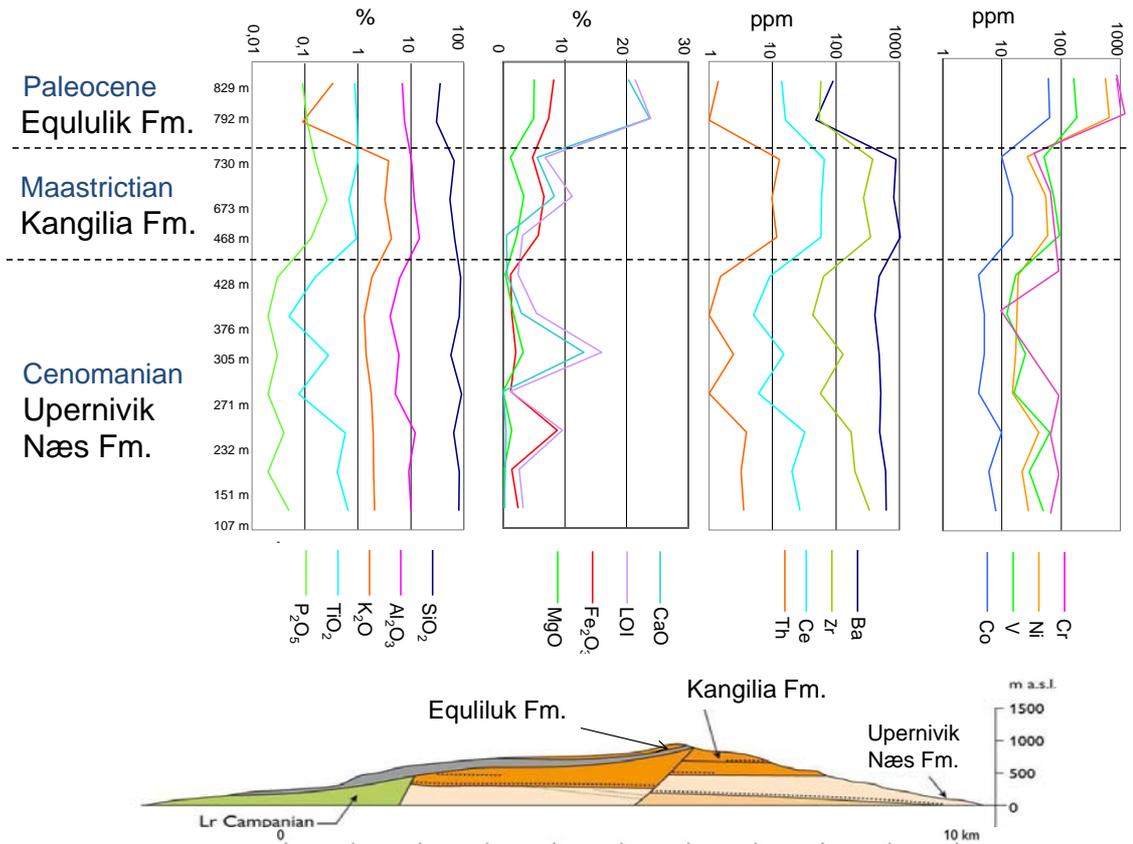
Figure 6.3. *Diagrams showing the geochemical variation in the samples from the Itsaku profile. The elevation above sea is indicated to the left. Note that diagram 1, 3 and 4 from left are logarithmic.*
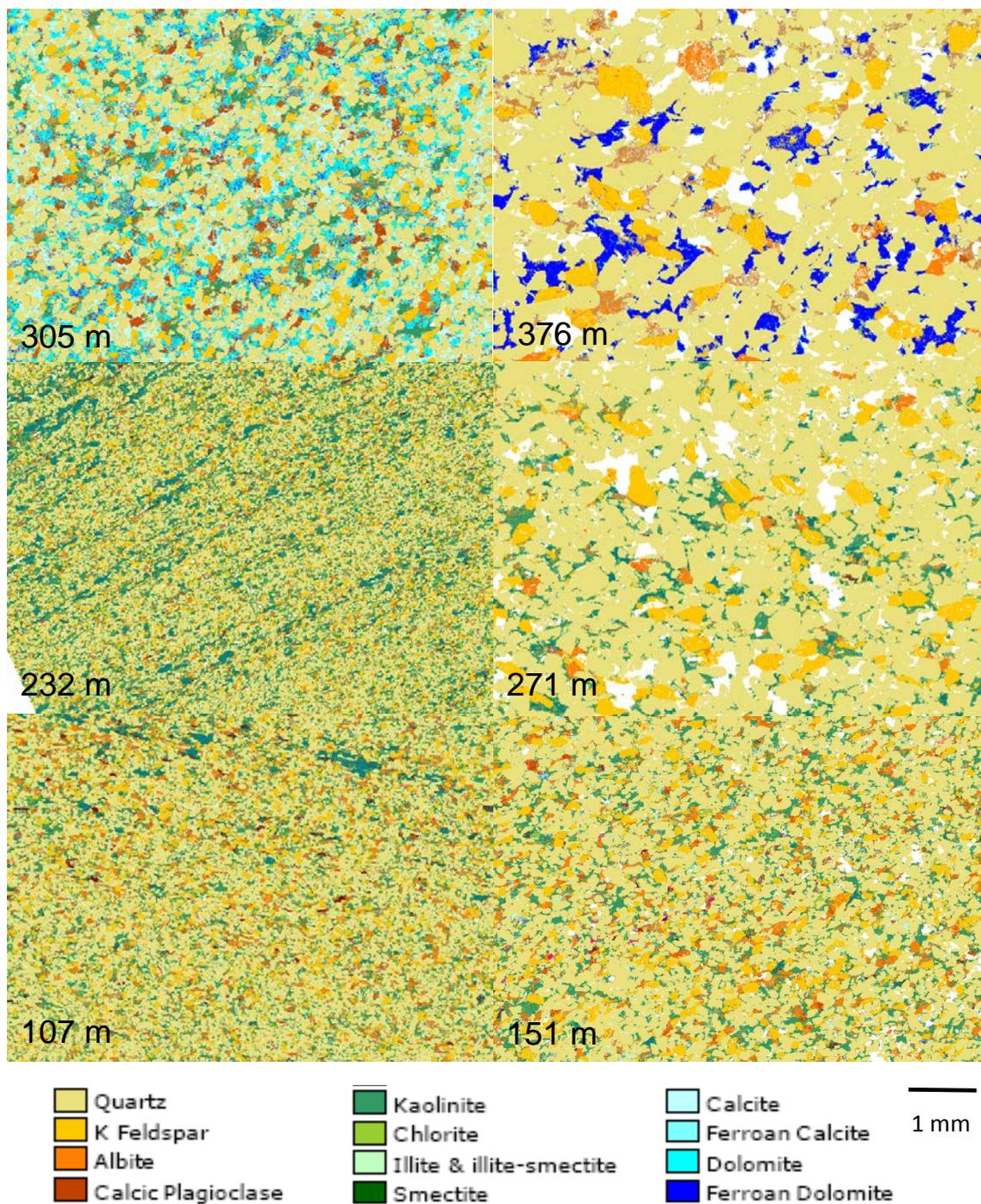
Figure 6.4. *Qemscan images of samples from the Upernivik Næs Formation. The level above sea is indicated. Sample numbers are given on Figure 7.*

	Quartz	25.6
	K Feldspar	15.6
	Albite	1.6
	Calcic Plagioclase	2.7
	Muscovite	2.9
	Biotite	6.6
	Kaolinite	1.2
	Chlorite	19.5
	Illite & illite-smectite	2.8
	Smectite	0.3
	Calcite	13.6
	Ferroan Calcite	4.6
	Dolomite	0.7
	Ferroan Dolomite	1.1
	Fe Oxide & siderite	0.1
	Chromite	0.0
	Pyrite	0.0
	Barite	0.0
	Ilmenite	0.2
	Rutile & Ti Silicates	0.5
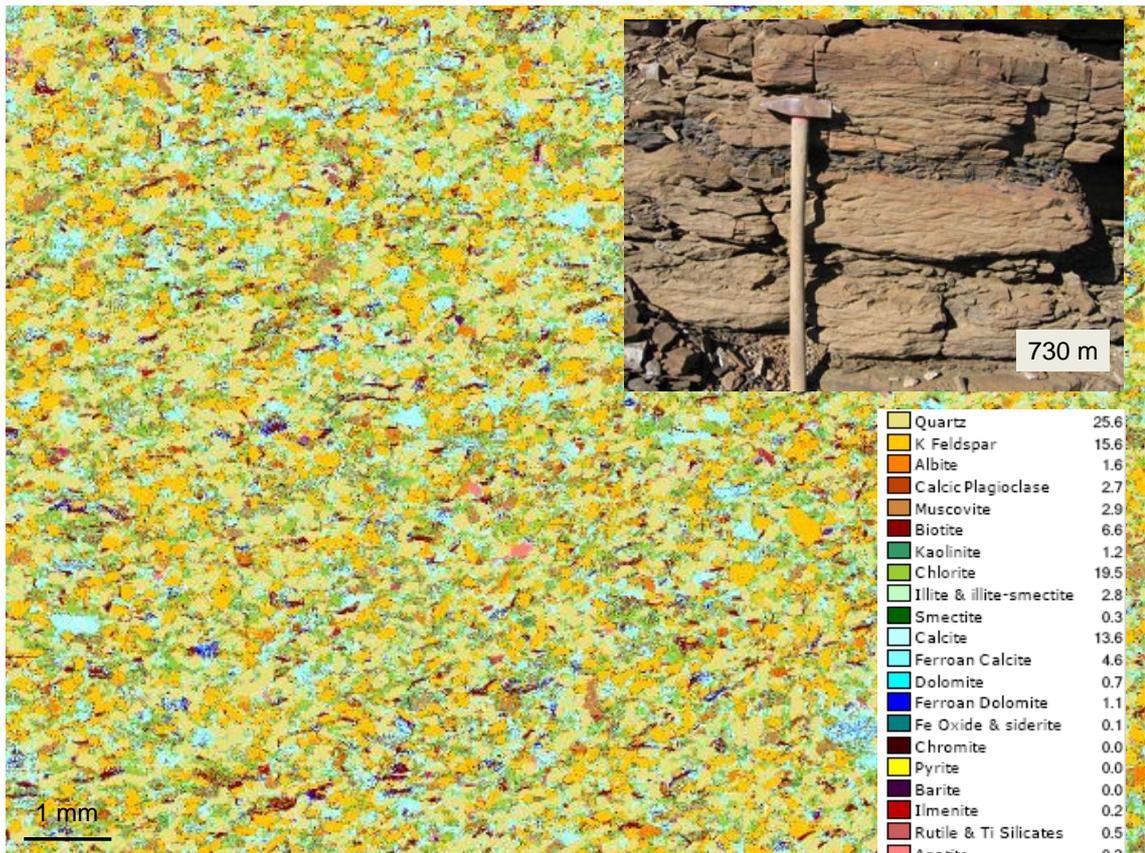
Figure 6.5. *Qemscan image of a sample GGU 463390 from the Kangilia Formation. The sample is taken 730 above sea level.*

GEUS
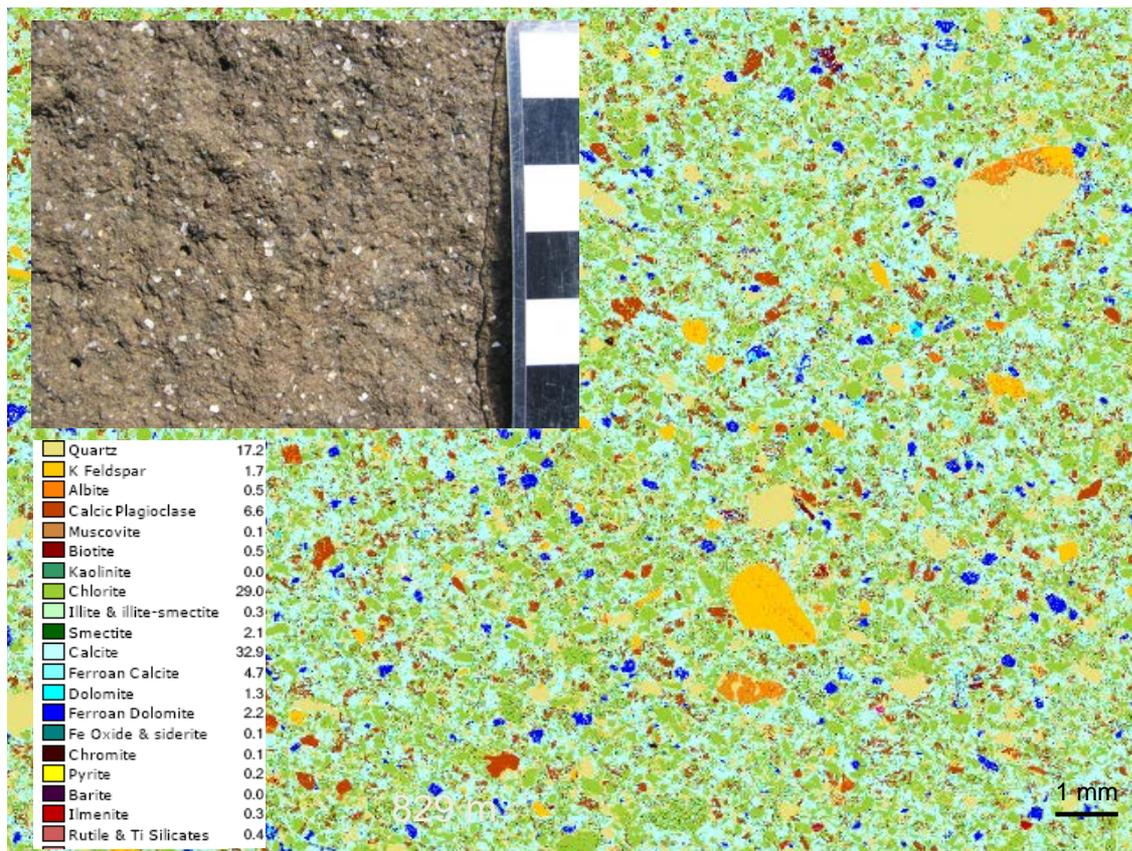
Figure 6.6. *Qemscan image of a sample GGU 463388 from the EF. The sample is taken 829 above sea level.*
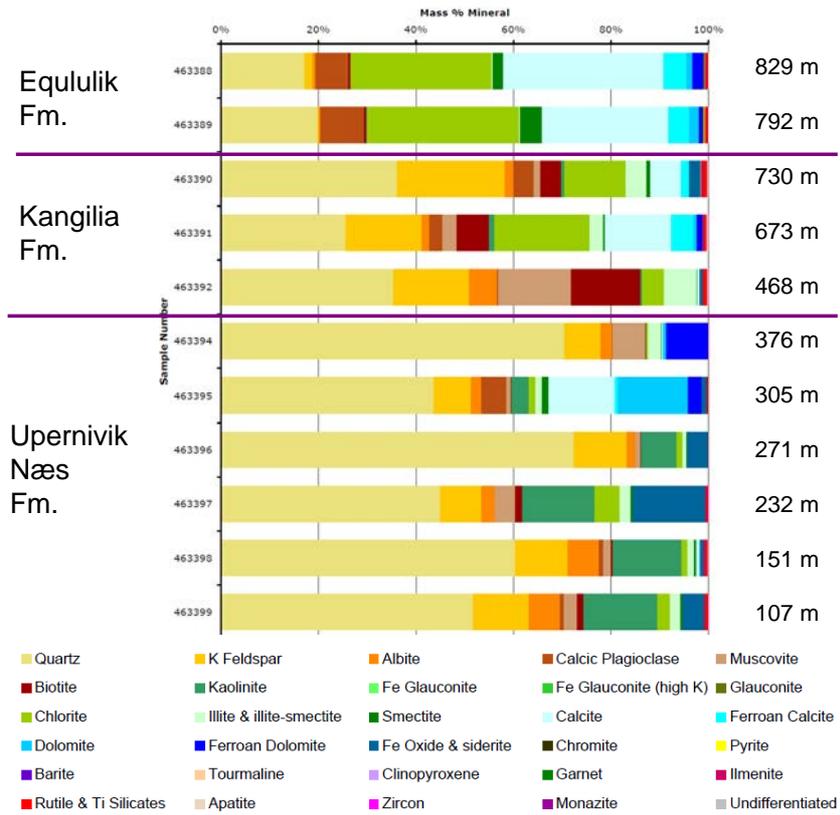
Figure 6.7. *Compilation of the mineralogical compositions of the samples in the Itsaku section analyzed using Qemscan.*
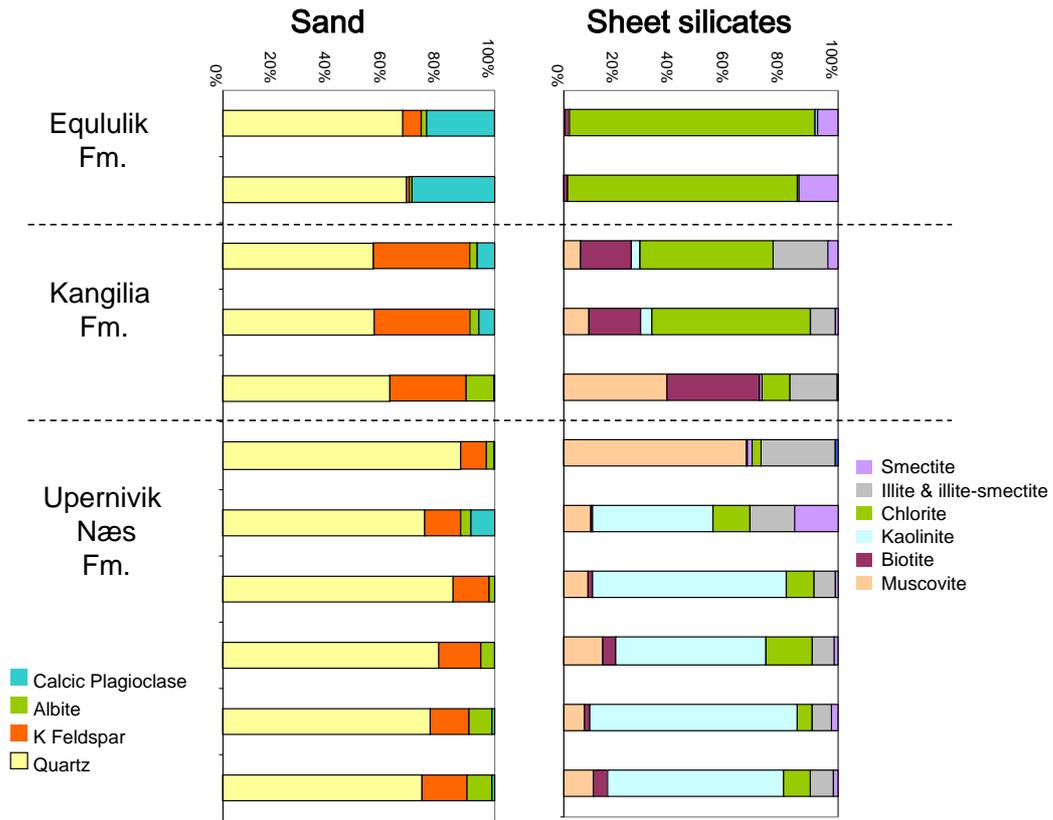
Figure 6.8. *The composition of the sand-fraction (left) and the sheet silicates (right) in the Itsaku section analyzed using Qemscan.*

Age of detrital zircons from present day drainage system
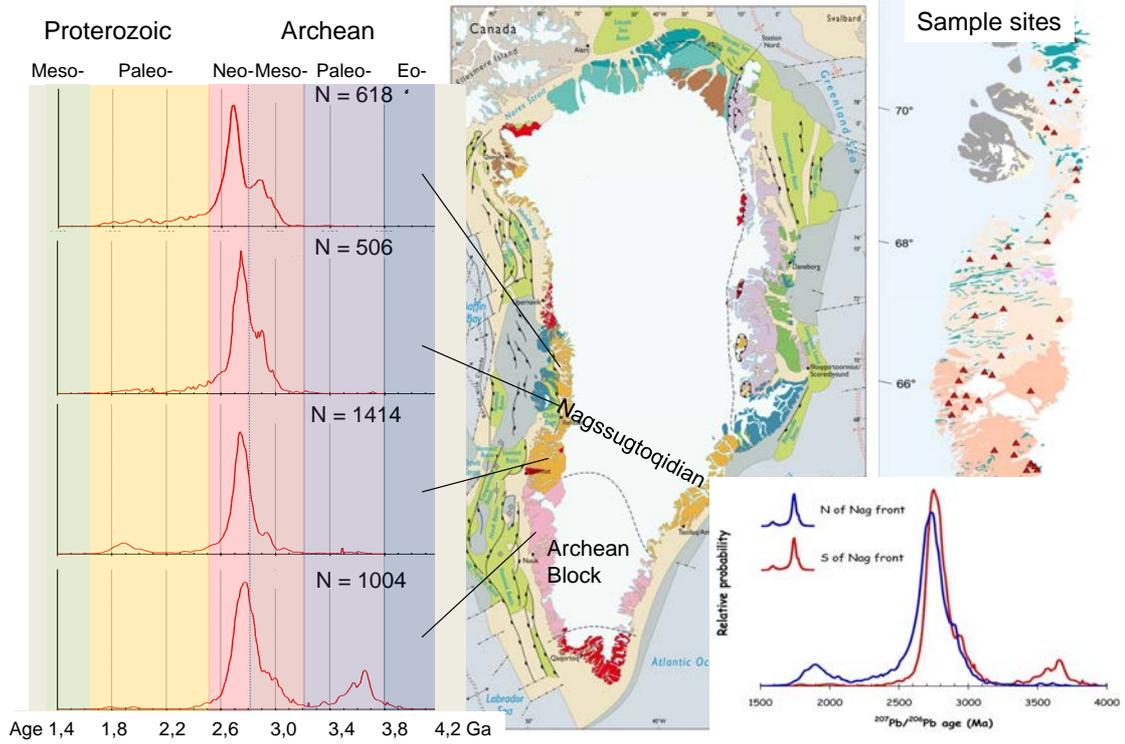
Figure 6.9. *$^{207}Pb/^{206}Pb$ age distribution of detrital zircons from present day drainage systems. Data from Scherstén el al. (2007).*

Detrital zirkon ages in Cretaceous sandstone

Figure 6.10. $^{207}Pb/^{206}Pb$ age distribution of detrital zircons from Cretaceous sandstones. Grønne Ejland at the base, Kingitooq above, GRO-3 in the middle, Paatut above this and Upernivik Ø at the top. Detrital zircon from Cretaceous sandstones and present day drainage systems are compared in the upper right corner. Data from Scherstén el al. (2007).

Figure 6.11. $^{207}Pb/^{206}Pb$ age distribution of detrital zircons from two profiles: Upernivik Ø to the right and Itsaku to the left. Data from Scherstén el al. (2007).

7. Summary of prospectivity and recommendations for future work

Oil and gas shows in cores and wells along with numerous oil seeps, attest to that fact there is a working petroleum system in the region. It is clear that the Disko–Nuussuaq region has all the components required for oil exploration. Five oil types from multiple source rocks of Mesozoic and Paleocene age have been documented. There are numerous formations within the Nuussuaq Basin stratigraphy with good reservoir properties and there are abundant potential seals and traps, both structural and stratigraphic. The combination of play types is thus extensive. Table 6.1 shows a summary of the various petroleum system components identified in the region. At present, our knowledge of the subsurface is still too immature to fully develop the most promising plays and identify specific prospects and calculate volumes.

Sources/Oil Types
- Itilli Fm: possible source of the Itilli and Niaqornaarsuk oils.
- Eqalulik Fm: source for the Marrat oil.
- Atane Fm: possible source for the Kuugannguaq oil.
- Unknown: Eqalulik oil.

Reservoirs
- Atane Fm: Fluvial sandstones, or shallow marine delta front sandstones.
- Itilli Fm: Thick sandstone successions in the Anariartorfik Mb, interbedded with mudstones.
- Kangilia Fm: The Annertuneq Conglomerate Mb could be locally important.
- Agatdal Fm: Sandstone beds in a channelized canyon environment.
- Anaanaa Mb of the Vaigat Fm: Highly permeable hyaloclastite that host most of the oil seeps in western Nuussuaq and Disko.

Seals
- Subaerial lava flows of the Vaigat Fm.
- Subaerial lava flows of the Maligât Fm. These are only preserved on Disko, however.
- Mudstones of the Itilli, Kangalia, and Eqalulik formations.

Traps
- Large anticlines within the volcanic rocks. Four-way closures unclear.
- Smaller anticlines within sedimentary sequences. Four-way closures unclear.
- Stratigraphic traps within interlayered sandstones and mudstones of the Itilli Fm.
- Rotated fault blocks?? Reverse faults??

Table 7.1. *Known petroleum systems components of the Nuussuaq Basin.*

Nevertheless, the number of oil accumulations that could be present is potentially large. Based on the work done by GEUS in the Marrat and Sikillingi areas on western Nuussuaq, Christiansen et al. (2006) estimated the amount of oil that was once present in just the volcanic rocks. The areal distribution of the Anaanaa Mb reservoir at Maraat was estimated to be 24 km^2 and at Sikillingi to be 16 km^2, resulting in volume estimates of 217 mill. barrels and 140 mill. barrels, respectively. Assuming that the Anaanaa Mb originally covered 800 km^2, as much as 1.8 bill. barrels of oil could have once been present. While this latter estimate is clearly a very optimistic scenario, there is no doubt that very large quantities of oil have migrated through Western Nuussuaq (Christiansen et al. 2006).

The structural anticline mapped in the Tunoqqu Mb surface here covers an area of ~250 km^2, suggesting that large areas of central-west Nuussuaq potentially contain significant structures that could serve as traps. The compressive stress field that caused this deformation affected the underlying sedimentary rocks as well, as indicated on seismic data in the Vaigat and north of Nuussuaq and the reversal of motion on faults observed along southern Nuussuaq. While the structures within the weaker sedimentary layers are smaller scale, possible trapping structures likely developed over a broad area.

A key uncertainty remains understanding the distribution, thickness, and quality of potential source rocks, however. Previous play concepts in the region generally assume that the main source rocks are to the west or southwest of the main oil seep areas, i.e., in the main deep marine depocentres. The areas farther east have been considered to be less prospective, since any oil would have to migrate longer distances and bypass these main areas between the Itilli and Kuugannguaq–Qunnilik faults Following this line of thought, the presence of oil seeps at Asuk, far to the east of the K–Q Fault, has always been enigmatic and have raised questions regarding the sources of these oils. Here, we suggest a new lead concept and propose that the central-west Nuussuaq and Uummannaq Fjord areas also hold potential source rocks. This would imply that the region from the Ikorfat and Saqqaqdalen faults and west is prospective on both Nuussuaq and on northern Disko. This hypothesis could also help to explain the Asuk oil seeps.

The Itilli and Kangilia formations are present under much of central-west Nuussuaq and Ummannaq Fjord as shown on the distribution maps of Figures 4.7 and 4.8. In addition, the gravity modelling from Chalmers 1998 shows that even though the deepest basins are west of the K–Q fault, there is still a considerable thickness of sediment indicated. Present day depth to basement is approximately 5 km, and is in places up to 7 km toward the Ikorfat Fault (Figure 3.3). Given that recent uplift and erosion has removed some of the overburden, the burial depths of the present day units were even greater in the past. Thus, it is possible that potential source rocks in the Itilli and Kangilia Fm beneath central Nuussuaq and Uummannaq Fjord were sufficiently buried and matured to generate oil. The migration path of the oils found at Asuk could very well be from the north, rather than the west.

Key questions to answer to develop this idea include:

- What is the distribution of potential marine source rock intervals west of the Ikorfat and Saqqaqdalen faults and what was their burial and uplift history?
- Where was the palaeo-shelf break and how far to the east and southeast did a deep marine environment prevail?

- What is the kinematic history of motion on the structures that control the main depocentres?
- What was the structural development during and after potential oil generation in the key source rock intervals?

Future work that could help to answer these questions and identify prospects in the region include:

1. Reprocessing of the 1995 deep seismic data north of Nuussuaq and in the Vaigat. These data were collected with the same seismic acquisition system as the East and West Greenland Kanumas seismic surveys in the mid-1990's. In 2009, Shell reprocessed the East Greenland data collected with this system with excellent results and demonstrated good imaging below the multiples.

2. New seismic reflection profiles onshore: High priority areas include Agatdalen and Aaffarsuaq. In addition, it could prove useful to collect a profile along the north coast of Nuussuaq between Ikorfat and the Itilli Valley to determine if a stratigraphic test well could prove useful here.

3. Active source seismic refraction to better determine larger scale crustal structure, including depth to basement in key areas.

4. Joint inversion of gravity and magnetic data for depth to basement and crustal thickness.

5. High resolution shallow 3D seismic surveys in Vaigat and north coast of Nuussuaq using the new P-Cable system at Aarhus. The 2000 seismic reflection survey demonstrated that excellent imaging down to the first multiple is possible. However, the spacing of the existing data is insufficient to confidently map faults and correlate structures given the complexity of the area. 3D imaging to multiple could resolve some of these problems and in conjunction with reprocessing of the deep seismic data from 1995 provide new insight into the structural history.

6. Multibeam seabed mapping in Vaigat and Uummannaq Fjord. A key problem interpreting the existing seismic data is that complex seabed features are difficult to interpret. It often cannot be determined if features disrupting the seabed are sills, pingos, slumps or debris flows. Seabed mapping would help to distinguish these. Multibeam mapping could be done using the new Lauge Koch research vessel while collecting P-Cable seismic data.

7. Onshore field campaigns to map the main faults and structures. A key problem for unravelling the structural history is that currently, almost nothing is known about the kinematic development of the faults. This can only be achieved by having structural geologists visit key locations.

8. Screen existing samples to do additional maturity data analyses (e.g., vitrinite reflectance) across key structural elements to determine there are significant differences in thermal history.

9. Additional work on existing cores and samples to determine the reservoir and seal characteristics of different units, including the volcanic succession.

Of these suggestions, 1, 6, 8 and 9 are particularly relevant for future research

Suggestions 2, 3, 5 are particularly relevant in a first phase of an exploration programme that can be followed by core drilling or full scale drilling in a second phase.

8. References

Alsulami, S., Paton, D.A., & Cornwell, D.G. 2015: Tectonic variation and structural evolution of the West Greenland continental margin. AAPG Bulletin **99,** 1689–1711, doi:10.1306/03021514023.

Andersen, G., 1996: Conventional core analysis on GANE-1 and GANE-1A cores. Danmarks og Grønlands Geologiske Undersøgelse Rapport **1996/117**, 1–36.

Anfinson, O. A., Leier, A. L., Embry, A. F., & Dewing, K. 2012: Detrital zircon geochronology and provenance of the Neoproterozoic to Late Devonian Franklinian basin, Canadian Arctic Islands. Geological Society of America Bulletin, **124**(3–4), 415–430.

Appel, A.U., Joensen, I.Á., 2014: Prograderende deltaaflejringer fra øvre Kridt, Atane Formationen, Nuususaqbassinet, centrale Vestgrønland. Bachelorprojekt geologi-geoscience. Københavns Universitet. 49pp (In Danish with English abstract).

Balkwill, H. R. & McMillan, N. J. 1990: Geology of the Labrador Shelf, Baffin Bay, and Davis Strait (Chapter 7 – Part 1). *In*: Keen, M. J. & Williams, G. L. (eds) *Geology of the Continental Margin of Eastern Canada*. Geological Survey of Canada, Geology of Canada, no. 2, 293–348.

Batten, D.J. & Lister, J.K. 1988: Evidence of freshwater dinoflagellates and other algae in the English Wealden (Early Cretaceous). Cretaceous Research **9**, 171–179.

Bint, A.N. 1986: Fossil Ceratiaceae: a restudy and new taxa from the mid-Cretaceous of the Western Interior, USA. Palynology, **10**, 135–180.

Birkelund, T. 1965: Ammonites from the Upper Cretaceous of West Greenland. Meddelelser om Grønland, **179**, No. 7, 192pp.

Bojesen-Koefoed, J. A., Christiansen, F. G., Nytoft, H. P. & Dalhoff, F. 1997: Organic geochemistry and thermal maturity of sediments in the GRO-3 well, Nuussuaq, West Greenland. Danmarks og Grønlands Geolologiske Undersøgelse Rapport **1997/43**, 18 pp.

Bojesen-Koefoed, J.A., Christiansen, F.G., Nytoft, H.P. & Pedersen, A.K. 1999: Oil seepage onshore West Greenland: evidence of multiple source rocks and oil mixing. In: Fleet, A.J. & Boldy, S.A.R. (eds) Petroleum Geology of Northwest Europe: Proceedings of the 5th Conference. Geological Society, London, 305–314.

Bojesen-Koefoed, J.A., Nytoft, H.P. & Christiansen, F.G. 2004: Age of oils in West Greenland: was there a Mesozoic seaway between Greenland and Canada. Geological Survey of Denmark and Greenland Bulletin **4**, 49–52.

Bojesen-Koefoed, J.A., Bidstrup, T., Christiansen, F.G., Dalhoff, F., Gregersen, U., Nytoft, H.P., Nøhr-Hansen, H., Pedersen, A.K. & Sønderholm, M. 2007: Petroleum seepages at Asuk, Disko, West Greenland: implications for regional petroleum exploration. Journal of Petroleum Geology, **30**, 219–236.

Boyd, A. 1998a. Macroleaf biostratigraphy of the Early Cretaceous beds in West Greenland. Zentralblatt für Geologie und Paläontologie Teil I, **11/12**, 1455–1468.

Boyd, A. 1998b. Cuticular and impressional angiosperm leaf remains from the Early Cretaceous floras of West Greenland. Palaeontographica Abteilung B, **247**, 1–53.

Boyd, A.1998c. The Bennettitales of the Early Cretaceous floras from West Greenland: Pseudocycas NATHORST. Palaeontographica Abt. B **247**, 123–155.

Boyd, A. 2000: Bennittales from the Early Cretaceous floras of West Greenland: *Pterophyllum* and *Nilssoniopteras.* Palaeontographica Abt. B **255,** 47–77.

Chalmers, J.A. & Pulvertaft, T.C.R. 2001: Development of the continental margins of the Labrador Sea: a review. Geological Society of London, Special Publications **187,** 77–105.

Chalmers, J.A., Pulvertaft, C.R., Marcussen, C., & Pedersen, A.K. 1998: New structure maps over the Nuussuaq Basin, central West Greenland. Geology of Greenland Survey Bulletin **180,** 18–27.

Chalmers, J.A., Marcussen, C. & Pedersen, A.K. 1999: New insight into the structure of the Nuussuaq Basin, central West Greenland. Marine and Petroleum Geology, **16**, 197–224.

Chalmers, J.A., Pulvertaft, T.C.R., Christiansen, F.G., Larsen, H.C., Laursen, K.H., & Ottesen, T.G. 1993: The southern West Greenland continental margin: rifting history, basin development, and petroleum potential. Geological Society, London, Petroleum Geology Conference Series **4,** 915–931, doi:10.1144/0040915.

Christiansen F.G., Bojesen-Koefoed, J., Larsen, L.M., Nytoft, H.P., & Pedersen, A.K. 2006 Amounts of oil present (or once present) in the volcanic rocks on Disko and Nuussuaq, West Greenland, GEUS-NOTAT No. 08-EN-06-16.

Clarke, D.B. & Pedersen, A.K. 1976: Tertiary volcanic province of West Greenland. In: A. Escher & W.S. Watt (eds) Geology of Greenland. Grønlands Geologiske Undersøgelse, Copenhagen, 365–385.

Connelly, J.N., Thrane, K., Krawiec, A.W., & Garde, A.A. 2006: Linking the Palaeoproterozoic Nagssugtoqidian and Rinkian orogens through the Disko Bugt region of West Greenland. Journal of the Geological Society **163,** 319–335, doi:10.1144/0016-764904-115.

Croxton, C.A. 1976: Sampling of measured sections for palynological and other investigations between 69° and 72°N, central West Greenland. Report Grønlands Geologiske Undersøgelse **80**, 36–39.

Croxton, C.A. 1978a. Report of field work undertaken between 69° and 72°N, central West Greenland in 1975 with preliminary palynological results. Grønlands Geologiske Undersøgelse Open File Report 78-1, 99 p.

Croxton, C.A. 1978b. Report of field work undertaken between 69° and 72°N, central West Greenland in 1977 with some preliminary palynological results. Unpublished Report Grønlands Geologiske Undersøgelse, Report file no. 28069, 24 p.

Dam, G. 2002: Sedimentology of magmatically and structurally controlled outburst valleys along rifted volcanic margins: examples from the Nuussuaq Basin, West Greenland. Sedimentology **49**, 505–532.

Dam, G. & Christensen, F.G., 1994: Well summary, Marraat-1, Nuussuaq, West Greenland. Open File Series Grønlands Geologiske Undersøgelse **94/11**, 27 pp.

Dam, G. & Nøhr-Hansen, H. 2001: Mantle plumes and sequence stratigraphy; Late Maastrichtian – Early Paleocene of West Greenland. Bulletin of the Geological Society of Denmark **48**, 189–207.

Dam, G. & Sønderholm, M. 1994: Lowstand slope channels of the Itilli succession (Maastrichtian–Lower Paleocene), Nuussuaq, West Greenland. Sedimentary Geology, **94**, 49–71.

Dam, G., Larsen, M. & Sønderholm, M. 1998: Sedimentary response to mantle plumes: implications from Paleocene onshore successions, West and East Greenland. Geology **26**, 207–210.

Dam, G., Nøhr-Hansen, H., Pedersen, G.K. & Sønderholm, M. 2000: Sedimentary and structural evidence of a new early Campanian rift phase in the Nuussuaq Basin, West Greenland. Cretaceous Research **21**, 127–154.

Dam, G., Nøhr-Hansen, H., Christiansen, F.G., Bojesen-Koefoed, J.A. & Laier, T. 1998: The oldest marine Cretaceous sediments in West Greenland (Umiivik-1 borehole) – record of the Cenomanian–Turonian Anoxic Event? Geology of Greenland Survey Bulletin **180**, 128–137.

Dam, G., Pedersen, G.K., Sønderholm, M., Midtgaard, H., Larsen, L.M., Nøhr-Hansen, H. & Pedersen, A.K. 2009: Lithostratigraphy of the Cretaceous–Paleocene Nuussuaq Group, Nuussuaq Basin, West Greenland. Geological Survey of Denmark and Greenland Bulletin **19**, 171 pp.

Dickie, K., Keen, C.E., Williams, G.L., & Dehler, S.A. 2011: Tectonostratigraphic evolution of the Labrador margin, Atlantic Canada. Marine and Petroleum Geology **28,** 1663–1675, doi:10.1016/j.marpetgeo.2011.05.009.

Fensome, R.A., Nøhr-Hansen, H., & Williams, G.L. 2016: Cretaceous and Cenozoic dinoflagellate cysts and other palynomorphs from the western and eastern margins of the Labrador–Baffin Seaway. Geological Survey of Denmark and Greenland Bulletin **36,** 143p

Floris, S. 1972: Scleractinian corals from the Upper Cretaceous and Lower Tertiary of Nûgssuaq, West Greenland. Grønlands Geologiske Undersøgelse Bulletin **100**, 132 p + 8 plates).

Funck, T., Jackson, H.R., Louden, K.E., & Klingelhoefer, F. 2007: Seismic study of the transform–rifted margin in Davis Strait between Baffin Island (Canada) and Greenland: What happens when a plume meets a transform. Journal Of Geophysical Research **112,** B04402, doi:10.1029/2006JB004308.

Garde, A. A. 1994: Precambrian geology between Qarajoq Isfjord and Jakobshavn Isfjord, West Greenland. 1:250 000 (geological map). Copenhagen: Geological Survey of Greenland.

Garde, A.A. & Steenfelt, A 1999: Precambrian geology of Nuussuaq and the area northeast of Disko Bugt, West Greenland. In: Kalsbeek, F. (ed.) Precambrian geology of the Disko Bugt region, West Greenland. Geology of Greenland Survey Bulletin **181**, 6–40.

Gerlings, J., Funck, T., Jackson, H.R., Louden, K.E., & Klingelhöfer, F. 2009: Seismic evidence for plume-derived volcanism during formation of the continental margin in southern Davis Strait and northern Labrador Sea. Geophysical Journal International **176,** 980–994, doi:10.1111/j.1365-246X.2008.04021.x.

Gradstein, F. M., Ogg, J. G., Schmitz, M. & Ogg, G.(eds) 2012: The Geologic Time Scale 2012. Amsterdam, Elsevier.

Green, P.F., Lidmar-Bergström, K., Japsen, P., Bonow, J.M., & Chalmers, J.A. 2013: Stratigraphic landscape analysis, thermochronology and the episodic development of elevated, passive continental margins. Geological of Survey of Denmark and Greenland Bulletin **30,** 150p

Gregersen, U. & Bidstrup, T. 2008: Structures and hydrocarbon prospectivity in the northern Davis Strait area, offshore West Greenland. Petroleum Geoscience **14,** 151–166, doi:10.1144/1354-079308-752.

Gregersen, U., Hopper, J.R. and Knutz, P.C. 2013: Basin seismic stratigraphy and aspects of prospectivity in the NE Baffin Bay, Northwest Greenland. Marine and Petroleum Geology **46**, 1–18.

Grímsson F., Zetter R., Grimm G.W., Pedersen G.K., Pedersen A.K.& Denk T. 2015: Fagaceae pollen from the early Cenozoic of West Greenland: revisiting Engler's and Chaney's Arcto-Tertiary hypotheses. Plant Systematics and Evolution **301**, 809–832.

Guarnieri, P. 2015: Pre-break-up palaeostress state along the East Greenland margin. Journal of the Geological Society **172,** 727–739, doi:10.1144/jgs2015-053.

Heer, O. 1883: Oversigt over Grønlands fossile Flora. Meddelelser om Grønland, 5, 79–202. Also published as "Allgemeine Bemerkungen" in Flora Fossilis Grønlandica, volume IV.

Henderson, G., Rosenkrantz, A. & Schiener, E.J. 1976: Cretaceous–Tertiary sedimentary rocks of West Greenland. In: Geology of Greenland. A. Escher and W.S. Watt (eds.). Grønlands Geologiske Undersøgelse, Copenhagen, 341–362.

Kalsbeek, F. 1999: Precambrian geology of the Disko Bugt region, West Greenland. Geology of Greenland Survey Bulletin **181,** 179p

Keen, C.E., Dickie, K., & Dehler, S.A. 2012: The volcanic margins of the northern Labrador Sea: Insights to the rifting process. Tectonics **31,** doi:10.1029/2011TC002985.

Kennedy, W.J., Nøhr-Hansen, H. & Dam, G. 1999: The youngest Maastrichtian ammonite faunas from Nuussuaq, West Greenland. Geology of Greenland Survey Bulletin **184**, 13–17.

Knutsen, S-M, Arendt, N.P., Runge, M.K., Stilling, J. & Brandt, M.P. 2012: Structural provinces offshore West Greenland and key geological variations influencing play assessment. First Break **30**, 43–55.

Knutz, P.C., Hopper, J.R., Gregersen, U., Nielsen, T., & Japsen, P. 2015: A contourite drift system on the Baffin Bay– West Greenland margin linking Pliocene Arctic warming to poleward ocean circulation. Geology, **43**, 907-910, doi: 10.1130/G36927.1.

Koch, B.E. 1959: Contribution to the stratigraphy of the non-marine Tertiary deposits on the south coast of the Nûgssuaq peninsula northwest Greenland with remarks on the fossil flora. Bulletin Grønlands Geologiske Undersøgelse **22**, 100 pp (also Meddelelser om Grønland **162**(1)).

Koppelhus, E.B. & Pedersen, G.K. 1993: A palynological and sedimentological study of Cretaceous floodplain deposits of the Atane Formation at Skansen and Igdlunguaq, Disko, West Greenland. Cretaceous Research, **14**, 707–734.

Lanstorp, J. 1999: En palynologisk undersøgelse af kretassiske og paleocæne sedimenter fra det sydøstlige Nuussuaq, Vestgrønland. Geologisk Tidsskrift 1999-1, 13–20.

Larsen, J.G. & Pulvertaft, T.C.R. 2000: The structure of the Cretaceous–Palaeogene sedimentary-volcanic area of Svartenhuk Halvø, central West Greenland. Geology of Greenland Survey Bulletin **188**, 40 pp.

Larsen, L.M. & Pedersen, A.K. 2009: Petrology of the Paleocene picrites and flood basalts on Disko and Nuussuaq, West Greenland. Journal of Petrology **50**, 1667–1711.

Larsen, L.M., Pedersen, A.K, Tegner, C., Duncan, R.A., Hald, N. & Larsen, J.G. 2015: Age of Tertiary volcanic rocks on the West Greenland continental margin: volcanic evolution and event correlation to other parts of the North Atlantic Igneous Province. Geological Magazine **153**, 487–511, doi: 10.1017/S0016756815000515

Larsen, L.M., Heaman, L.M., Creaser, R.A., Duncan, R.A., Frei, R., & Hutchinson, M. 2009: Tectonomagmatic events during stretching and basin formation in the Labrador Sea and the Davis Strait: evidence from age and composition of Mesozoic to Palaeogene dyke swarms in West Greenland. Journal of the Geological Society **166,** 999–1012, doi:10.1144/0016-76492009-038.

Lenniger, M., Nøhr-Hansen, H., Hills, L.V. & Bjerrum, C.J. 2014: Arctic black shale formation during Cretaceous Oceanic Anoxic Event 2. Geology **42**, 1–4; Data Repository item 2014290; doi:10.1130/G35732.1.

Marcussen, C., Skaarup, N., & Chalmers, J.A. 2002: EFP Project NuussuaqSeis 2000: Structure and hydrocarbon potential of the Nuussuaq Basin: acquisition and interpretation of high resolution multichannel seismic data. Danmarks og Grønlands Geologiske Undersøgelse Rapport **2002/33**.

McIntyre, D.J. 1994a. Report on Cretaceous palynology of eight samples from Kugssinera-juk, Disko Island, West Greenland (Map 70 V.1 Syd). Geological Survey of Canada (Calgary), Paleontological Report 3-DJM-1994, unpubl. 3 p.

McIntyre, D.J. 1994b. Palynology of five Cretaceous samples from Kugssinerajuk, Disko Island, West Greenland (Map 70 V.1 S). Geological Survey of Canada (Calgary), Paleontological Report 6-DJM-1994, unpubl. 3 p.

Midtgaard, H.H. 1996a. Inner-shelf to lower shore-face hummocky sandstone bodies with evidence for geostrophic influenced combined flow, Lower Cretaceous, West Greenland. Journal of Sedimentary Research, **66**, 343–353.

Midtgaard, H.H. 1996b. Sedimentology and sequence stratigraphy of coalbearing synrift sediments on Nuussuaq and Upernivik Ø (Upper Albian–Lower Cenomanian), Central West Greenland. Unpublished Ph.D. thesis, University of Copenhagen, 175 p + appendices + plates.

Morley, C.K., Haranya, C., Phoosongsee, W., Pongwapee, S., Kornsawan, A., & Won-ganan, N. 2004: Activation of rift oblique and rift parallel pre-existing fabrics during extension and their effect on deformation style: examples from the rifts of Thailand. Journal of Structural Geology **26,** 1803-1829, doi:10.1016/j.jsg.2004.02.014.

Nielsen, T.K., Larsen, H.C., & Hopper, J.R. 2002: Contrasting rifted margin styles south of Greenland: implications for mantle plume dynamics. Earth and Planetary Science Letters **200,** 271-286, doi:10.1016/ S0012-821X(02)00616-7.

Núñez-Betelu, L.K. 1994: Sequence stratigraphy of a coastal to offshore transition, sedimentological and Rock-Eval characterization of a depositional sequence, northeastern Sverdrup Basin, Canadian Arctic, 569 pUnpublished Ph.D. thesis, Department of Geology and Geophysics, University of Calgary, Calgary, Canada.

Nøhr-Hansen, H. 1996: Upper Cretaceous dinoflagellate cyst stratigraphy, onshore West Greenland. Bulletin Grønlands Geologiske Undersøgelse **170**, 104 p + plates.

Nøhr-Hansen, H. 2003: Dinoflagellate cyst stratigraphy of the Palaeogene strata from the Hellefisk-1, Ikermiut-1, Kangâmiut-1, Nukik-1, Nukik-2 and Qulleq-1 wells, offshore West Greenland. Marine and Petroleum Geology **20**, 987–1016.

Nøhr-Hansen, H. 2006: Palynostratigraphy of brackish to marine deposits of mid Cretaceous age from the Asuk area, north coast of Disko, West Greenland. GEUS-NOTAT No.: 08-EN-06-14, unpubl. 15

Nøhr-Hansen, H. & Dam, G. 1997: Palynology and sedimentology across a new Cretaceous–Tertiary boundary section on Nuussuaq, West Greenland. Geology, **25**, 851–854

Nøhr-Hansen, H., Sheldon, E. & Dam, G. 2002: A new biostratigraphic scheme for the Paleocene onshore West Greenland and its implications for the timing of the pre-volcanic evolution. In: Jolley, D.W. & Bell, B.R. (eds): The North Atlantic igneous province: stratigraphy, tectonic, volcanic and magmatic processes. Geological Society London Special Publication, **197**, 111–156.

Oakey, G.N. & Chalmers, J.A. 2012: A new model for the Paleogene motion of Greenland relative to North America: Plate reconstructions of the Davis Strait and Nares Strait regions between Canada and Greenland. Journal of Geophysical Research **117,** doi:10.1029/2011JB008942.

Olshefsky, K. & Jerome, M. 1994: Report on 1993 Exploration activities for prospecting licence # 156 and exploration licences 02/91, 03/91. GEUS Report File no. 21356.

Pearce, M.A. 2010: New organic-walled dinoflagellate cysts from the Cenomanian to Maastrichtian of the Trunch borehole, UK. Journal of Micropalaeontology, **29**, 51–72.

Pedersen, A.K. 1985: Lithostratigraphy of the Tertiary Vaigat Formation on Disko, central West Greenland. Rapport Grønlands Geologiske Undersøgelse **124**, 30 p.

Pedersen, A.K. & Dueholm, K.S. 1992: New methods for the geological analysis of Tertiary volcanic formations on Nuussuaq and Disko, central West Greenland, using multi-model photogrammetry. Rapport Grønlands Geologiske Undersøgelse **156,** 19-34.

Pedersen, A.K. & Larsen, L.M. 2006: The Ilugissoq graphite andesite volcano, Nuussuaq, central West Greenland. Lithos **92**, 1–19.

Pedersen, A.K., Larsen, L.M. & Dueholm, K.S. 1993: Geological section along the south coast of Nuussuaq, central West Greenland. 1:20 000 coloured geological sheet. Copenhagen: The Geological Survey of Greenland.

Pedersen, A.K., Larsen, L.M., & Dueholm, K.S. 1996: Filling and plugging of a marine basin by volcanic rocks: the Tunoqqu Member of the Lower Tertiary Viagat Formation on Nuussuaq, central West Greenland. Bulletin Grønlands Geologiske Undersøgelse **171,** 5-28.

Pedersen, A.K., Larsen, L.M. & Dueholm, K.S. 2002: Geological section along the north side of the Aaffarsuaq valley and central Nuussuaq, central West Greenland. 1:20 000 coloured geological sheet. Copenhagen: The Geological Survey of Denmark and Greenland.

Pedersen, A.K., Larsen, L.M. & Dueholm, K.S. 2005: Geological section across north central Disko from Nordfjord to Pingo, central West Greenland. 1:20 000 coloured geological sheet. Copenhagen: The Geological Survey of Denmark and Greenland.

Pedersen, A.K., Larsen, L.M., Pedersen, G.K., Heinesen, M.V. & Dueholm, A.K. 2003: Geological section along the south and south- west coast of Disko, central West Greenland. 1:20 000 coloured geological sheet. Copenhagen: The Geological Survey of Denmark and Greenland.

Pedersen, A.K., Larsen, L.M., Pedersen, G.K., Sønderholm, M., Midtgaard, H.H., Pulvertaft, T.C.R. & Dueholm, K.S. 2006: Geological section along the north coast of Nuussuaq, central West Greenland. 1:20 000 coloured geological sheet. Copenhagen: The Geological Survey of Denmark and Greenland.

Pedersen, G.K., Andersen, L.A., Lundsteen, E.B., Petersen, H.I., Bojesen-Koefoed, J.A. & Nytoft, H.P. 2006: Depositional environments, organic maturity and petroleum potential of the Cretaceous coal-bearing Atane Formation at Qullissat, Nuussuaq Basin, West Greenland. Journal of Petroleum Geology **29**, 3-26.

Pedersen, G. K., Larsen, L. M., Pedersen, A. K. & Hjortkjær, B. F. 1998: The synvolcanic Naajaat lake, Paleocene of West Greenland. Palaeogeography, Palaeoclimatology, Palaeoecology **140**, 271–287.

Pedersen, G.K. & Nøhr-Hansen, H. 2014: Cretaceous sedimentology and palynology of the Nuussuaq Basin, West Greenland —outcrops at the eastern margin of the Baffin Bay Basin Bulletin of Canadian Petroleum Geology **62**, 216–244.

Pedersen, G.K. & Pulvertaft, T.C.R. 1992: The nonmarine Cretaceous of the West Greenland Basin, onshore West Greenland. Cretaceous Research **13**, 263–272.

Pedersen, G. K., Schovsbo, N.H. & Nøhr-Hansen, H., 2013: Calibration of spectral gamma-ray logs to deltaic sedimentary facies from the Cretaceous Atane Formation, Nuussuaq Basin, West Greenland. Bulletin of the Geological Survey **28**, 61–64.

Petersen, G.H. & Vedelsby, A. 2000: An illustrated catalogue of the Paleocene Bivalvia from Nuussuaq, Northwest Greenland: Their environment and the paleoclimate. Steenstrupia **25**, 25-120.

Pulvertaft, T.C.R. 1979: Lower Cretaceous fluvial-deltaic sediments at Kûk, Nûgssuaq, West Greenland. Bulletin of the geological Society of Denmark **28**, 57–72.

Pulvertaft, T.C.R. 1989a. Reinvestigation of the Cretaceous boundary fault in Sarqaqdalen, Nûgssuaq, central West Greenland. Rapport Grønlands Geologiske Undersøgelse **145**, 28 32.

Pulvertaft, T.C.R. 1989b. The geology of Sarqaqdalen, West Greenland, with special reference to the Cretaceous boundary fault system. Open file Series, Grønlands Geologiske Undersøgelse, **89/5**, 36 p.

Pulvertaft, T.C.R. & Chalmers, J.A. 1990: Are there Late Cretaceous unconformities in the onshore outcrops of the West Greenland basin? Report Grønlands Geologiske Undersøgelse **148**, 75–82.

Rasmussen, J.A. & Sheldon, E. 2003: Microfossil biostratigraphy of the Palaeogene succession in the Davis Strait, offshore West Greenland. Marine and petroleum geology **20,** 1017-1030, doi:10.1016/S0264-8172(02)00114-9.

Rasmussen, J.A., Nøhr-Hansen, H., & Sheldon, E. 2003: Palaeoecology and palaeoenvironments of the lower Palaeogene succession, offshore West Greenland. Marine and Petroleum Geology **20,** 1043-1073, doi: 10.1016/j.marpetgeo.2003.11.001.

Ring, U. 1994: The influence of preexisting structure on the evolution of the Cenozoic Malawi rift (East African rift system). Tectonics **13,** 313-326, doi:10.1029/93TC03188.

Rolle, F. 1985: Late Cretaceous – Tertiary sediments offshore central West Greenland: lithostratigraphy, sedimentary evolution, and petroleum potential. Canadian Journal of Earth Sciences **22,** 1001-1019, doi: 10.1139/e85-105.

Rosenkrantz, A. 1970: Marine Upper Cretaceous and lowermost Tertiary deposits in West Greenland. Bulletin of the Geological Society of Denmark **19**, 406–453.

Rosenkrantz, A. & Pulvertaft, T.C.R. 1969: Cretaceous-Tertiary stratigraphy and tectonics in Northern West Greenland. The American Association of Petroleum Geologists Memoir **12**, 883–898.

Scherstén, A., Sønderholm, M. & Steenfelt, A. 2007: Provenance of West Greenland Cretaceous and Paleocene sandstones and stream sediment samples based on U-Pb dating of detrital zircon: data and results. Danmarks og Grønlands Geologiske Undersøgelse Rapport **2007/21**, 121 pp.

Scherstén, A., & Sønderholm, M. 2007: Provenance of Cretaceous and Paleocene sandstones in the West Greenland basins based on detrital zircon dating. Geological Survey of Denmark and Greenland Bulletin, **13**.

Schiener, E.J. 1977: Sedimentological observations on the Early Cretaceous sediments in eastern parts of the Nûgssuaq Embayment. Rapport Grønlands Geologiske Undersøgelse **79**, 45–61.

Schlanger, S.O. & Jenkyns, H.C. 1976: Cretaceous oceanic anoxic events: causes and consequences. Geologie en Mijnbouw **55**, 179–184.

Shekhar, S.C., Frandsen, N. & Thomsen, E. 1982: Coal on Nûgssuaq, West Greenland. Unpublished Report Grønlands Geologiske Undersøgelse, 82pp + appendices.

Singh, C. 1983: Cenomanian microfloras of the Peace River area, northwestern Alberta: Alberta Research Council, Bulletin 44.

Storey, M., Duncan, R.A., Pedersen, A.K., Larsen, L.M., & Larsen, H.C. 1998: Ar-40/Ar-39 geochronology of the West Greenland Tertiary volcanic province. Earth And Planetary Science Letters **160,** 569-586.

Sønderholm, M., Dam, G., 1998: Reservoir characterisation of western Nuussuaq, central West Greenland. Danmarks og Grønlands Geologiske Undersøgelse Rapport **1998/6**, 1–36.

Sørensen, E. V. 2011. Implementation of digital Multi-Model Photogrammetry for building of 3D-models and interpretation of the geological and tectonic evolution of the Nuussuaq Basin. Unpublished PhD thesis.

Tappe, S., Foley, S.F., Stracke, A., Romer, R.L., Kjarsgaard, B.A., Heaman, L.M., & Joyce, N. 2007: Craton reactivation on the Labrador Sea margins: Ar-40/Ar-39 age and Sr-Nd-Hf-Pb isotope constraints from alkaline and carbonatite intrusives. Earth And Planetary Science Letters **256,** 433-454, doi:10.1016/j.epsl.2007.01.036.

Thorning, L. & Stemp, R.W. 1998: Airborne geophysical surveys in central West Greenland and central East Greenland in 1997: Geology of Greenland Survey Bulletin **180,** 63-66.

Tröger, K.-A. 2009: Katalog oberkretazischer Inoceramen. Geologica Saxonica **55**, 188 pp.

Whittaker, R.C., Hamann, N.E., & Pulvertaft, T.C.R. 1997: A new frontier province offshore northwest Greenland: Structure, basin development, and petroleum potential of the Melville Bay area. AAPG Bull **81,** 978-998.

Wilgus, C.K. et al. (eds) 1988: Sea level changes: an integrated approach. SEPM Special Publication **42**, 407 pp.